(54) Title: POWER INTERNAL MEDICAL DEVICES WITH GUIDED SURFACE WAVES
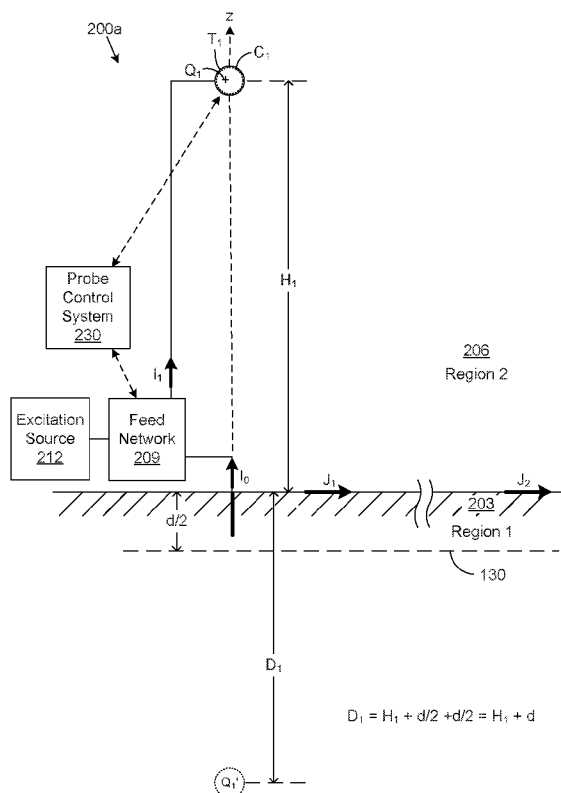
FIG. 3

(57) Abstract: Disclosed is an implantable medical device and
methods of using the medical device. The medical device may in-
clude a guided surface wave receive structure configured to receive
a guided surface wave transmitted by a guided surface waveguide
probe. The guided surface wave receive structure in the medical
device generates an alternating current signal when the guided sur-
face wave is received. The medical device includes a power circuit
that is coupled to the guided surface wave receive structure. The
power circuit includes a power storage circuit to store the power
signal. The medical device includes a medical circuit that com-
prises a stimulus circuit, a monitoring circuit, and potentially other
components. The stimulus circuit provides a stimulus to a human
body. The monitoring circuit measures a characteristic of the hu-
man body.

TZ, UG, ZM, ZW), Eurasian (AM, AZ, BY, KG, KZ, RU, TJ, TM), European (AL, AT, BE, BG, CH, CY, CZ, DE, DK, EE, ES, FI, FR, GB, GR, HR, HU, IE, IS, IT, LT, LU, LV, MC, MK, MT, NL, NO, PL, PT, RO, RS, SE, SI, SK, SM, TR), OAPI (BF, BJ, CF, CG, CI, CM, GA, GN, GQ, GW, KM, ML, MR, NE, SN, TD, TG).

Declarations under Rule 4.17:

— *as to applicant's entitlement to apply for and be granted a patent (Rule 4.17(ii))*

— *as to the applicant's entitlement to claim the priority of the earlier application (Rule 4.17(iii))*

Published:

— *with international search report (Art. 21(3))*

POWER INTERNAL MEDICAL DEVICES WITH GUIDED SURFACE WAVES

CROSS-REFERENCE TO RELATED APPLICATION

[0001]   This application claims priority to and the benefit of, U.S. Application No. 62/215,868, filed on 09 September 2015, herein incorporated by reference in its entirety.

[0002]   This application is related to co-pending U.S. Non-provisional Patent Application entitled "Excitation and Use of Guided Surface Wave Modes on Lossy Media," which was filed on March 7, 2013 and assigned Application Number 13/789,538, and was published on September 11, 2014 as Publication Number US2014/0252886 A1, and which is incorporated herein by reference in its entirety. This application is also related to co-pending U.S. Non-provisional Patent Application entitled "Excitation and Use of Guided Surface Wave Modes on Lossy Media," which was filed on March 7, 2013 and assigned Application Number 13/789,525, and was published on September 11, 2014 as Publication Number US2014/0252865 A1, and which is incorporated herein by reference in its entirety. This application is further related to co-pending U.S. Non-provisional Patent Application entitled "Excitation and Use of Guided Surface Wave Modes on Lossy Media," which was filed on September 10, 2014 and assigned Application Number 14/483,089, and which is incorporated herein by reference in its entirety. This application is further related to co-pending U.S. Non-provisional Patent Application entitled "Excitation and Use of Guided Surface Waves," which was filed on June 2, 2015 and assigned Application Number 14/728,507, and which is incorporated herein by reference in its entirety. This application is further related to co-pending U.S. Non-provisional Patent Application entitled "Excitation and Use of Guided Surface Waves," which was filed on June 2, 2015 and assigned Application Number 14/728,492, and which is incorporated herein by reference in its entirety.

BACKGROUND

[0003]   In the medical industry, medical devices are commonly implanted into patients to provide continuous care for patients that are high risk. For instance, a patient with a heart arrhythmia may have a pacemaker implanted within the chest cavity with electronic leads connected to the heart in order to provide an electric impulse to the heart if the patient's heartbeat requires defibrillation. Such devices may need to be replaced every few years due to the fact that batteries in such devices become discharged or worn out. Such replacement can involve surgery that presents a risk to patients.

SUMMARY

[0004]   According to one embodiment, a medical device includes a guided surface wave receive structure that is configured to receive a guided surface wave traveling along a terrestrial medium generated by a guided surface waveguide probe. A power circuit is electrically coupled to the guided surface wave receive structure. The power circuit generates a power signal from an alternating current signal generated by the guided surface wave receive structure. A medical circuit is electrically coupled to the power circuit. The medical circuit includes a monitoring circuit configured to measure a characteristic of a human body.

[0005]   The medical circuit includes a stimulus circuit configured to provide a stimulus to the human body. The medical circuit is implanted within a human body. The power circuit includes a power storage circuit configured to store the power signal. The monitoring circuit is configured to measure a pulse, a blood pressure, a temperature, a respiration rate, an electric signal, a nerve impulse, a muscle twitch, a resistance value, a protein turnover level, an oxygen level, or another characteristic of the human body.

[0006]   The medical circuit includes a computing device coupled to the stimulus circuit and the monitoring circuit. The computing device is configured to receive a measurement from the monitoring circuit and cause the stimulus circuit to provide the stimulus to the human body. The guided surface wave receive structure is coupled to the power circuit through an impedance matching network. The impedance matching network is configured to minimize a reflection of the alternating current signal back to the guided surface wave receive structure.

[0007]   The stimulus includes one or more of an electrical stimulus to a peroneal nerve, an electrical stimulus to a heart chamber, an electrical stimulus to the surface of a stomach, an electrical stimulus to an auditory nerve, a secretion of insulin, or another stimulus. The medical circuit includes a computing device connected to the power circuit and the computing device is configured to obtain a measurement from a sensing device and initiate the stimulus to the human body based at least in part on the measurement.

[0008]   According to another embodiment, a guided wave receive structure generates an alternating current (AC) signal from a guided surface wave. Power circuitry supplies electrical energy generated embodied in the AC signal to medical circuitry comprising a monitoring circuit and a stimulus circuit. The monitoring circuit determines one or more measurement from a human body. The stimulus circuit provides, via the stimulus circuit, the stimulus circuit to provide a stimulus to the human body.

[0009]   The medical circuitry includes a computing device. The computing device receives measurements from the monitoring circuit. The computing device causes the

2

stimulus circuit to provide the stimulus. The computing device receives preconfigured impulses and transmit information describing the measurements from the monitoring circuit over a network connection.

[0010]   The computing device receives a request to modify at least one threshold for providing the stimulus and modify the threshold based on the request to generate the threshold. The computing device causes the stimulus circuit to provide the stimulus based on the modified threshold. The computing device receives a software package via a network connection. The software package includes a hash of the software package, which the computing device verifies based on the hash. The computing device receives a request to program the software package into a memory associated with the computing device. The computing device stores the software package in the memory. The computing device validates that the software package was successfully stored and execute the software package. The computing device receives a request from a server via a network connection. The computing device authenticates the request based on a security credential.

[0011]   Other systems, methods, features, and advantages of the present disclosure will be or become apparent to one with skill in the art upon examination of the following drawings and detailed description. It is intended that all such additional systems, methods, features, and advantages be included within this description, be within the scope of the present disclosure, and be protected by the accompanying claims.

[0012]   In addition, all optional and preferred features and modifications of the described embodiments are usable in all aspects of the entire disclosure taught herein. Furthermore, the individual features of the dependent claims, as well as all optional and preferred features and modifications of the described embodiments are combinable and interchangeable with one another.

BRIEF DESCRIPTION OF THE DRAWINGS

[0013]   Many aspects of the present disclosure can be better understood with reference to the following drawings. The components in the drawings are not necessarily to scale, emphasis instead being placed upon clearly illustrating the principles of the disclosure. Moreover, in the drawings, like reference numerals designate corresponding parts throughout the several views.

[0014]   FIG. 1 is a chart that depicts field strength as a function of distance for a guided electromagnetic field and a radiated electromagnetic field.

[0015]   FIG. 2 is a drawing that illustrates a propagation interface with two regions employed for transmission of a guided surface wave according to various embodiments of the present disclosure.

[0016] FIG. 3 is a drawing that illustrates a guided surface waveguide probe disposed with respect to a propagation interface of FIG. 2 according to various embodiments of the present disclosure.

[0017] FIG. 4 is a plot of an example of the magnitudes of close-in and far-out asymptotes of first order Hankel functions according to various embodiments of the present disclosure.

[0018] FIGS. 5A and 5B are drawings that illustrate a complex angle of incidence of an electric field synthesized by a guided surface waveguide probe according to various embodiments of the present disclosure.

[0019] FIG. 6 is a graphical representation illustrating the effect of elevation of a charge terminal on the location where the electric field of FIG. 5A intersects with the lossy conducting medium at a Brewster angle according to various embodiments of the present disclosure.

[0020] FIG. 7 is a graphical representation of an example of a guided surface waveguide probe according to various embodiments of the present disclosure.

[0021] FIGS. 8A through 8C are graphical representations illustrating examples of equivalent image plane models of the guided surface waveguide probe of FIGS. 3 and 7 according to various embodiments of the present disclosure.

[0022] FIGS. 9A and 9B are graphical representations illustrating examples of single-wire transmission line and classic transmission line models of the equivalent image plane models of FIGS. 8B and 8C according to various embodiments of the present disclosure.

[0023] FIG. 10 is a flow chart illustrating an example of adjusting a guided surface waveguide probe of FIGS. 3 and 7 to launch a guided surface wave along the surface of a lossy conducting medium according to various embodiments of the present disclosure.

[0024] FIG. 11 is a plot illustrating an example of the relationship between a wave tilt angle and the phase delay of a guided surface waveguide probe of FIGS. 3 and 7 according to various embodiments of the present disclosure.

[0025] FIG. 12 is a drawing that illustrates an example of a guided surface waveguide probe according to various embodiments of the present disclosure.

[0026] FIG. 13 is a graphical representation illustrating the incidence of a synthesized electric field at a complex Brewster angle to match the guided surface waveguide mode at the Hankel crossover distance according to various embodiments of the present disclosure.

[0027] FIG. 14 is a graphical representation of an example of a guided surface waveguide probe of FIG. 12 according to various embodiments of the present disclosure.

[0028] FIG. 15A includes plots of an example of the imaginary and real parts of a phase delay (Φ_U) of a charge terminal T_1 of a guided surface waveguide probe according to various embodiments of the present disclosure.

[0029] FIG. 15B is a schematic diagram of the guided surface waveguide probe of FIG. 14 according to various embodiments of the present disclosure.

[0030] FIG. 16 is a drawing that illustrates an example of a guided surface waveguide probe according to various embodiments of the present disclosure.

[0031] FIG. 17 is a graphical representation of an example of a guided surface waveguide probe of FIG. 16 according to various embodiments of the present disclosure.

[0032] FIGS. 18A through 18C depict examples of receiving structures that can be employed to receive energy transmitted in the form of a guided surface wave launched by a guided surface waveguide probe according to the various embodiments of the present disclosure.

[0033] FIG. 18D is a flow chart illustrating an example of adjusting a receiving structure according to various embodiments of the present disclosure.

[0034] FIG. 19 depicts an example of an additional receiving structure that can be employed to receive energy transmitted in the form of a guided surface wave launched by a guided surface waveguide probe according to the various embodiments of the present disclosure.

[0035] FIGS. 20A through 20E depict examples of various schematic symbols according to various embodiments of the present disclosure.

[0036] FIG. 21 is an illustration of a medical environment according to various embodiments of the present disclosure.

[0037] FIG. 22 depicts a medical device according to various embodiments of the present disclosure.

[0038] FIG. 23 depicts medical circuitry according to various embodiments of the present disclosure.

[0039] FIG. 24 depicts power circuitry according to various embodiments of the present disclosure.

[0040] FIG. 25 is a flowchart illustrating one example of functionality implemented as portions of logic in a medical device of FIG. 21 according to various embodiments of the present disclosure.

[0041] FIG. 26 is a flowchart illustrating one example of functionality implemented as portions of logic in a medical device of FIG. 21 according to various embodiments of the present disclosure.

[0042] FIG. 27 is a schematic block diagram that provides one example illustration of a computing environment employed in the medical environment of FIG. 21 and the computing device employed in the medical circuitry of FIG. 23 according to various embodiments of the present disclosure.

DETAILED DESCRIPTION

[0043] To begin, some terminology shall be established to provide clarity in the discussion of concepts to follow. First, as contemplated herein, a formal distinction is drawn between *radiated* electromagnetic fields and *guided* electromagnetic fields.

[0044] As contemplated herein, a radiated electromagnetic field comprises electromagnetic energy that is emitted from a source structure in the form of waves that are not bound to a waveguide. For example, a radiated electromagnetic field is generally a field that leaves an electric structure such as an antenna and propagates through the atmosphere or other medium and is not bound to any waveguide structure. Once radiated electromagnetic waves leave an electric structure such as an antenna, they continue to propagate in the medium of propagation (such as air) independent of their source until they dissipate regardless of whether the source continues to operate. Once electromagnetic waves are radiated, they are not recoverable unless intercepted, and, if not intercepted, the energy inherent in the radiated electromagnetic waves is lost forever. Electrical structures such as antennas are designed to radiate electromagnetic fields by maximizing the ratio of the radiation resistance to the structure loss resistance. Radiated energy spreads out in space and is lost regardless of whether a receiver is present. The energy density of the radiated fields is a function of distance due to geometric spreading. Accordingly, the term "radiate" in all its forms as used herein refers to this form of electromagnetic propagation.

[0045] A guided electromagnetic field is a propagating electromagnetic wave whose energy is concentrated within or near boundaries between media having different electromagnetic properties. In this sense, a guided electromagnetic field is one that is bound to a waveguide and may be characterized as being conveyed by the current flowing in the waveguide. If there is no load to receive and/or dissipate the energy conveyed in a guided electromagnetic wave, then no energy is lost except for that dissipated in the conductivity of the guiding medium. Stated another way, if there is no load for a guided electromagnetic wave, then no energy is consumed. Thus, a generator or other source generating a guided electromagnetic field does not deliver real power unless a resistive load is present. To this end, such a generator or other source essentially runs idle until a load is presented. This is akin to running a generator to generate a 60 Hertz electromagnetic wave that is transmitted over power lines where there is no electrical load. It should be noted that a guided

electromagnetic field or wave is the equivalent to what is termed a "transmission line mode." This contrasts with radiated electromagnetic waves in which real power is supplied at all times in order to generate radiated waves. Unlike radiated electromagnetic waves, guided electromagnetic energy does not continue to propagate along a finite length waveguide after the energy source is turned off. Accordingly, the term "guide" in all its forms as used herein refers to this transmission mode of electromagnetic propagation.

[0046] Referring now to FIG. 1, shown is a graph 100 of field strength in decibels (dB) above an arbitrary reference in volts per meter as a function of distance in kilometers on a log-dB plot to further illustrate the distinction between radiated and guided electromagnetic fields. The graph 100 of FIG. 1 depicts a guided field strength curve 103 that shows the field strength of a guided electromagnetic field as a function of distance. This guided field strength curve 103 is essentially the same as a transmission line mode. Also, the graph 100 of FIG. 1 depicts a radiated field strength curve 106 that shows the field strength of a radiated electromagnetic field as a function of distance.

[0047] Of interest are the shapes of the curves 103 and 106 for *guided wave* and for *radiation* propagation, respectively. The radiated field strength curve 106 falls off geometrically ($1/d$, where d is distance), which is depicted as a straight line on the log-log scale. The guided field strength curve 103, on the other hand, has a characteristic exponential decay of $e^{-\alpha d}/\sqrt{d}$ and exhibits a distinctive knee 109 on the log-log scale. The guided field strength curve 103 and the radiated field strength curve 106 intersect at point 112, which occurs at a crossing distance. At distances less than the crossing distance at intersection point 112, the field strength of a guided electromagnetic field is significantly greater at most locations than the field strength of a radiated electromagnetic field. At distances greater than the crossing distance, the opposite is true. Thus, the guided and radiated field strength curves 103 and 106 further illustrate the fundamental propagation difference between guided and radiated electromagnetic fields. For an informal discussion of the difference between guided and radiated electromagnetic fields, reference is made to Milligan, T., Modern Antenna Design, McGraw-Hill, 1st Edition, 1985, pp.8-9, which is incorporated herein by reference in its entirety.

[0048] The distinction between radiated and guided electromagnetic waves, made above, is readily expressed formally and placed on a rigorous basis. That two such diverse solutions could emerge from one and the same linear partial differential equation, the wave equation, analytically follows from the boundary conditions imposed on the problem. The Green function for the wave equation, itself, contains the distinction between the nature of radiation and guided waves.

[0049] In empty space, the wave equation is a differential operator whose eigenfunctions possess a *continuous* spectrum of eigenvalues on the complex wave-number plane. This transverse electro-magnetic (TEM) field is called the radiation field, and those propagating fields are called "Hertzian waves." However, in the presence of a conducting boundary, the wave equation plus boundary conditions mathematically lead to a spectral representation of wave-numbers composed of a continuous spectrum *plus* a sum of *discrete* spectra. To this end, reference is made to Sommerfeld, A., "Uber die Ausbreitung der Wellen in der Drahtlosen Telegraphie," Annalen der Physik, Vol. 28, 1909, pp. 665-736. Also see Sommerfeld, A., "Problems of Radio," published as Chapter 6 in Partial Differential Equations in Physics – Lectures on Theoretical Physics: Volume VI, Academic Press, 1949, pp. 236-289, 295-296; Collin, R. E., "Hertzian Dipole Radiating Over a Lossy Earth or Sea: Some Early and Late 20th Century Controversies," IEEE Antennas and Propagation Magazine, Vol. 46, No. 2, April 2004, pp. 64-79; and Reich, H. J., Ordnung, P.F, Krauss, H.L., and Skalnik, J.G., Microwave Theory and Techniques, Van Nostrand, 1953, pp. 291-293, each of these references being incorporated herein by reference in its entirety.

[0050] The terms *"ground wave"* and *"surface wave"* identify two distinctly different physical propagation phenomena. A surface wave arises analytically from a distinct *pole* yielding a *discrete* component in the plane wave spectrum. See, e.g., "The Excitation of Plane Surface Waves" by Cullen, A.L., (Proceedings of the IEE (British), Vol. 101, Part IV, August 1954, pp. 225-235). In this context, a *surface wave* is considered to be a guided *surface wave*. The *surface wave* (in the Zenneck-Sommerfeld guided wave sense) is, physically and mathematically, <u>not</u> the same as the *ground wave* (in the Weyl-Norton-FCC sense) that is now so familiar from radio broadcasting. These two propagation mechanisms arise from the excitation of different types of eigenvalue spectra (continuum or discrete) on the complex plane. The field strength of the guided *surface wave* decays exponentially with distance as illustrated by curve 103 of FIG. 1 (much like propagation in a lossy waveguide) and resembles propagation in a radial transmission line, as opposed to the classical Hertzian radiation of the *ground wave*, which propagates spherically, possesses a *continuum* of eigenvalues, falls off geometrically as illustrated by curve 106 of FIG. 1, and results from branch-cut integrals. As experimentally demonstrated by C.R. Burrows in "The Surface Wave in Radio Propagation over Plane Earth" (Proceedings of the IRE, Vol. 25, No. 2, February, 1937, pp. 219-229) and "The Surface Wave in Radio Transmission" (Bell Laboratories Record, Vol. 15, June 1937, pp. 321-324), vertical antennas radiate *ground waves* but do not launch guided *surface waves*.

[0051] To summarize the above, first, the *continuous* part of the wave-number eigenvalue spectrum, corresponding to *branch-cut integrals*, produces the radiation field,

and second, the *discrete* spectra, and corresponding *residue sum* arising from the poles enclosed by the contour of integration, result in non-TEM traveling surface waves that are exponentially damped in the direction transverse to the propagation. Such surface waves are guided transmission line modes. For further explanation, reference is made to Friedman, B., Principles and Techniques of Applied Mathematics, Wiley, 1956, pp. pp. 214, 283-286, 290, 298-300.

[0052] In free space, antennas excite the *continuum* eigenvalues of the wave equation, which is a radiation field, where the outwardly propagating RF energy with E_z and H_ϕ in-phase is lost forever. On the other hand, waveguide probes excite *discrete* eigenvalues, which results in transmission line propagation. See Collin, R. E., Field Theory of Guided Waves, McGraw-Hill, 1960, pp. 453, 474-477. While such theoretical analyses have held out the hypothetical possibility of launching open surface guided waves over planar or spherical surfaces of lossy, homogeneous media, for more than a century no known structures in the engineering arts have existed for accomplishing this with any practical efficiency. Unfortunately, since it emerged in the early 1900's, the theoretical analysis set forth above has essentially remained a theory and there have been no known structures for practically accomplishing the launching of open surface guided waves over planar or spherical surfaces of lossy, homogeneous media.

[0053] According to the various embodiments of the present disclosure, various guided surface waveguide probes are described that are configured to excite electric fields that couple into a guided surface waveguide mode along the surface of a lossy conducting medium. Such guided electromagnetic fields are substantially mode-matched in magnitude and phase to a guided surface wave mode on the surface of the lossy conducting medium. Such a guided surface wave mode can also be termed a Zenneck waveguide mode. By virtue of the fact that the resultant fields excited by the guided surface waveguide probes described herein are substantially mode-matched to a guided surface waveguide mode on the surface of the lossy conducting medium, a guided electromagnetic field in the form of a guided surface wave is launched along the surface of the lossy conducting medium. According to one embodiment, the lossy conducting medium comprises a terrestrial medium such as the Earth.

[0054] Referring to FIG. 2, shown is a propagation interface that provides for an examination of the boundary value solutions to Maxwell's equations derived in 1907 by Jonathan Zenneck as set forth in his paper Zenneck, J., "On the Propagation of Plane Electromagnetic Waves Along a Flat Conducting Surface and their Relation to Wireless Telegraphy," Annalen der Physik, Serial 4, Vol. 23, September 20, 1907, pp. 846-866. FIG. 2 depicts cylindrical coordinates for radially propagating waves along the interface between

a lossy conducting medium specified as Region 1 and an insulator specified as Region 2. Region 1 can comprise, for example, any lossy conducting medium. In one example, such a lossy conducting medium can comprise a terrestrial medium such as the Earth or other medium. Region 2 is a second medium that shares a boundary interface with Region 1 and has different constitutive parameters relative to Region 1. Region 2 can comprise, for example, any insulator such as the atmosphere or other medium. The reflection coefficient for such a boundary interface goes to zero only for incidence at a *complex* Brewster angle. See Stratton, J.A., Electromagnetic Theory, McGraw-Hill, 1941, p. 516.

[0055]   According to various embodiments, the present disclosure sets forth various guided surface waveguide probes that generate electromagnetic fields that are substantially mode-matched to a guided surface waveguide mode on the surface of the lossy conducting medium comprising Region 1. According to various embodiments, such electromagnetic fields substantially synthesize a wave front incident at a complex Brewster angle of the lossy conducting medium that can result in zero reflection.

[0056]   To explain further, in Region 2, where an $e^{j\omega t}$ field variation is assumed and where $\rho \neq 0$ and $z \geq 0$ (with z being the vertical coordinate normal to the surface of Region 1, and ρ being the radial dimension in cylindrical coordinates), Zenneck's closed-form exact solution of Maxwell's equations satisfying the boundary conditions along the interface are expressed by the following electric field and magnetic field components:

$$H_{2\phi} = Ae^{-u_2 z}\ H_1^{(2)}(-j\gamma\rho), \tag{1}$$

$$E_{2\rho} = A\left(\frac{u_2}{j\omega\varepsilon_o}\right)e^{-u_2 z}\ H_1^{(2)}(-j\gamma\rho),\ \text{and} \tag{2}$$

$$E_{2z} = A\left(\frac{-\gamma}{\omega\varepsilon_o}\right)e^{-u_2 z}\ H_0^{(2)}(-j\gamma\rho). \tag{3}$$

[0057]   In Region 1, where the $e^{j\omega t}$ field variation is assumed and where $\rho \neq 0$ and $z \leq 0$, Zenneck's closed-form exact solution of Maxwell's equations satisfying the boundary conditions along the interface is expressed by the following electric field and magnetic field components:

$$H_{1\phi} = Ae^{u_1 z}\ H_1^{(2)}(-j\gamma\rho), \tag{4}$$

$$E_{1\rho} = A\left(\frac{-u_1}{\sigma_1 + j\omega\varepsilon_1}\right)e^{u_1 z}\ H_1^{(2)}(-j\gamma\rho),\ \text{and} \tag{5}$$

$$E_{1z} = A\left(\frac{-j\gamma}{\sigma_1 + j\omega\varepsilon_1}\right)e^{u_1 z}\ H_0^{(2)}(-j\gamma\rho). \tag{6}$$

[0058]   In these expressions, z is the vertical coordinate normal to the surface of Region 1 and ρ is the radial coordinate, $H_n^{(2)}(-j\gamma\rho)$ is a complex argument Hankel function of the second kind and order n, u_1 is the propagation constant in the positive vertical (z) direction in Region 1, u_2 is the propagation constant in the vertical (z) direction in Region 2, σ_1 is the conductivity of Region 1, ω is equal to $2\pi f$, where f is a frequency of excitation, ε_o is the

permittivity of free space, ε_1 is the permittivity of Region 1, A is a source constant imposed by the source, and γ is a surface wave radial propagation constant.

[0059]   The propagation constants in the $\pm z$ directions are determined by separating the wave equation above and below the interface between Regions 1 and 2, and imposing the boundary conditions. This exercise gives, in Region 2,

$$u_2 = \frac{-jk_o}{\sqrt{1+(\varepsilon_r-jx)}} \tag{7}$$

and gives, in Region 1,

$$u_1 = -u_2(\varepsilon_r - jx). \tag{8}$$

The radial propagation constant γ is given by

$$\gamma = j\sqrt{k_o^2 + u_2^2} = j\frac{k_o n}{\sqrt{1+n^2}}, \tag{9}$$

which is a complex expression where n is the complex index of refraction given by

$$n = \sqrt{\varepsilon_r - jx}. \tag{10}$$

In all of the above Equations,

$$x = \frac{\sigma_1}{\omega\varepsilon_o}, \text{ and} \tag{11}$$

$$k_o = \omega\sqrt{\mu_o\varepsilon_o} = \frac{\lambda_o}{2\pi}, \tag{12}$$

where ε_r comprises the relative permittivity of Region 1, σ_1 is the conductivity of Region 1, ε_o is the permittivity of free space, and μ_o comprises the permeability of free space. Thus, the generated surface wave propagates parallel to the interface and exponentially decays vertical to it. This is known as evanescence.

[0060]   Thus, Equations (1)-(3) can be considered to be a cylindrically-symmetric, radially-propagating waveguide mode. See Barlow, H. M., and Brown, J., Radio Surface Waves, Oxford University Press, 1962, pp. 10-12, 29-33. The present disclosure details structures that excite this "open boundary" waveguide mode. Specifically, according to various embodiments, a guided surface waveguide probe is provided with a charge terminal of appropriate size that is fed with voltage and/or current and is positioned relative to the boundary interface between Region 2 and Region 1. This may be better understood with reference to FIG. 3, which shows an example of a guided surface waveguide probe 200a that includes a charge terminal T_1 elevated above a lossy conducting medium 203 (e.g., the Earth) along a vertical axis z that is normal to a plane presented by the lossy conducting medium 203. The lossy conducting medium 203 makes up Region 1, and a second medium 206 makes up Region 2 and shares a boundary interface with the lossy conducting medium 203.

[0061]   According to one embodiment, the lossy conducting medium 203 can comprise a terrestrial medium such as the planet Earth. To this end, such a terrestrial medium comprises all structures or formations included thereon whether natural or man-made. For

example, such a terrestrial medium can comprise natural elements such as rock, soil, sand, fresh water, sea water, trees, vegetation, and all other natural elements that make up our planet. In addition, such a terrestrial medium can comprise man-made elements such as concrete, asphalt, building materials, and other man-made materials. In other embodiments, the lossy conducting medium 203 can comprise some medium other than the Earth, whether naturally occurring or man-made. In other embodiments, the lossy conducting medium 203 can comprise other media such as man-made surfaces and structures such as automobiles, aircraft, man-made materials (such as plywood, plastic sheeting, or other materials) or other media.

[0062]   In the case where the lossy conducting medium 203 comprises a terrestrial medium or Earth, the second medium 206 can comprise the atmosphere above the ground. As such, the atmosphere can be termed an "atmospheric medium" that comprises air and other elements that make up the atmosphere of the Earth. In addition, it is possible that the second medium 206 can comprise other media relative to the lossy conducting medium 203.

[0063]   The guided surface waveguide probe 200a includes a feed network 209 that couples an excitation source 212 to the charge terminal T_1 via, e.g., a vertical feed line conductor. According to various embodiments, a charge Q_1 is imposed on the charge terminal T_1 to synthesize an electric field based upon the voltage applied to terminal T_1 at any given instant. Depending on the angle of incidence (θ_i) of the electric field (E), it is possible to substantially mode-match the electric field to a guided surface waveguide mode on the surface of the lossy conducting medium 203 comprising Region 1.

[0064]   By considering the Zenneck closed-form solutions of Equations (1)-(6), the Leontovich impedance boundary condition between Region 1 and Region 2 can be stated as

$$\hat{z} \times \vec{H}_2(\rho, \varphi, 0) = \vec{J}_s, \qquad (13)$$

where $\hat{z}$ is a unit normal in the positive vertical $(+z)$ direction and $\vec{H}_2$ is the magnetic field strength in Region 2 expressed by Equation (1) above. Equation (13) implies that the electric and magnetic fields specified in Equations (1)-(3) may result in a radial surface current density along the boundary interface, where the radial surface current density can be specified by

$$J_\rho(\rho') = -A\, H_1^{(2)}(-j\gamma\rho') \qquad (14)$$

where A is a constant. Further, it should be noted that close-in to the guided surface waveguide probe 200 (for $\rho \ll \lambda$), Equation (14) above has the behavior

$$J_{close}(\rho') = \frac{-A(j2)}{\pi(-j\gamma\rho')} = -H_\phi = -\frac{I_o}{2\pi\rho'}. \qquad (15)$$

The negative sign means that when source current (I_o) flows vertically upward as illustrated in FIG. 3, the "close-in" ground current flows radially *inward*. By field matching on H_ϕ "close-in," it can be determined that

$$A = -\frac{I_o \gamma}{4} = -\frac{\omega q_1 \gamma}{4} \tag{16}$$

where $q_1 = C_1 V_1$, in Equations (1)-(6) and (14). Therefore, the radial surface current density of Equation (14) can be restated as

$$J_\rho(\rho') = \frac{I_o \gamma}{4} H_1^{(2)}(-j\gamma\rho'). \tag{17}$$

The fields expressed by Equations (1)-(6) and (17) have the nature of a *transmission line mode* bound to a lossy interface, *not radiation fields* that are associated with groundwave propagation. See Barlow, H. M. and Brown, J., Radio Surface Waves, Oxford University Press, 1962, pp. 1-5.

[0065] At this point, a review of the nature of the Hankel functions used in Equations (1)-(6) and (17) is provided for these solutions of the wave equation. One might observe that the Hankel functions of the first and second kind and order n are defined as complex combinations of the standard Bessel functions of the first and second kinds

$$H_n^{(1)}(x) = J_n(x) + jN_n(x), \text{ and} \tag{18}$$

$$H_n^{(2)}(x) = J_n(x) - jN_n(x), \tag{19}$$

These functions represent cylindrical waves propagating radially inward ($H_n^{(1)}$) and outward ($H_n^{(2)}$), respectively. The definition is analogous to the relationship $e^{\pm jx} = \cos x \pm j \sin x$. See, for example, Harrington, R.F., Time-Harmonic Fields, McGraw-Hill, 1961, pp. 460-463.

[0066] That $H_n^{(2)}(k_\rho \rho)$ is an outgoing wave can be recognized from its large argument asymptotic behavior that is obtained directly from the series definitions of $J_n(x)$ and $N_n(x)$. Far-out from the guided surface waveguide probe:

$$H_n^{(2)}(x) \xrightarrow[x \to \infty]{} \sqrt{\frac{2j}{\pi x}} j^n e^{-jx} = \sqrt{\frac{2}{\pi x}} j^n e^{-j\left(x - \frac{\pi}{4}\right)}, \tag{20a}$$

which, when multiplied by $e^{j\omega t}$, is an outward propagating cylindrical wave of the form $e^{j(\omega t - k\rho)}$ with a $1/\sqrt{\rho}$ spatial variation. The first order ($n = 1$) solution can be determined from Equation (20a) to be

$$H_1^{(2)}(x) \xrightarrow[x \to \infty]{} j\sqrt{\frac{2j}{\pi x}} e^{-jx} = \sqrt{\frac{2}{\pi x}} e^{-j\left(x - \frac{\pi}{2} - \frac{\pi}{4}\right)}. \tag{20b}$$

Close-in to the guided surface waveguide probe (for $\rho \ll \lambda$), the Hankel function of first order and the second kind behaves as

$$H_1^{(2)}(x) \xrightarrow[x \to 0]{} \frac{2j}{\pi x}. \tag{21}$$

Note that these asymptotic expressions are complex quantities. When x is a real quantity, Equations (20b) and (21) differ in phase by $\sqrt{j}$, which corresponds to an extra phase advance or "phase boost" of 45° or, equivalently, $\lambda/8$. The close-in and far-out asymptotes of the first order Hankel function of the second kind have a Hankel "crossover" or transition point where they are of equal magnitude at a distance of $\rho = R_x$.

[0067] Thus, beyond the Hankel crossover point the "far out" representation predominates over the "close-in" representation of the Hankel function. The distance to the Hankel crossover point (or Hankel crossover distance) can be found by equating Equations (20b) and (21) for $-j\gamma\rho$, and solving for R_x. With $x = \sigma/\omega\varepsilon_o$, it can be seen that the far-out and close-in Hankel function asymptotes are frequency dependent, with the Hankel crossover point moving out as the frequency is lowered. It should also be noted that the Hankel function asymptotes may also vary as the conductivity (σ) of the lossy conducting medium changes. For example, the conductivity of the soil can vary with changes in weather conditions.

[0068] Referring to FIG. 4, shown is an example of a plot of the magnitudes of the first order Hankel functions of Equations (20b) and (21) for a Region 1 conductivity of σ = 0.010 mhos/m and relative permittivity ε_r = 15, at an operating frequency of 1850 kHz. Curve 115 is the magnitude of the far-out asymptote of Equation (20b) and curve 118 is the magnitude of the close-in asymptote of Equation (21), with the Hankel crossover point 121 occurring at a distance of R_x = 54 feet. While the magnitudes are equal, a phase offset exists between the two asymptotes at the Hankel crossover point 121. It can also be seen that the Hankel crossover distance is much less than a wavelength of the operation frequency.

[0069] Considering the electric field components given by Equations (2) and (3) of the Zenneck closed-form solution in Region 2, it can be seen that the ratio of E_z and E_ρ asymptotically passes to

$$\frac{E_z}{E_\rho} = \left(\frac{-j\gamma}{u_2}\right)\frac{H_0^{(2)}(-j\gamma\rho)}{H_1^{(2)}(-j\gamma\rho)} \xrightarrow[\rho\to\infty]{} \sqrt{\varepsilon_r - j\frac{\sigma}{\omega\varepsilon_o}} = n = \tan\theta_i, \tag{22}$$

where n is the complex index of refraction of Equation (10) and θ_i is the angle of incidence of the electric field. In addition, the vertical component of the mode-matched electric field of Equation (3) asymptotically passes to

$$E_{2z} \xrightarrow[\rho\to\infty]{} \left(\frac{q_{free}}{\varepsilon_o}\right)\sqrt{\frac{\gamma^3}{8\pi}}\,e^{-u_2 z}\,\frac{e^{-j(\gamma\rho-\pi/4)}}{\sqrt{\rho}}, \tag{23}$$

which is linearly proportional to free charge on the isolated component of the elevated charge terminal's capacitance at the terminal voltage, $q_{free} = C_{free} \times V_T$.

[0070] For example, the height H_1 of the elevated charge terminal T_1 in FIG. 3 affects the amount of free charge on the charge terminal T_1. When the charge terminal T_1 is near the ground plane of Region 1, most of the charge Q_1 on the terminal is "bound." As the charge terminal T_1 is elevated, the bound charge is lessened until the charge terminal T_1 reaches a height at which substantially all of the isolated charge is free.

[0071] The advantage of an increased capacitive elevation for the charge terminal T_1 is that the charge on the elevated charge terminal T_1 is further removed from the ground plane, resulting in an increased amount of free charge q_{free} to couple energy into the guided surface waveguide mode. As the charge terminal T_1 is moved away from the ground plane, the charge distribution becomes more uniformly distributed about the surface of the terminal. The amount of free charge is related to the self-capacitance of the charge terminal T_1.

[0072] For example, the capacitance of a spherical terminal can be expressed as a function of physical height above the ground plane. The capacitance of a sphere at a physical height of h above a perfect ground is given by

$$C_{\text{elevated sphere}} = 4\pi\varepsilon_o a(1 + M + M^2 + M^3 + 2M^4 + 3M^5 + \cdots), \qquad (24)$$

where the diameter of the sphere is $2a$, and where $M = a/2h$ with h being the height of the spherical terminal. As can be seen, an increase in the terminal height h reduces the capacitance C of the charge terminal. It can be shown that for elevations of the charge terminal T_1 that are at a height of about four times the diameter ($4D = 8a$) or greater, the charge distribution is approximately uniform about the spherical terminal, which can improve the coupling into the guided surface waveguide mode.

[0073] In the case of a sufficiently isolated terminal, the self-capacitance of a conductive sphere can be approximated by $C = 4\pi\varepsilon_o a$, where a is the radius of the sphere in meters, and the self-capacitance of a disk can be approximated by $C = 8\varepsilon_o a$, where a is the radius of the disk in meters. The charge terminal T_1 can include any shape such as a sphere, a disk, a cylinder, a cone, a torus, a hood, one or more rings, or any other randomized shape or combination of shapes. An equivalent spherical diameter can be determined and used for positioning of the charge terminal T_1.

[0074] This may be further understood with reference to the example of FIG. 3, where the charge terminal T_1 is elevated at a physical height of $h_p = H_1$ above the lossy conducting medium 203. To reduce the effects of the "bound" charge, the charge terminal T_1 can be positioned at a physical height that is at least four times the spherical diameter (or equivalent spherical diameter) of the charge terminal T_1 to reduce the bounded charge effects.

[0075] Referring next to FIG. 5A, shown is a ray optics interpretation of the electric field produced by the elevated charge Q_1 on charge terminal T_1 of FIG. 3. As in optics, minimizing the reflection of the incident electric field can improve and/or maximize the

energy coupled into the guided surface waveguide mode of the lossy conducting medium 203. For an electric field $(E_{\parallel})$ that is polarized parallel to the plane of incidence (not the boundary interface), the amount of reflection of the incident electric field may be determined using the Fresnel reflection coefficient, which can be expressed as

$$\Gamma_{\parallel}(\theta_i) = \frac{E_{\parallel,R}}{E_{\parallel,i}} = \frac{\sqrt{(\varepsilon_r - jx) - \sin^2\theta_i} - (\varepsilon_r - jx)\cos\theta_i}{\sqrt{(\varepsilon_r - jx) - \sin^2\theta_i} + (\varepsilon_r - jx)\cos\theta_i},\qquad(25)$$

where θ_i is the conventional angle of incidence measured with respect to the surface normal.

[0076]   In the example of FIG. 5A, the ray optic interpretation shows the incident field polarized parallel to the plane of incidence having an angle of incidence of θ_i, which is measured with respect to the surface normal $(\hat{z})$. There will be no reflection of the incident electric field when $\Gamma_{\parallel}(\theta_i) = 0$ and thus the incident electric field will be completely coupled into a guided surface waveguide mode along the surface of the lossy conducting medium 203. It can be seen that the numerator of Equation (25) goes to zero when the angle of incidence is

$$\theta_i = \arctan\left(\sqrt{\varepsilon_r - jx}\right) = \theta_{i,B},\qquad(26)$$

where $x = \sigma/\omega\varepsilon_o$. This complex angle of incidence $(\theta_{i,B})$ is referred to as the Brewster angle. Referring back to Equation (22), it can be seen that the same complex Brewster angle $(\theta_{i,B})$ relationship is present in both Equations (22) and (26).

[0077]   As illustrated in FIG. 5A, the electric field vector E can be depicted as an incoming non-uniform plane wave, polarized parallel to the plane of incidence. The electric field vector E can be created from independent horizontal and vertical components as

$$\vec{E}(\theta_i) = E_\rho\,\hat{\rho} + E_z\,\hat{z}.\qquad(27)$$

Geometrically, the illustration in FIG. 5A suggests that the electric field vector E can be given by

$$E_\rho(\rho,z) = E(\rho,z)\cos\theta_i,\ \text{and}\qquad(28a)$$

$$E_z(\rho,z) = E(\rho,z)\cos\left(\frac{\pi}{2} - \theta_i\right) = E(\rho,z)\sin\theta_i,\qquad(28b)$$

which means that the field ratio is

$$\frac{E_\rho}{E_z} = \frac{1}{\tan\theta_i} = \tan\psi_i.\qquad(29)$$

[0078]   A generalized parameter W, called "wave tilt," is noted herein as the ratio of the horizontal electric field component to the vertical electric field component given by

$$W = \frac{E_\rho}{E_z} = |W|e^{j\Psi},\ \text{or}\qquad(30a)$$

$$\frac{1}{W} = \frac{E_z}{E_\rho} = \tan\theta_i = \frac{1}{|W|}e^{-j\Psi},\qquad(30b)$$

which is complex and has both magnitude and phase. For an electromagnetic wave in Region 2, the wave tilt angle (Ψ) is equal to the angle between the normal of the wave-front at the boundary interface with Region 1 and the tangent to the boundary interface. This may be easier to see in FIG. 5B, which illustrates equi-phase surfaces of an electromagnetic wave and their normals for a radial cylindrical guided surface wave. At the boundary interface (z = 0) with a perfect conductor, the wave-front normal is parallel to the tangent of the boundary interface, resulting in W = 0. However, in the case of a lossy dielectric, a wave tilt W exists because the wave-front normal is not parallel with the tangent of the boundary interface at z = 0.

[0079] Applying Equation (30b) to a guided surface wave gives

$$\tan \theta_{i,B} = \frac{E_z}{E_\rho} = \frac{u_2}{\gamma} = \sqrt{\varepsilon_r - jx} = n = \frac{1}{W} = \frac{1}{|W|}e^{-j\Psi}. \tag{31}$$

With the angle of incidence equal to the complex Brewster angle ($\theta_{i,B}$), the Fresnel reflection coefficient of Equation (25) vanishes, as shown by

$$\Gamma_{\parallel}(\theta_{i,B}) = \left.\frac{\sqrt{(\varepsilon_r - jx) - \sin^2 \theta_i} - (\varepsilon_r - jx)\cos\theta_i}{\sqrt{(\varepsilon_r - jx) - \sin^2 \theta_i} + (\varepsilon_r - jx)\cos\theta_i}\right|_{\theta_i = \theta_{i,B}} = 0. \tag{32}$$

By adjusting the complex field ratio of Equation (22), an incident field can be synthesized to be incident at a complex angle at which the reflection is reduced or eliminated. Establishing this ratio as $n = \sqrt{\varepsilon_r - jx}$ results in the synthesized electric field being incident at the complex Brewster angle, making the reflections vanish.

[0080] The concept of an electrical effective height can provide further insight into synthesizing an electric field with a complex angle of incidence with a guided surface waveguide probe 200. The electrical effective height (h_{eff}) has been defined as

$$h_{eff} = \frac{1}{I_0} \int_0^{h_p} I(z)dz \tag{33}$$

for a monopole with a physical height (or length) of h_p. Since the expression depends upon the magnitude and phase of the source distribution along the structure, the effective height (or length) is complex in general. The integration of the distributed current $I(z)$ of the structure is performed over the physical height of the structure (h_p), and normalized to the ground current (I_0) flowing upward through the base (or input) of the structure. The distributed current along the structure can be expressed by

$$I(z) = I_C \cos(\beta_0 z), \tag{34}$$

where β_0 is the propagation factor for current propagating on the structure. In the example of FIG. 3, I_C is the current that is distributed along the vertical structure of the guided surface waveguide probe 200a.

[0081] For example, consider a feed network 209 that includes a low loss coil (e.g., a helical coil) at the bottom of the structure and a vertical feed line conductor connected

between the coil and the charge terminal T_1. The phase delay due to the coil (or helical delay line) is $\theta_c = \beta_p l_C$, with a physical length of l_C and a propagation factor of

$$\beta_p = \frac{2\pi}{\lambda_p} = \frac{2\pi}{V_f \lambda_0}, \qquad (35)$$

where V_f is the velocity factor on the structure, λ_0 is the wavelength at the supplied frequency, and λ_p is the propagation wavelength resulting from the velocity factor V_f. The phase delay is measured relative to the ground (stake) current I_0.

[0082]   In addition, the spatial phase delay along the length l_w of the vertical feed line conductor can be given by $\theta_y = \beta_w l_w$ where β_w is the propagation phase constant for the vertical feed line conductor.   In some implementations, the spatial phase delay may be approximated by $\theta_y = \beta_w h_p$, since the difference between the physical height h_p of the guided surface waveguide probe 200a and the vertical feed line conductor length l_w is much less than a wavelength at the supplied frequency (λ_0).   As a result, the total phase delay through the coil and vertical feed line conductor is $\Phi = \theta_c + \theta_y$, and the current fed to the top of the coil from the bottom of the physical structure is

$$I_C(\theta_c + \theta_y) = I_0 e^{j\Phi}, \qquad (36)$$

with the total phase delay Φ measured relative to the ground (stake) current I_0. Consequently, the electrical effective height of a guided surface waveguide probe 200 can be approximated by

$$h_{eff} = \frac{1}{I_0} \int_0^{h_p} I_0 e^{j\Phi} \cos(\beta_0 z)\, dz \cong h_p e^{j\Phi}, \qquad (37)$$

for the case where the physical height $h_p \ll \lambda_0$. The complex effective height of a monopole, $h_{eff} = h_p$ at an angle (or phase shift) of Φ, may be adjusted to cause the source fields to match a guided surface waveguide mode and cause a guided surface wave to be launched on the lossy conducting medium 203.

[0083]   In the example of FIG. 5A, ray optics are used to illustrate the complex angle trigonometry of the incident electric field (E) having a complex Brewster angle of incidence $(\theta_{i,B})$ at the Hankel crossover distance (R_x) 121.   Recall from Equation (26) that, for a lossy conducting medium, the Brewster angle is complex and specified by

$$\tan \theta_{i,B} = \sqrt{\varepsilon_r - j\frac{\sigma}{\omega\varepsilon_o}} = n . \qquad (38)$$

Electrically, the geometric parameters are related by the electrical effective height (h_{eff}) of the charge terminal T_1 by

$$R_x \tan \psi_{i,B} = R_x \times W = h_{eff} = h_p e^{j\Phi}, \qquad (39)$$

where $\psi_{i,B} = (\pi/2) - \theta_{i,B}$ is the Brewster angle measured from the surface of the lossy conducting medium.   To couple into the guided surface waveguide mode, the wave tilt of the

electric field at the Hankel crossover distance can be expressed as the ratio of the electrical effective height and the Hankel crossover distance

$$\frac{h_{eff}}{R_x} = \tan \psi_{i,B} = W_{Rx}. \tag{40}$$

Since both the physical height (h_p) and the Hankel crossover distance (R_x) are real quantities, the angle (Ψ) of the desired guided surface wave tilt at the Hankel crossover distance (R_x) is equal to the phase (Φ) of the complex effective height (h_{eff}). This implies that by varying the phase at the supply point of the coil, and thus the phase shift in Equation (37), the phase, Φ, of the complex effective height can be manipulated to match the angle of the wave tilt, Ψ, of the guided surface waveguide mode at the Hankel crossover point 121: $\Phi = \Psi$.

[0084]   In FIG. 5A, a right triangle is depicted having an adjacent side of length R_x along the lossy conducting medium surface and a complex Brewster angle $\psi_{i,B}$ measured between a ray 124 extending between the Hankel crossover point 121 at R_x and the center of the charge terminal T$_1$, and the lossy conducting medium surface 127 between the Hankel crossover point 121 and the charge terminal T$_1$. With the charge terminal T$_1$ positioned at physical height h_p and excited with a charge having the appropriate phase delay Φ, the resulting electric field is incident with the lossy conducting medium boundary interface at the Hankel crossover distance R_x, and at the Brewster angle. Under these conditions, the guided surface waveguide mode can be excited without reflection or substantially negligible reflection.

[0085]   If the physical height of the charge terminal T$_1$ is decreased without changing the phase shift Φ of the effective height (h_{eff}), the resulting electric field intersects the lossy conducting medium 203 at the Brewster angle at a reduced distance from the guided surface waveguide probe 200. FIG. 6 graphically illustrates the effect of decreasing the physical height of the charge terminal T$_1$ on the distance where the electric field is incident at the Brewster angle. As the height is decreased from h$_3$ through h$_2$ to h$_1$, the point where the electric field intersects with the lossy conducting medium (e.g., the Earth) at the Brewster angle moves closer to the charge terminal position. However, as Equation (39) indicates, the height H$_1$ (FIG. 3) of the charge terminal T$_1$ should be at or higher than the physical height (h_p) in order to excite the far-out component of the Hankel function. With the charge terminal T$_1$ positioned at or above the effective height (h_{eff}), the lossy conducting medium 203 can be illuminated at the Brewster angle of incidence ($\psi_{i,B} = (\pi/2) - \theta_{i,B}$) at or beyond the Hankel crossover distance (R_x) 121 as illustrated in FIG. 5A. To reduce or minimize the bound charge on the charge terminal T$_1$, the height should be at least four times the

spherical diameter (or equivalent spherical diameter) of the charge terminal T_1 as mentioned above.

[0086] A guided surface waveguide probe 200 can be configured to establish an electric field having a wave tilt that corresponds to a wave illuminating the surface of the lossy conducting medium 203 at a complex Brewster angle, thereby exciting radial surface currents by substantially mode-matching to a guided surface wave mode at (or beyond) the Hankel crossover point 121 at R_x.

[0087] Referring to FIG. 7, shown is a graphical representation of an example of a guided surface waveguide probe 200b that includes a charge terminal T_1. An AC source 212 acts as the excitation source for the charge terminal T_1, which is coupled to the guided surface waveguide probe 200b through a feed network 209 (FIG. 3) comprising a coil 215 such as, *e.g.*, a helical coil. In other implementations, the AC source 212 can be inductively coupled to the coil 215 through a primary coil. In some embodiments, an impedance matching network may be included to improve and/or maximize coupling of the AC source 212 to the coil 215.

[0088] As shown in FIG. 7, the guided surface waveguide probe 200b can include the upper charge terminal T_1 (*e.g.*, a sphere at height h_p) that is positioned along a vertical axis z that is substantially normal to the plane presented by the lossy conducting medium 203. A second medium 206 is located above the lossy conducting medium 203. The charge terminal T_1 has a self-capacitance C_T. During operation, charge Q_1 is imposed on the terminal T_1 depending on the voltage applied to the terminal T_1 at any given instant.

[0089] In the example of FIG. 7, the coil 215 is coupled to a ground stake 218 at a first end and to the charge terminal T_1 via a vertical feed line conductor 221. In some implementations, the coil connection to the charge terminal T_1 can be adjusted using a tap 224 of the coil 215 as shown in FIG. 7. The coil 215 can be energized at an operating frequency by the AC source 212 through a tap 227 at a lower portion of the coil 215. In other implementations, the AC source 212 can be inductively coupled to the coil 215 through a primary coil.

[0090] The construction and adjustment of the guided surface waveguide probe 200 is based upon various operating conditions, such as the transmission frequency, conditions of the lossy conducting medium (*e.g.*, soil conductivity σ and relative permittivity ε_r), and size of the charge terminal T_1. The index of refraction can be calculated from Equations (10) and (11) as

$$n = \sqrt{\varepsilon_r - jx}, \qquad\qquad (41)$$

where $x = \sigma/\omega\varepsilon_o$ with $\omega = 2\pi f$. The conductivity σ and relative permittivity ε_r can be determined through test measurements of the lossy conducting medium 203. The complex

Brewster angle $(\theta_{i,B})$ measured from the surface normal can also be determined from Equation (26) as

$$\theta_{i,B} = \arctan\left(\sqrt{\varepsilon_r - jx}\right),\tag{42}$$

or measured from the surface as shown in FIG. 5A as

$$\psi_{i,B} = \frac{\pi}{2} - \theta_{i,B}.\tag{43}$$

The wave tilt at the Hankel crossover distance (W_{Rx}) can also be found using Equation (40).

[0091]   The Hankel crossover distance can also be found by equating the magnitudes of Equations (20b) and (21) for $-j\gamma\rho$, and solving for R_x as illustrated by FIG. 4. The electrical effective height can then be determined from Equation (39) using the Hankel crossover distance and the complex Brewster angle as

$$h_{eff} = h_p e^{j\Phi} = R_x \tan \psi_{i,B}.\tag{44}$$

As can be seen from Equation (44), the complex effective height (h_{eff}) includes a magnitude that is associated with the physical height (h_p) of the charge terminal T₁ and a phase delay (Φ) that is to be associated with the angle (Ψ) of the wave tilt at the Hankel crossover distance (R_x). With these variables and the selected charge terminal T₁ configuration, it is possible to determine the configuration of a guided surface waveguide probe 200.

[0092]   With the charge terminal T₁ positioned at or above the physical height (h_p), the feed network 209 (FIG. 3) and/or the vertical feed line connecting the feed network to the charge terminal T₁ can be adjusted to match the phase (Φ) of the charge Q₁ on the charge terminal T₁ to the angle (Ψ) of the wave tilt (W). The size of the charge terminal T₁ can be chosen to provide a sufficiently large surface for the charge Q₁ imposed on the terminals. In general, it is desirable to make the charge terminal T₁ as large as practical. The size of the charge terminal T₁ should be large enough to avoid ionization of the surrounding air, which can result in electrical discharge or sparking around the charge terminal.

[0093]   The phase delay θ_c of a helically-wound coil can be determined from Maxwell's equations as has been discussed by Corum, K.L. and J.F. Corum, "RF Coils, Helical Resonators and Voltage Magnification by Coherent Spatial Modes," Microwave Review, Vol. 7, No. 2, September 2001, pp. 36-45., which is incorporated herein by reference in its entirety. For a helical coil with $H/D > 1$, the ratio of the velocity of propagation (v) of a wave along the coil's longitudinal axis to the speed of light (c), or the "velocity factor," is given by

$$V_f = \frac{v}{c} = \frac{1}{\sqrt{1 + 20\left(\frac{D}{s}\right)^{2.5}\left(\frac{D}{\lambda_o}\right)^{0.5}}},\tag{45}$$

where H is the axial length of the solenoidal helix, D is the coil diameter, N is the number of turns of the coil, $s = H/N$ is the turn-to-turn spacing (or helix pitch) of the coil, and λ_o is the

free-space wavelength. Based upon this relationship, the electrical length, or phase delay, of the helical coil is given by

$$\theta_c = \beta_p H = \frac{2\pi}{\lambda_p} H = \frac{2\pi}{V_f \lambda_0} H. \tag{46}$$

The principle is the same if the helix is wound spirally or is short and fat, but V_f and θ_c are easier to obtain by experimental measurement. The expression for the characteristic (wave) impedance of a helical transmission line has also been derived as

$$Z_c = \frac{60}{V_f}\left[\ell n \left(\frac{V_f \lambda_0}{D}\right) - 1.027\right]. \tag{47}$$

[0094] The spatial phase delay θ_y of the structure can be determined using the traveling wave phase delay of the vertical feed line conductor 221 (FIG. 7). The capacitance of a cylindrical vertical conductor above a prefect ground plane can be expressed as

$$C_A = \frac{2\pi\varepsilon_0 h_w}{\ell n\left(\frac{h}{a}\right) - 1} \text{ Farads,} \tag{48}$$

where h_w is the vertical length (or height) of the conductor and a is the radius (in mks units). As with the helical coil, the traveling wave phase delay of the vertical feed line conductor can be given by

$$\theta_y = \beta_w h_w = \frac{2\pi}{\lambda_w} h_w = \frac{2\pi}{V_w \lambda_0} h_w, \tag{49}$$

where β_w is the propagation phase constant for the vertical feed line conductor, h_w is the vertical length (or height) of the vertical feed line conductor, V_w is the velocity factor on the wire, λ_0 is the wavelength at the supplied frequency, and λ_w is the propagation wavelength resulting from the velocity factor V_w. For a uniform cylindrical conductor, the velocity factor is a constant with $V_w \approx 0.94$, or in a range from about 0.93 to about 0.98. If the mast is considered to be a uniform transmission line, its average characteristic impedance can be approximated by

$$Z_w = \frac{60}{V_w}\left[\ell n \left(\frac{h_w}{a}\right) - 1\right], \tag{50}$$

where $V_w \approx 0.94$ for a uniform cylindrical conductor and a is the radius of the conductor. An alternative expression that has been employed in amateur radio literature for the characteristic impedance of a single-wire feed line can be given by

$$Z_w = 138 \log\left(\frac{1.123 \, V_w \lambda_0}{2\pi a}\right). \tag{51}$$

Equation (51) implies that Z_w for a single-wire feeder varies with frequency. The phase delay can be determined based upon the capacitance and characteristic impedance.

[0095] With a charge terminal T_1 positioned over the lossy conducting medium 203 as shown in FIG. 3, the feed network 209 can be adjusted to excite the charge terminal T_1 with the phase shift (Φ) of the complex effective height (h_{eff}) equal to the angle (Ψ) of the wave tilt at the Hankel crossover distance, or $\Phi = \Psi$. When this condition is met, the electric field

produced by the charge oscillating Q_1 on the charge terminal T_1 is coupled into a guided surface waveguide mode traveling along the surface of a lossy conducting medium 203. For example, if the Brewster angle $(\theta_{i,B})$, the phase delay (θ_y) associated with the vertical feed line conductor 221 (FIG. 7), and the configuration of the coil 215 (FIG. 7) are known, then the position of the tap 224 (FIG. 7) can be determined and adjusted to impose an oscillating charge Q_1 on the charge terminal T_1 with phase $\Phi = \Psi$. The position of the tap 224 may be adjusted to maximize coupling the traveling surface waves into the guided surface waveguide mode. Excess coil length beyond the position of the tap 224 can be removed to reduce the capacitive effects. The vertical wire height and/or the geometrical parameters of the helical coil may also be varied.

[0096] The coupling to the guided surface waveguide mode on the surface of the lossy conducting medium 203 can be improved and/or optimized by tuning the guided surface waveguide probe 200 for standing wave resonance with respect to a complex image plane associated with the charge Q_1 on the charge terminal T_1. By doing this, the performance of the guided surface waveguide probe 200 can be adjusted for increased and/or maximum voltage (and thus charge Q_1) on the charge terminal T_1. Referring back to FIG. 3, the effect of the lossy conducting medium 203 in Region 1 can be examined using image theory analysis.

[0097] Physically, an elevated charge Q_1 placed over a perfectly conducting plane attracts the free charge on the perfectly conducting plane, which then "piles up" in the region under the elevated charge Q_1. The resulting distribution of "bound" electricity on the perfectly conducting plane is similar to a bell-shaped curve. The superposition of the potential of the elevated charge Q_1, plus the potential of the induced "piled up" charge beneath it, forces a zero equipotential surface for the perfectly conducting plane. The boundary value problem solution that describes the fields in the region above the perfectly conducting plane may be obtained using the classical notion of image charges, where the field from the elevated charge is superimposed with the field from a corresponding "image" charge below the perfectly conducting plane.

[0098] This analysis may also be used with respect to a lossy conducting medium 203 by assuming the presence of an effective image charge Q_1' beneath the guided surface waveguide probe 200. The effective image charge Q_1' coincides with the charge Q_1 on the charge terminal T_1 about a conducting image ground plane 130, as illustrated in FIG. 3. However, the image charge Q_1' is not merely located at some real depth and 180° out of phase with the primary source charge Q_1 on the charge terminal T_1, as they would be in the case of a perfect conductor. Rather, the lossy conducting medium 203 (e.g., a terrestrial medium) presents a *phase shifted* image. That is to say, the image charge Q_1' is at a

complex depth below the surface (or physical boundary) of the lossy conducting medium 203. For a discussion of complex image depth, reference is made to Wait, J. R., "Complex Image Theory—Revisited," IEEE Antennas and Propagation Magazine, Vol. 33, No. 4, August 1991, pp. 27-29, which is incorporated herein by reference in its entirety.

[0099]   Instead of the image charge Q_1' being at a depth that is equal to the physical height (H_1) of the charge Q_1, the conducting image ground plane 130 (representing a perfect conductor) is located at a complex depth of $z = -d/2$ and the image charge Q_1' appears at a complex depth (i.e., the "depth" has both magnitude and phase), given by $-D_1 = -(d/2 + d/2 + H_1) \neq H_1$. For vertically polarized sources over the Earth,

$$d = \frac{2\sqrt{\gamma_e^2 + k_0^2}}{\gamma_e^2} \approx \frac{2}{\gamma_e} = d_r + jd_i = |d|\angle\zeta ,   \tag{52}$$

where

$$\gamma_e^2 = j\omega\mu_1\sigma_1 - \omega^2\mu_1\varepsilon_1, \text{and}   \tag{53}$$

$$k_o = \omega\sqrt{\mu_o\varepsilon_o},   \tag{54}$$

as indicated in Equation (12). The complex spacing of the image charge, in turn, implies that the external field will experience *extra phase shifts* not encountered when the interface is either a dielectric or a perfect conductor. In the lossy conducting medium, the wave front normal is parallel to the tangent of the conducting image ground plane 130 at $z = -d/2$, and not at the boundary interface between Regions 1 and 2.

[0100]   Consider the case illustrated in FIG. 8A where the lossy conducting medium 203 is a finitely conducting Earth 133 with a physical boundary 136. The *finitely* conducting Earth 133 may be replaced by a *perfectly* conducting image ground plane 139 as shown in FIG.8B, which is located at a complex depth z_1 below the physical boundary 136. This equivalent representation exhibits the *same* impedance when looking down into the interface at the physical boundary 136. The equivalent representation of FIG. 8B can be modeled as an equivalent transmission line, as shown in FIG. 8C. The cross-section of the equivalent structure is represented as a (z-directed) end-loaded transmission line, with the impedance of the perfectly conducting image plane being a short circuit ($z_s = 0$). The depth z_1 can be determined by equating the TEM wave impedance looking down at the Earth to an image ground plane impedance z_{in} seen looking into the transmission line of FIG. 8C.

[0101]   In the case of FIG. 8A, the propagation constant and wave intrinsic impedance in the upper region (air) 142 are

$$\gamma_o = j\omega\sqrt{\mu_o\varepsilon_o} = 0 + j\beta_o , \text{and}   \tag{55}$$

$$z_o = \frac{j\omega\mu_o}{\gamma_o} = \sqrt{\frac{\mu_o}{\varepsilon_o}}.   \tag{56}$$

In the lossy Earth 133, the propagation constant and wave intrinsic impedance are

$$\gamma_e = \sqrt{j\omega\mu_1(\sigma_1 + j\omega\varepsilon_1)} \text{ , and} \tag{57}$$

$$Z_e = \frac{j\omega\mu_1}{\gamma_e}. \tag{58}$$

For normal incidence, the equivalent representation of FIG. 8B is equivalent to a TEM transmission line whose characteristic impedance is that of air (z_o), with propagation constant of γ_o, and whose length is z_1. As such, the image ground plane impedance Z_{in} seen at the interface for the shorted transmission line of FIG. 8C is given by

$$Z_{in} = Z_o \tanh(\gamma_o z_1). \tag{59}$$

Equating the image ground plane impedance Z_{in} associated with the equivalent model of FIG. 8C to the normal incidence wave impedance of FIG. 8A and solving for z_1 gives the distance to a short circuit (the *perfectly conducting* image ground plane 139) as

$$z_1 = \frac{1}{\gamma_o}\tanh^{-1}\left(\frac{Z_e}{Z_o}\right) = \frac{1}{\gamma_o}\tanh^{-1}\left(\frac{\gamma_o}{\gamma_e}\right) \approx \frac{1}{\gamma_e}, \tag{60}$$

where only the first term of the series expansion for the inverse hyperbolic tangent is considered for this approximation. Note that in the air region 142, the propagation constant is $\gamma_o = j\beta_o$, so $Z_{in} = jZ_o \tan\beta_o z_1$ (which is a purely imaginary quantity for a real z_1), but z_e is a complex value if $\sigma \neq 0$. Therefore, $Z_{in} = Z_e$ only when z_1 is a *complex distance*.

[0102] Since the equivalent representation of FIG. 8B includes a *perfectly conducting* image ground plane 139, the image depth for a charge or current *lying at the surface of the Earth* (physical boundary 136) is equal to distance z_1 on the other side of the image ground plane 139, or $d = 2 \times z_1$ beneath the Earth's surface (which is located at $z = 0$). Thus, the distance to the perfectly conducting image ground plane 139 can be approximated by

$$d = 2z_1 \approx \frac{2}{\gamma_e}. \tag{61}$$

Additionally, the "image charge" will be *"equal and opposite"* to the real charge, so the potential of the perfectly conducting image ground plane 139 at depth $z_1 = -d/2$ will be zero.

[0103] If a charge Q_1 is elevated a distance H_1 above the surface of the Earth as illustrated in FIG. 3, then the image charge Q_1' resides at a complex distance of $D_1 = d + H_1$ below the surface, or a complex distance of $d/2 + H_1$ below the image ground plane 130. The guided surface waveguide probe 200b of FIG. 7 can be modeled as an equivalent single-wire transmission line image plane model that can be based upon the perfectly conducting image ground plane 139 of FIG. 8B. FIG. 9A shows an example of the equivalent single-wire transmission line image plane model, and FIG. 9B illustrates an example of the equivalent classic transmission line model, including the shorted transmission line of FIG. 8C.

[0104] In the equivalent image plane models of FIGS. 9A and 9B, $\Phi = \theta_y + \theta_c$ is the traveling wave phase delay of the guided surface waveguide probe 200 referenced to Earth

133 (or the lossy conducting medium 203), $\theta_c = \beta_p H$ is the electrical length of the coil 215 (FIG. 7), of physical length H, expressed in degrees, $\theta_y = \beta_w h_w$ is the electrical length of the vertical feed line conductor 221 (FIG. 7), of physical length h_w, expressed in degrees, and $\theta_d = \beta_o d/2$ is the phase shift between the image ground plane 139 and the physical boundary 136 of the Earth 133 (or lossy conducting medium 203). In the example of FIGS. 9A and 9B, Z_w is the characteristic impedance of the elevated vertical feed line conductor 221 in ohms, Z_c is the characteristic impedance of the coil 215 in ohms, and Z_O is the characteristic impedance of free space.

[0105] At the base of the guided surface waveguide probe 200, the impedance seen "looking up" into the structure is $Z_\uparrow = Z_{base}$. With a load impedance of:

$$Z_L = \frac{1}{j\omega C_T},\qquad(62)$$

where C_T is the self-capacitance of the charge terminal T$_1$, the impedance seen "looking up" into the vertical feed line conductor 221 (FIG. 7) is given by:

$$Z_2 = Z_W \frac{Z_L + Z_w \tanh(j\beta_w h_w)}{Z_w + Z_L \tanh(j\beta_w h_w)} = Z_W \frac{Z_L + Z_w \tanh(j\theta_y)}{Z_w + Z_L \tanh(j\theta_y)},\qquad(63)$$

and the impedance seen "looking up" into the coil 215 (FIG. 7) is given by:

$$Z_{base} = Z_c \frac{Z_2 + Z_c \tanh(j\beta_p H)}{Z_c + Z_2 \tanh(j\beta_p H)} = Z_c \frac{Z_2 + Z_c \tanh(j\theta_c)}{Z_c + Z_2 \tanh(j\theta_c)}.\qquad(64)$$

At the base of the guided surface waveguide probe 200, the impedance seen "looking down" into the lossy conducting medium 203 is $Z_\downarrow = Z_{in}$, which is given by:

$$Z_{in} = Z_o \frac{Z_s + Z_o \tanh[j\beta_o(d/2)]}{Z_o + Z_s \tanh[j\beta_o(d/2)]} = Z_o \tanh(j\theta_d),\qquad(65)$$

where $Z_s = 0$.

[0106] Neglecting losses, the equivalent image plane model can be tuned to resonance when $Z_\downarrow + Z_\uparrow = 0$ at the physical boundary 136. Or, in the low loss case, $X_\downarrow + X_\uparrow = 0$ at the physical boundary 136, where X is the corresponding reactive component. Thus, the impedance at the physical boundary 136 "looking up" into the guided surface waveguide probe 200 is the conjugate of the impedance at the physical boundary 136 "looking down" into the lossy conducting medium 203. By adjusting the load impedance Z_L of the charge terminal T$_1$ while maintaining the traveling wave phase delay Φ equal to the angle of the media's wave tilt Ψ, so that $\Phi = \Psi$, which improves and/or maximizes coupling of the probe's electric field to a guided surface waveguide mode along the surface of the lossy conducting medium 203 (e.g., Earth), the equivalent image plane models of FIGS. 9A and 9B can be tuned to resonance with respect to the image ground plane 139. In this way, the impedance of the equivalent complex image plane model is purely resistive, which maintains a superposed standing wave on the probe structure that maximizes the voltage and elevated

charge on terminal T_1, and by equations (1)-(3) and (16) maximizes the propagating surface wave.

[0107]   It follows from the Hankel solutions, that the guided surface wave excited by the guided surface waveguide probe 200 is an outward propagating <u>traveling wave</u>. The source distribution along the feed network 209 between the charge terminal T_1 and the ground stake 218 of the guided surface waveguide probe 200 (FIGS. 3 and 7) is actually composed of a superposition of a <u>traveling wave</u> plus a <u>standing wave</u> on the structure. With the charge terminal T_1 positioned at or above the physical height h_p, the phase delay of the traveling wave moving through the feed network 209 is matched to the angle of the wave tilt associated with the lossy conducting medium 203. This mode-matching allows the traveling wave to be launched along the lossy conducting medium 203. Once the phase delay has been established for the traveling wave, the load impedance Z_L of the charge terminal T_1 is adjusted to bring the probe structure into standing wave resonance with respect to the image ground plane (130 of FIG. 3 or 139 of FIG. 8), which is at a complex depth of $-d/2$. In that case, the impedance seen from the image ground plane has zero reactance and the charge on the charge terminal T_1 is maximized.

[0108]   The distinction between the traveling wave phenomenon and standing wave phenomena is that (1) the phase delay of traveling waves $(\theta = \beta d)$ on a section of transmission line of length d (sometimes called a "delay line") is due to propagation time delays; whereas (2) the position-dependent phase of standing waves (which are composed of forward and backward propagating waves) depends on <u>both</u> the line length propagation time delay <u>and</u> impedance transitions at interfaces between line sections of different characteristic impedances. In <u>addition</u> to the phase delay that arises due to the physical length of a section of transmission line operating in sinusoidal steady-state, there is an extra reflection coefficient phase at impedance discontinuities that is due to the ratio of Z_{oa}/Z_{ob}, where Z_{oa} and Z_{ob} are the characteristic impedances of two sections of a transmission line such as, e.g., a helical coil section of characteristic impedance $Z_{oa} = Z_c$ (FIG. 9B) and a straight section of vertical feed line conductor of characteristic impedance $Z_{ob} = Z_w$ (FIG. 9B).

[0109]   As a result of this phenomenon, two *relatively short* transmission line sections of widely differing characteristic impedance may be used to provide a *very large* phase shift. For example, a probe structure composed of two sections of transmission line, one of low impedance and one of high impedance, together totaling a physical length of, say, 0.05 λ, may be fabricated to provide a phase shift of 90° which is equivalent to a 0.25 λ resonance. This is due to the large jump in characteristic impedances. In this way, a physically short probe structure can be electrically longer than the two physical lengths combined. This is

illustrated in FIGS. 9A and 9B, where the discontinuities in the impedance ratios provide large jumps in phase. The impedance discontinuity provides a substantial phase shift where the sections are joined together.

[0110]   Referring to FIG. 10, shown is a flow chart 150 illustrating an example of adjusting a guided surface waveguide probe 200 (FIGS. 3 and 7) to substantially mode-match to a guided surface waveguide mode on the surface of the lossy conducting medium, which launches a guided surface traveling wave along the surface of a lossy conducting medium 203 (FIG. 3). Beginning with 153, the charge terminal T_1 of the guided surface waveguide probe 200 is positioned at a defined height above a lossy conducting medium 203. Utilizing the characteristics of the lossy conducting medium 203 and the operating frequency of the guided surface waveguide probe 200, the Hankel crossover distance can also be found by equating the magnitudes of Equations (20b) and (21) for $-j\gamma\rho$, and solving for R_x as illustrated by FIG. 4. The complex index of refraction (n) can be determined using Equation (41), and the complex Brewster angle $(\theta_{i,B})$ can then be determined from Equation (42). The physical height (h_p) of the charge terminal T_1 can then be determined from Equation (44). The charge terminal T_1 should be at or higher than the physical height (h_p) in order to excite the far-out component of the Hankel function. This height relationship is initially considered when launching surface waves. To reduce or minimize the bound charge on the charge terminal T_1, the height should be at least four times the spherical diameter (or equivalent spherical diameter) of the charge terminal T_1.

[0111]   At 156, the electrical phase delay Φ of the elevated charge Q_1 on the charge terminal T_1 is matched to the complex wave tilt angle Ψ. The phase delay (θ_c) of the helical coil and/or the phase delay (θ_y) of the vertical feed line conductor can be adjusted to make Φ equal to the angle (Ψ) of the wave tilt (W). Based on Equation (31), the angle (Ψ) of the wave tilt can be determined from:

$$W = \frac{E_\rho}{E_z} = \frac{1}{\tan\theta_{i,B}} = \frac{1}{n} = |W|e^{j\Psi}. \qquad (66)$$

The electrical phase Φ can then be matched to the angle of the wave tilt. This angular (or phase) relationship is next considered when launching surface waves. For example, the electrical phase delay $\Phi = \theta_c + \theta_y$ can be adjusted by varying the geometrical parameters of the coil 215 (FIG. 7) and/or the length (or height) of the vertical feed line conductor 221 (FIG. 7). By matching $\Phi = \Psi$, an electric field can be established at or beyond the Hankel crossover distance (R_x) with a complex Brewster angle at the boundary interface to excite the surface waveguide mode and launch a traveling wave along the lossy conducting medium 203.

[0112]   Next at 159, the load impedance of the charge terminal T$_1$ is tuned to resonate the equivalent image plane model of the guided surface waveguide probe 200. The depth $(d/2)$ of the conducting image ground plane 139 of FIG. 9A and 9B (or 130 of FIG. 3) can be determined using Equations (52), (53) and (54) and the values of the lossy conducting medium 203 (e.g., the Earth), which can be measured. Using that depth, the phase shift (θ_d) between the image ground plane 139 and the physical boundary 136 of the lossy conducting medium 203 can be determined using $\theta_d = \beta_o \, d/2$. The impedance (Z_{in}) as seen "looking down" into the lossy conducting medium 203 can then be determined using Equation (65). This resonance relationship can be considered to maximize the launched surface waves.

[0113]   Based upon the adjusted parameters of the coil 215 and the length of the vertical feed line conductor 221, the velocity factor, phase delay, and impedance of the coil 215 and vertical feed line conductor 221 can be determined using Equations (45) through (51). In addition, the self-capacitance (C_T) of the charge terminal T$_1$ can be determined using, e.g., Equation (24). The propagation factor (β_p) of the coil 215 can be determined using Equation (35) and the propagation phase constant (β_w) for the vertical feed line conductor 221 can be determined using Equation (49). Using the self-capacitance and the determined values of the coil 215 and vertical feed line conductor 221, the impedance (Z_{base}) of the guided surface waveguide probe 200 as seen "looking up" into the coil 215 can be determined using Equations (62), (63) and (64).

[0114]   The equivalent image plane model of the guided surface waveguide probe 200 can be tuned to resonance by adjusting the load impedance Z_L such that the reactance component X_{base} of Z_{base} cancels out the reactance component X_{in} of Z_{in}, or $X_{base} + X_{in} = 0$. Thus, the impedance at the physical boundary 136 "looking up" into the guided surface waveguide probe 200 is the conjugate of the impedance at the physical boundary 136 "looking down" into the lossy conducting medium 203. The load impedance Z_L can be adjusted by varying the capacitance (C_T) of the charge terminal T$_1$ without changing the electrical phase delay $\Phi = \theta_c + \theta_y$ of the charge terminal T$_1$. An iterative approach may be taken to tune the load impedance Z_L for resonance of the equivalent image plane model with respect to the conducting image ground plane 139 (or 130). In this way, the coupling of the electric field to a guided surface waveguide mode along the surface of the lossy conducting medium 203 (e.g., Earth) can be improved and/or maximized.

[0115]   This may be better understood by illustrating the situation with a numerical example. Consider a guided surface waveguide probe 200 comprising a top-loaded vertical stub of physical height h_p with a charge terminal T$_1$ at the top, where the charge terminal T$_1$ is excited through a helical coil and vertical feed line conductor at an operational frequency (f_o) of 1.85 MHz. With a height (H$_1$) of 16 feet and the lossy conducting medium 203 (e.g.,

Earth) having a relative permittivity of $\varepsilon_r = 15$ and a conductivity of $\sigma_1 = 0.010$ mhos/m, several surface wave propagation parameters can be calculated for $f_o = 1.850$ MHz. Under these conditions, the Hankel crossover distance can be found to be $R_x = 54.5$ feet with a physical height of $h_p = 5.5$ feet, which is well below the actual height of the charge terminal T_1. While a charge terminal height of $H_1 = 5.5$ feet could have been used, the taller probe structure reduced the bound capacitance, permitting a greater percentage of free charge on the charge terminal T_1 providing greater field strength and excitation of the traveling wave.

[0116]   The wave length can be determined as:

$$\lambda_o = \frac{c}{f_o} = 162.162 \text{ meters,} \tag{67}$$

where c is the speed of light. The complex index of refraction is:

$$n = \sqrt{\varepsilon_r - jx} = 7.529 - j\,6.546, \tag{68}$$

from Equation (41), where $x = \sigma_1/\omega\varepsilon_o$ with $\omega = 2\pi f_o$, and the complex Brewster angle is:

$$\theta_{i,B} = \arctan\left(\sqrt{\varepsilon_r - jx}\right) = 85.6 - j\,3.744°. \tag{69}$$

from Equation (42). Using Equation (66), the wave tilt values can be determined to be:

$$W = \frac{1}{\tan\theta_{i,B}} = \frac{1}{n} = |W|e^{j\Psi} = 0.101e^{j40.614°}. \tag{70}$$

Thus, the helical coil can be adjusted to match $\Phi = \Psi = 40.614°$

[0117]   The velocity factor of the vertical feed line conductor (approximated as a uniform cylindrical conductor with a diameter of 0.27 inches) can be given as $V_w \approx 0.93$. Since $h_p \ll \lambda_o$, the propagation phase constant for the vertical feed line conductor can be approximated as:

$$\beta_w = \frac{2\pi}{\lambda_w} = \frac{2\pi}{V_w\lambda_0} = 0.042 \text{ m}^{-1}. \tag{71}$$

From Equation (49) the phase delay of the vertical feed line conductor is:

$$\theta_y = \beta_w h_w \approx \beta_w h_p = 11.640°. \tag{72}$$

By adjusting the phase delay of the helical coil so that $\theta_c = 28.974° = 40.614° - 11.640°$, Φ will equal Ψ to match the guided surface waveguide mode. To illustrate the relationship between Φ and Ψ, FIG. 11 shows a plot of both over a range of frequencies. As both Φ and Ψ are frequency dependent, it can be seen that their respective curves cross over each other at approximately 1.85 MHz.

[0118]   For a helical coil having a conductor diameter of 0.0881 inches, a coil diameter (D) of 30 inches and a turn-to-turn spacing (s) of 4 inches, the velocity factor for the coil can be determined using Equation (45) as:

$$V_f = \frac{1}{\sqrt{1+20\left(\frac{D}{s}\right)^{2.5}\left(\frac{D}{\lambda_o}\right)^{0.5}}} = 0.069 \;, \tag{73}$$

and the propagation factor from Equation (35) is:

$$\beta_p = \frac{2\pi}{V_f \lambda_0} = 0.564 \text{ m}^{-1}. \tag{74}$$

With $\theta_c = 28.974°$, the axial length of the solenoidal helix (H) can be determined using Equation (46) such that:

$$H = \frac{\theta_c}{\beta_p} = 35.2732 \text{ inches .} \tag{75}$$

This height determines the location on the helical coil where the vertical feed line conductor is connected, resulting in a coil with 8.818 turns ($N = H/s$).

[0119]   With the traveling wave phase delay of the coil and vertical feed line conductor adjusted to match the wave tilt angle ($\Phi = \theta_c + \theta_y = \Psi$), the load impedance ($Z_L$) of the charge terminal T_1 can be adjusted for standing wave resonance of the equivalent image plane model of the guided surface wave probe 200.   From the measured permittivity, conductivity and permeability of the Earth, the radial propagation constant can be determined using Equation (57)

$$\gamma_e = \sqrt{j\omega u_1(\sigma_1 + j\omega\varepsilon_1)} = 0.25 + j\, 0.292 \text{ m}^{-1}, \tag{76}$$

And the complex depth of the conducting image ground plane can be approximated from Equation (52) as:

$$d \approx \frac{2}{\gamma_e} = 3.364 + j\, 3.963 \text{ meters ,} \tag{77}$$

with a corresponding phase shift between the conducting image ground plane and the physical boundary of the Earth given by:

$$\theta_d = \beta_o(d/2) = 4.015 - j\, 4.73°. \tag{78}$$

Using Equation (65), the impedance seen "looking down" into the lossy conducting medium 203 (i.e., Earth) can be determined as:

$$Z_{in} = Z_o \tanh(j\theta_d) = R_{in} + jX_{in} = 31.191 + j\, 26.27 \text{ ohms.} \tag{79}$$

[0120]   By matching the reactive component (X_{in}) seen "looking down" into the lossy conducting medium 203 with the reactive component (X_{base}) seen "looking up" into the guided surface wave probe 200, the coupling into the guided surface waveguide mode may be maximized.   This can be accomplished by adjusting the capacitance of the charge terminal T_1 without changing the traveling wave phase delays of the coil and vertical feed line conductor.   For example, by adjusting the charge terminal capacitance (C_T) to 61.8126 pF, the load impedance from Equation (62) is:

$$Z_L = \frac{1}{j\omega C_T} = -j\, 1392 \text{ ohms,} \tag{80}$$

and the reactive components at the boundary are matched.

[0121]   Using Equation (51), the impedance of the vertical feed line conductor (having a diameter ($2a$) of 0.27 inches) is given as

$$Z_w = 138 \, log\left(\frac{1.123\, V_w \lambda_0}{2\pi a}\right) = 537.534 \text{ ohms,} \tag{81}$$

and the impedance seen "looking up" into the vertical feed line conductor is given by Equation (63) as:

$$Z_2 = Z_W \frac{Z_L + Z_w \tanh(j\theta_y)}{Z_w + Z_L \tanh(j\theta_y)} = -j\, 835.438 \text{ ohms.} \tag{82}$$

Using Equation (47), the characteristic impedance of the helical coil is given as

$$Z_c = \frac{60}{V_f}\left[\ell n\left(\frac{V_f \lambda_0}{D}\right) - 1.027\right] = 1446 \text{ ohms,} \tag{83}$$

and the impedance seen "looking up" into the coil at the base is given by Equation (64) as:

$$Z_{base} = Z_c \frac{Z_2 + Z_c \tanh(j\theta_c)}{Z_c + Z_2 \tanh(j\theta_c)} = -j\, 26.271 \text{ ohms.} \tag{84}$$

When compared to the solution of Equation (79), it can be seen that the reactive components are opposite and approximately equal, and thus are conjugates of each other. Thus, the impedance (Z_{ip}) seen "looking up" into the equivalent image plane model of FIGS. 9A and 9B from the perfectly conducting image ground plane is only resistive or $Z_{ip} = R + j0$.

[0122]   When the electric fields produced by a guided surface waveguide probe 200 (FIG. 3) are established by matching the traveling wave phase delay of the feed network to the wave tilt angle and the probe structure is resonated with respect to the perfectly conducting image ground plane at complex depth $z = -d/2$, the fields are substantially mode-matched to a guided surface waveguide mode on the surface of the lossy conducting medium, a guided surface traveling wave is launched along the surface of the lossy conducting medium.   As illustrated in FIG. 1, the guided field strength curve 103 of the guided electromagnetic field has a characteristic exponential decay of $e^{-\alpha d}/\sqrt{d}$ and exhibits a distinctive knee 109 on the log-log scale.

[0123]   In summary, both analytically and experimentally, the *traveling wave* component on the structure of the guided surface waveguide probe 200 has a phase delay (Φ) at its upper terminal that matches the angle (Ψ) of the wave tilt of the surface traveling wave (Φ = Ψ).   Under this condition, the surface waveguide may be considered to be "mode-matched".   Furthermore, the resonant *standing wave* component on the structure of the guided surface waveguide probe 200 has a V$_\text{MAX}$ at the charge terminal T$_1$ and a V$_\text{MIN}$ down at the image plane 139 (FIG. 8B) where $Z_{ip} = R_{ip} + j\,0$ at a complex depth of $z = -\text{d}/2$, not at the connection at the physical boundary 136 of the lossy conducting medium 203 (FIG. 8B).   Lastly, the charge terminal T$_1$ is of sufficient height H$_1$ of FIG. 3 ($h \geq R_x \tan\psi_{i,B}$) so that electromagnetic waves incident onto the lossy conducting medium 203 at the complex Brewster angle do so out at a distance ($\geq R_x$) where the $1/\sqrt{r}$ term is predominant.   Receive circuits can be utilized with one or more guided surface waveguide probes to facilitate wireless transmission and/or power delivery systems.

[0124] Referring back to FIG. 3, operation of a guided surface waveguide probe 200 may be controlled to adjust for variations in operational conditions associated with the guided surface waveguide probe 200. For example, an adaptive probe control system 230 can be used to control the feed network 209 and/or the charge terminal T_1 to control the operation of the guided surface waveguide probe 200. Operational conditions can include, but are not limited to, variations in the characteristics of the lossy conducting medium 203 (e.g., conductivity σ and relative permittivity ε_r), variations in field strength and/or variations in loading of the guided surface waveguide probe 200. As can be seen from Equations (31), (41) and (42), the index of refraction (n), the complex Brewster angle ($\theta_{i,B}$), and the wave tilt ($|W|e^{j\Psi}$) can be affected by changes in soil conductivity and permittivity resulting from, e.g., weather conditions.

[0125] Equipment such as, e.g., conductivity measurement probes, permittivity sensors, ground parameter meters, field meters, current monitors and/or load receivers can be used to monitor for changes in the operational conditions and provide information about current operational conditions to the adaptive probe control system 230. The probe control system 230 can then make one or more adjustments to the guided surface waveguide probe 200 to maintain specified operational conditions for the guided surface waveguide probe 200. For instance, as the moisture and temperature vary, the conductivity of the soil will also vary. Conductivity measurement probes and/or permittivity sensors may be located at multiple locations around the guided surface waveguide probe 200. Generally, it would be desirable to monitor the conductivity and/or permittivity at or about the Hankel crossover distance R_x for the operational frequency. Conductivity measurement probes and/or permittivity sensors may be located at multiple locations (e.g., in each quadrant) around the guided surface waveguide probe 200.

[0126] The conductivity measurement probes and/or permittivity sensors can be configured to evaluate the conductivity and/or permittivity on a periodic basis and communicate the information to the probe control system 230. The information may be communicated to the probe control system 230 through a network such as, but not limited to, a LAN, WLAN, cellular network, or other appropriate wired or wireless communication network. Based upon the monitored conductivity and/or permittivity, the probe control system 230 may evaluate the variation in the index of refraction (n), the complex Brewster angle ($\theta_{i,B}$), and/or the wave tilt ($|W|e^{j\Psi}$) and adjust the guided surface waveguide probe 200 to maintain the phase delay (Φ) of the feed network 209 equal to the wave tilt angle (Ψ) and/or maintain resonance of the equivalent image plane model of the guided surface waveguide probe 200. This can be accomplished by adjusting, e.g., θ_y, θ_c and/or C_T. For instance, the probe control system 230 can adjust the self-capacitance of the charge

terminal T_1 and/or the phase delay (θ_y, θ_c) applied to the charge terminal T_1 to maintain the electrical launching efficiency of the guided surface wave at or near its maximum. For example, the self-capacitance of the charge terminal T_1 can be varied by changing the size of the terminal. The charge distribution can also be improved by increasing the size of the charge terminal T_1, which can reduce the chance of an electrical discharge from the charge terminal T_1. In other embodiments, the charge terminal T_1 can include a variable inductance that can be adjusted to change the load impedance Z_L. The phase applied to the charge terminal T_1 can be adjusted by varying the tap position on the coil 215 (FIG. 7), and/or by including a plurality of predefined taps along the coil 215 and switching between the different predefined tap locations to maximize the launching efficiency.

[0127]   Field or field strength (FS) meters may also be distributed about the guided surface waveguide probe 200 to measure field strength of fields associated with the guided surface wave. The field or FS meters can be configured to detect the field strength and/or changes in the field strength (e.g., electric field strength) and communicate that information to the probe control system 230. The information may be communicated to the probe control system 230 through a network such as, but not limited to, a LAN, WLAN, cellular network, or other appropriate communication network. As the load and/or environmental conditions change or vary during operation, the guided surface waveguide probe 200 may be adjusted to maintain specified field strength(s) at the FS meter locations to ensure appropriate power transmission to the receivers and the loads they supply.

[0128]   For example, the phase delay ($\Phi = \theta_y + \theta_c$) applied to the charge terminal T_1 can be adjusted to match the wave tilt angle (Ψ). By adjusting one or both phase delays, the guided surface waveguide probe 200 can be adjusted to ensure the wave tilt corresponds to the complex Brewster angle. This can be accomplished by adjusting a tap position on the coil 215 (FIG. 7) to change the phase delay supplied to the charge terminal T_1. The voltage level supplied to the charge terminal T_1 can also be increased or decreased to adjust the electric field strength. This may be accomplished by adjusting the output voltage of the excitation source 212 or by adjusting or reconfiguring the feed network 209. For instance, the position of the tap 227 (FIG. 7) for the AC source 212 can be adjusted to increase the voltage seen by the charge terminal T_1. Maintaining field strength levels within predefined ranges can improve coupling by the receivers, reduce ground current losses, and avoid interference with transmissions from other guided surface waveguide probes 200.

[0129]   The probe control system 230 can be implemented with hardware, firmware, software executed by hardware, or a combination thereof. For example, the probe control system 230 can include processing circuitry including a processor and a memory, both of which can be coupled to a local interface such as, for example, a data bus with an

accompanying control/address bus as can be appreciated by those with ordinary skill in the art. A probe control application may be executed by the processor to adjust the operation of the guided surface waveguide probe 200 based upon monitored conditions. The probe control system 230 can also include one or more network interfaces for communicating with the various monitoring devices. Communications can be through a network such as, but not limited to, a LAN, WLAN, cellular network, or other appropriate communication network. The probe control system 230 may comprise, for example, a computer system such as a server, desktop computer, laptop, or other system with like capability.

[0130]   Referring back to the example of FIG. 5A, the complex angle trigonometry is shown for the ray optic interpretation of the incident electric field (E) of the charge terminal T_1 with a complex Brewster angle ($\theta_{i,B}$) at the Hankel crossover distance (R_x). Recall that, for a lossy conducting medium, the Brewster angle is complex and specified by equation (38). Electrically, the geometric parameters are related by the electrical effective height (h_{eff}) of the charge terminal T_1 by equation (39). Since both the physical height (h_p) and the Hankel crossover distance (R_x) are real quantities, the angle of the desired guided surface wave tilt at the Hankel crossover distance (W_{Rx}) is equal to the phase (Φ) of the complex effective height (h_{eff}). With the charge terminal T_1 positioned at the physical height h_p and excited with a charge having the appropriate phase Φ, the resulting electric field is incident with the lossy conducting medium boundary interface at the Hankel crossover distance R_x, and at the Brewster angle. Under these conditions, the guided surface waveguide mode can be excited without reflection or substantially negligible reflection.

[0131]   However, Equation (39) means that the physical height of the guided surface waveguide probe 200 can be relatively small. While this will excite the guided surface waveguide mode, this can result in an unduly large bound charge with little free charge. To compensate, the charge terminal T_1 can be raised to an appropriate elevation to increase the amount of free charge. As one example rule of thumb, the charge terminal T_1 can be positioned at an elevation of about 4-5 times (or more) the effective diameter of the charge terminal T_1. FIG. 6 illustrates the effect of raising the charge terminal T_1 above the physical height (h_p) shown in FIG. 5A. The increased elevation causes the distance at which the wave tilt is incident with the lossy conductive medium to move beyond the Hankel crossover point 121 (FIG. 5A). To improve coupling in the guided surface waveguide mode, and thus provide for a greater launching efficiency of the guided surface wave, a lower compensation terminal T_2 can be used to adjust the total effective height (h_{TE}) of the charge terminal T_1 such that the wave tilt at the Hankel crossover distance is at the Brewster angle.

[0132]   Referring to FIG. 12, shown is an example of a guided surface waveguide probe 200c that includes an elevated charge terminal T_1 and a lower compensation terminal T_2 that

are arranged along a vertical axis z that is normal to a plane presented by the lossy conducting medium 203. In this respect, the charge terminal T_1 is placed directly above the compensation terminal T_2 although it is possible that some other arrangement of two or more charge and/or compensation terminals T_N can be used. The guided surface waveguide probe 200c is disposed above a lossy conducting medium 203 according to an embodiment of the present disclosure. The lossy conducting medium 203 makes up Region 1 with a second medium 206 that makes up Region 2 sharing a boundary interface with the lossy conducting medium 203.

[0133]   The guided surface waveguide probe 200c includes a feed network 209 that couples an excitation source 212 to the charge terminal T_1 and the compensation terminal T_2. According to various embodiments, charges Q_1 and Q_2 can be imposed on the respective charge and compensation terminals T_1 and T_2, depending on the voltages applied to terminals T_1 and T_2 at any given instant. I_1 is the conduction current feeding the charge Q_1 on the charge terminal T_1 via the terminal lead, and I_2 is the conduction current feeding the charge Q_2 on the compensation terminal T_2 via the terminal lead.

[0134]   According to the embodiment of FIG. 12, the charge terminal T_1 is positioned over the lossy conducting medium 203 at a physical height H_1, and the compensation terminal T_2 is positioned directly below T_1 along the vertical axis z at a physical height H_2, where H_2 is less than H_1. The height h of the transmission structure may be calculated as h = H_1 - H_2. The charge terminal T_1 has an isolated (or self) capacitance C_1, and the compensation terminal T_2 has an isolated (or self) capacitance C_2. A mutual capacitance C_M can also exist between the terminals T_1 and T_2 depending on the distance therebetween. During operation, charges Q_1 and Q_2 are imposed on the charge terminal T_1 and the compensation terminal T_2, respectively, depending on the voltages applied to the charge terminal T_1 and the compensation terminal T_2 at any given instant.

[0135]   Referring next to FIG. 13, shown is a ray optics interpretation of the effects produced by the elevated charge Q_1 on charge terminal T_1 and compensation terminal T_2 of FIG. 12. With the charge terminal T_1 elevated to a height where the ray intersects with the lossy conductive medium at the Brewster angle at a distance greater than the Hankel crossover point 121 as illustrated by line 163, the compensation terminal T_2 can be used to adjust h_{TE} by compensating for the increased height. The effect of the compensation terminal T_2 is to reduce the electrical effective height of the guided surface waveguide probe (or effectively raise the lossy medium interface) such that the wave tilt at the Hankel crossover distance is at the Brewster angle as illustrated by line 166.

[0136]   The total effective height can be written as the superposition of an upper effective height (h_{UE}) associated with the charge terminal T$_1$ and a lower effective height (h_{LE}) associated with the compensation terminal T$_2$ such that

$$h_{TE} = h_{UE} + h_{LE} = h_p e^{j(\beta h_p + \Phi_U)} + h_d e^{j(\beta h_d + \Phi_L)} = R_x \times W, \qquad (85)$$

where Φ_U is the phase delay applied to the upper charge terminal T$_1$, Φ_L is the phase delay applied to the lower compensation terminal T$_2$, $\beta = 2\pi/\lambda_p$ is the propagation factor from Equation (35), h_p is the physical height of the charge terminal T$_1$ and h_d is the physical height of the compensation terminal T$_2$. If extra lead lengths are taken into consideration, they can be accounted for by adding the charge terminal lead length z to the physical height h_p of the charge terminal T$_1$ and the compensation terminal lead length y to the physical height h_d of the compensation terminal T$_2$ as shown in

$$h_{TE} = \left(h_p + z\right)e^{j(\beta(h_p+z)+\Phi_U)} + (h_d + y)e^{j(\beta(h_d+y)+\Phi_L)} = R_x \times W. \qquad (86)$$

The lower effective height can be used to adjust the total effective height (h_{TE}) to equal the complex effective height (h_{eff}) of FIG. 5A.

[0137]   Equations (85) or (86) can be used to determine the physical height of the lower disk of the compensation terminal T$_2$ and the phase angles to feed the terminals in order to obtain the desired wave tilt at the Hankel crossover distance. For example, Equation (86) can be rewritten as the phase shift applied to the charge terminal T$_1$ as a function of the compensation terminal height (h_d) to give

$$\Phi_U(h_d) = -\beta\left(h_p + z\right) - j \ln\left(\frac{R_x \times W - (h_d+y)e^{j(\beta h_d + \beta y + \Phi_L)}}{(h_p+z)}\right). \qquad (87)$$

[0138]   To determine the positioning of the compensation terminal T$_2$, the relationships discussed above can be utilized. First, the total effective height (h_{TE}) is the superposition of the complex effective height (h_{UE}) of the upper charge terminal T$_1$ and the complex effective height (h_{LE}) of the lower compensation terminal T$_2$ as expressed in Equation (86). Next, the tangent of the angle of incidence can be expressed geometrically as

$$\tan\psi_E = \frac{h_{TE}}{R_x}, \qquad (88)$$

which is equal to the definition of the wave tilt, W. Finally, given the desired Hankel crossover distance R_x, the h_{TE} can be adjusted to make the wave tilt of the incident ray match the complex Brewster angle at the Hankel crossover point 121. This can be accomplished by adjusting h_p, Φ_U, and/or h_d.

[0139]   These concepts may be better understood when discussed in the context of an example of a guided surface waveguide probe. Referring to FIG. 14, shown is a graphical representation of an example of a guided surface waveguide probe 200d including an upper charge terminal T$_1$ (e.g., a sphere at height h_T) and a lower compensation terminal T$_2$ (e.g.,

a disk at height h_d) that are positioned along a vertical axis z that is substantially normal to the plane presented by the lossy conducting medium 203. During operation, charges Q_1 and Q_2 are imposed on the charge and compensation terminals T_1 and T_2, respectively, depending on the voltages applied to the terminals T_1 and T_2 at any given instant.

[0140] An AC source 212 acts as the excitation source for the charge terminal T_1, which is coupled to the guided surface waveguide probe 200d through a feed network 209 comprising a coil 215 such as, e.g., a helical coil. The AC source 212 can be connected across a lower portion of the coil 215 through a tap 227, as shown in FIG. 14, or can be inductively coupled to the coil 215 by way of a primary coil. The coil 215 can be coupled to a ground stake 218 at a first end and the charge terminal T_1 at a second end. In some implementations, the connection to the charge terminal T_1 can be adjusted using a tap 224 at the second end of the coil 215. The compensation terminal T_2 is positioned above and substantially parallel with the lossy conducting medium 203 (e.g., the ground or Earth), and energized through a tap 233 coupled to the coil 215. An ammeter 236 located between the coil 215 and ground stake 218 can be used to provide an indication of the magnitude of the current flow (I_0) at the base of the guided surface waveguide probe. Alternatively, a current clamp may be used around the conductor coupled to the ground stake 218 to obtain an indication of the magnitude of the current flow (I_0).

[0141] In the example of FIG. 14, the coil 215 is coupled to a ground stake 218 at a first end and the charge terminal T_1 at a second end via a vertical feed line conductor 221. In some implementations, the connection to the charge terminal T_1 can be adjusted using a tap 224 at the second end of the coil 215 as shown in FIG. 14. The coil 215 can be energized at an operating frequency by the AC source 212 through a tap 227 at a lower portion of the coil 215. In other implementations, the AC source 212 can be inductively coupled to the coil 215 through a primary coil. The compensation terminal T_2 is energized through a tap 233 coupled to the coil 215. An ammeter 236 located between the coil 215 and ground stake 218 can be used to provide an indication of the magnitude of the current flow at the base of the guided surface waveguide probe 200d. Alternatively, a current clamp may be used around the conductor coupled to the ground stake 218 to obtain an indication of the magnitude of the current flow. The compensation terminal T_2 is positioned above and substantially parallel with the lossy conducting medium 203 (e.g., the ground).

[0142] In the example of FIG. 14, the connection to the charge terminal T_1 located on the coil 215 above the connection point of tap 233 for the compensation terminal T_2. Such an adjustment allows an increased voltage (and thus a higher charge Q_1) to be applied to the upper charge terminal T_1. In other embodiments, the connection points for the charge terminal T_1 and the compensation terminal T_2 can be reversed. It is possible to adjust the

total effective height (h_{TE}) of the guided surface waveguide probe 200d to excite an electric field having a guided surface wave tilt at the Hankel crossover distance R_x. The Hankel crossover distance can also be found by equating the magnitudes of equations (20b) and (21) for $-j\gamma\rho$, and solving for R_x as illustrated by FIG. 4. The index of refraction (n), the complex Brewster angle ($\theta_{i,B}$ and $\psi_{i,B}$), the wave tilt ($|W|e^{j\Psi}$) and the complex effective height ($h_{eff} = h_p e^{j\Phi}$) can be determined as described with respect to Equations (41) – (44) above.

[0143] With the selected charge terminal T₁ configuration, a spherical diameter (or the effective spherical diameter) can be determined. For example, if the charge terminal T₁ is not configured as a sphere, then the terminal configuration may be modeled as a spherical capacitance having an effective spherical diameter. The size of the charge terminal T₁ can be chosen to provide a sufficiently large surface for the charge Q₁ imposed on the terminals. In general, it is desirable to make the charge terminal T₁ as large as practical. The size of the charge terminal T₁ should be large enough to avoid ionization of the surrounding air, which can result in electrical discharge or sparking around the charge terminal. To reduce the amount of bound charge on the charge terminal T₁, the desired elevation to provide free charge on the charge terminal T₁ for launching a guided surface wave should be at least 4-5 times the effective spherical diameter above the lossy conductive medium (*e.g.*, the Earth). The compensation terminal T₂ can be used to adjust the total effective height (h_{TE}) of the guided surface waveguide probe 200d to excite an electric field having a guided surface wave tilt at R_x. The compensation terminal T₂ can be positioned below the charge terminal T₁ at $h_d = h_T - h_p$, where h_T is the total physical height of the charge terminal T₁. With the position of the compensation terminal T₂ fixed and the phase delay Φ_U applied to the upper charge terminal T₁, the phase delay Φ_L applied to the lower compensation terminal T₂ can be determined using the relationships of Equation (86), such that:

$$\Phi_U(h_d) = -\beta(h_d + y) - j \ln\left(\frac{R_x \times W - (h_p + z)e^{j(\beta h_p + \beta z + \Phi_L)}}{(h_d + y)}\right). \tag{89}$$

In alternative embodiments, the compensation terminal T₂ can be positioned at a height h_d where $\text{Im}\{\Phi_L\} = 0$. This is graphically illustrated in FIG. 15A, which shows plots 172 and 175 of the imaginary and real parts of Φ_U, respectively. The compensation terminal T₂ is positioned at a height h_d where $\text{Im}\{\Phi_U\} = 0$, as graphically illustrated in plot 172. At this fixed height, the coil phase Φ_U can be determined from $\text{Re}\{\Phi_U\}$, as graphically illustrated in plot 175.

[0144] With the AC source 212 coupled to the coil 215 (*e.g.*, at the 50Ω point to maximize coupling), the position of tap 233 may be adjusted for parallel resonance of the compensation terminal T₂ with at least a portion of the coil at the frequency of operation.

FIG. 15B shows a schematic diagram of the general electrical hookup of FIG. 14 in which V_1 is the voltage applied to the lower portion of the coil 215 from the AC source 212 through tap 227, V_2 is the voltage at tap 224 that is supplied to the upper charge terminal T_1, and V_3 is the voltage applied to the lower compensation terminal T_2 through tap 233. The resistances R_p and R_d represent the ground return resistances of the charge terminal T_1 and compensation terminal T_2, respectively. The charge and compensation terminals T_1 and T_2 may be configured as spheres, cylinders, toroids, rings, hoods, or any other combination of capacitive structures. The size of the charge and compensation terminals T_1 and T_2 can be chosen to provide a sufficiently large surface for the charges Q_1 and Q_2 imposed on the terminals. In general, it is desirable to make the charge terminal T_1 as large as practical. The size of the charge terminal T_1 should be large enough to avoid ionization of the surrounding air, which can result in electrical discharge or sparking around the charge terminal. The self-capacitance C_p and C_d of the charge and compensation terminals T_1 and T_2 respectively, can be determined using, for example, equation (24).

[0145]   As can be seen in FIG. 15B, a resonant circuit is formed by at least a portion of the inductance of the coil 215, the self-capacitance C_d of the compensation terminal T_2, and the ground return resistance R_d associated with the compensation terminal T_2. The parallel resonance can be established by adjusting the voltage V_3 applied to the compensation terminal T_2 (*e.g.*, by adjusting a tap 233 position on the coil 215) or by adjusting the height and/or size of the compensation terminal T_2 to adjust C_d. The position of the coil tap 233 can be adjusted for parallel resonance, which will result in the ground current through the ground stake 218 and through the ammeter 236 reaching a maximum point. After parallel resonance of the compensation terminal T_2 has been established, the position of the tap 227 for the AC source 212 can be adjusted to the 50Ω point on the coil 215.

[0146]   Voltage V_2 from the coil 215 can be applied to the charge terminal T_1, and the position of tap 224 can be adjusted such that the phase (Φ) of the total effective height (h_{TE}) approximately equals the angle of the guided surface wave tilt (W_{Rx}) at the Hankel crossover distance (R_x). The position of the coil tap 224 can be adjusted until this operating point is reached, which results in the ground current through the ammeter 236 increasing to a maximum. At this point, the resultant fields excited by the guided surface waveguide probe 200d are substantially mode-matched to a guided surface waveguide mode on the surface of the lossy conducting medium 203, resulting in the launching of a guided surface wave along the surface of the lossy conducting medium 203. This can be verified by measuring field strength along a radial extending from the guided surface waveguide probe 200.

[0147]   Resonance of the circuit including the compensation terminal T_2 may change with the attachment of the charge terminal T_1 and/or with adjustment of the voltage applied

to the charge terminal T$_1$ through tap 224. While adjusting the compensation terminal circuit for resonance aids the subsequent adjustment of the charge terminal connection, it is not necessary to establish the guided surface wave tilt (W_{Rx}) at the Hankel crossover distance (R_x). The system may be further adjusted to improve coupling by iteratively adjusting the position of the tap 227 for the AC source 212 to be at the 50Ω point on the coil 215 and adjusting the position of tap 233 to maximize the ground current through the ammeter 236. Resonance of the circuit including the compensation terminal T$_2$ may drift as the positions of taps 227 and 233 are adjusted, or when other components are attached to the coil 215.

[0148]   In other implementations, the voltage V$_2$ from the coil 215 can be applied to the charge terminal T$_1$, and the position of tap 233 can be adjusted such that the phase (Φ) of the total effective height (h_{TE}) approximately equals the angle (Ψ) of the guided surface wave tilt at R_x. The position of the coil tap 224 can be adjusted until the operating point is reached, resulting in the ground current through the ammeter 236 substantially reaching a maximum. The resultant fields are substantially mode-matched to a guided surface waveguide mode on the surface of the lossy conducting medium 203, and a guided surface wave is launched along the surface of the lossy conducting medium 203. This can be verified by measuring field strength along a radial extending from the guided surface waveguide probe 200. The system may be further adjusted to improve coupling by iteratively adjusting the position of the tap 227 for the AC source 212 to be at the 50Ω point on the coil 215 and adjusting the position of tap 224 and/or 233 to maximize the ground current through the ammeter 236.

[0149]   Referring back to FIG. 12, operation of a guided surface waveguide probe 200 may be controlled to adjust for variations in operational conditions associated with the guided surface waveguide probe 200. For example, a probe control system 230 can be used to control the feed network 209 and/or positioning of the charge terminal T$_1$ and/or compensation terminal T$_2$ to control the operation of the guided surface waveguide probe 200. Operational conditions can include, but are not limited to, variations in the characteristics of the lossy conducting medium 203 (e.g., conductivity σ and relative permittivity ε_r), variations in field strength and/or variations in loading of the guided surface waveguide probe 200. As can be seen from Equations (41) – (44), the index of refraction (n), the complex Brewster angle ($\theta_{i,B}$ and $\psi_{i,B}$), the wave tilt ($|W|e^{j\Psi}$) and the complex effective height ($h_{eff} = h_p e^{j\Phi}$) can be affected by changes in soil conductivity and permittivity resulting from, e.g., weather conditions.

[0150]   Equipment such as, e.g., conductivity measurement probes, permittivity sensors, ground parameter meters, field meters, current monitors and/or load receivers can be used to monitor for changes in the operational conditions and provide information about current

operational conditions to the probe control system 230. The probe control system 230 can then make one or more adjustments to the guided surface waveguide probe 200 to maintain specified operational conditions for the guided surface waveguide probe 200. For instance, as the moisture and temperature vary, the conductivity of the soil will also vary. Conductivity measurement probes and/or permittivity sensors may be located at multiple locations around the guided surface waveguide probe 200. Generally, it would be desirable to monitor the conductivity and/or permittivity at or about the Hankel crossover distance R_x for the operational frequency. Conductivity measurement probes and/or permittivity sensors may be located at multiple locations (e.g., in each quadrant) around the guided surface waveguide probe 200.

[0151] With reference then to FIG. 16, shown is an example of a guided surface waveguide probe 200e that includes a charge terminal T_1 and a charge terminal T_2 that are arranged along a vertical axis z. The guided surface waveguide probe 200e is disposed above a lossy conducting medium 203, which makes up Region 1. In addition, a second medium 206 shares a boundary interface with the lossy conducting medium 203 and makes up Region 2. The charge terminals T_1 and T_2 are positioned over the lossy conducting medium 203. The charge terminal T_1 is positioned at height H_1, and the charge terminal T_2 is positioned directly below T_1 along the vertical axis z at height H_2, where H_2 is less than H_1. The height h of the transmission structure presented by the guided surface waveguide probe 200e is h = $H_1 - H_2$. The guided surface waveguide probe 200e includes a feed network 209 that couples an excitation source 212 to the charge terminals T_1 and T_2.

[0152] The charge terminals T_1 and/or T_2 include a conductive mass that can hold an electrical charge, which may be sized to hold as much charge as practically possible. The charge terminal T_1 has a self-capacitance C_1, and the charge terminal T_2 has a self-capacitance C_2, which can be determined using, for example, equation (24). By virtue of the placement of the charge terminal T_1 directly above the charge terminal T_2, a mutual capacitance C_M is created between the charge terminals T_1 and T_2. Note that the charge terminals T_1 and T_2 need not be identical, but each can have a separate size and shape, and can include different conducting materials. Ultimately, the field strength of a guided surface wave launched by a guided surface waveguide probe 200e is directly proportional to the quantity of charge on the terminal T_1. The charge Q_1 is, in turn, proportional to the self-capacitance C_1 associated with the charge terminal T_1 since $Q_1 = C_1V$, where V is the voltage imposed on the charge terminal T_1.

[0153] When properly adjusted to operate at a predefined operating frequency, the guided surface waveguide probe 200e generates a guided surface wave along the surface of the lossy conducting medium 203. The excitation source 212 can generate electrical energy

at the predefined frequency that is applied to the guided surface waveguide probe 200e to excite the structure. When the electromagnetic fields generated by the guided surface waveguide probe 200e are substantially mode-matched with the lossy conducting medium 203, the electromagnetic fields substantially synthesize a wave front incident at a complex Brewster angle that results in little or no reflection. Thus, the surface waveguide probe 200e does not produce a radiated wave, but launches a guided surface traveling wave along the surface of a lossy conducting medium 203. The energy from the excitation source 212 can be transmitted as Zenneck surface currents to one or more receivers that are located within an effective transmission range of the guided surface waveguide probe 200e.

[0154] One can determine asymptotes of the radial Zenneck surface current $J_\rho(\rho)$ on the surface of the lossy conducting medium 203 to be $J_1(\rho)$ close-in and $J_2(\rho)$ far-out, where

$$\text{Close-in } (\rho < \lambda/8): J_\rho(\rho) \sim J_1 = \frac{I_1 + I_2}{2\pi\rho} + \frac{E_\rho^{QS}(Q_1) + E_\rho^{QS}(Q_2)}{Z_\rho}, \text{ and} \qquad (90)$$

$$\text{Far-out } (\rho \gg \lambda/8): J_\rho(\rho) \sim J_2 = \frac{j\gamma\omega Q_1}{4} \times \sqrt{\frac{2\gamma}{\pi}} \times \frac{e^{-(\alpha+j\beta)\rho}}{\sqrt{\rho}}. \qquad (91)$$

where I_1 is the conduction current feeding the charge Q_1 on the first charge terminal T_1, and I_2 is the conduction current feeding the charge Q_2 on the second charge terminal T_2. The charge Q_1 on the upper charge terminal T_1 is determined by $Q_1 = C_1 V_1$, where C_1 is the isolated capacitance of the charge terminal T_1. Note that there is a third component to J_1 set forth above given by $\left(E_\rho^{Q_1}\right)/Z_\rho$, which follows from the Leontovich boundary condition and is the radial current contribution in the lossy conducting medium 203 pumped by the quasi-static field of the elevated oscillating charge on the first charge terminal Q_1. The quantity $Z_\rho = j\omega\mu_o/\gamma_e$ is the radial impedance of the lossy conducting medium, where $\gamma_e = (j\omega\mu_1\sigma_1 - \omega^2\mu_1\varepsilon_1)^{1/2}$.

[0155] The asymptotes representing the radial current close-in and far-out as set forth by equations (90) and (91) are complex quantities. According to various embodiments, a physical surface current $\mathbf{J}(\rho)$, is synthesized to match as close as possible the current asymptotes in *magnitude* and *phase*. That is to say close-in, $|\mathbf{J}(\rho)|$ is to be tangent to $|J_1|$, and far-out $|\mathbf{J}(\rho)|$ is to be tangent to $|J_2|$. Also, according to the various embodiments, the phase of $\mathbf{J}(\rho)$ should transition from the phase of J_1 close-in to the phase of J_2 far-out.

[0156] In order to match the guided surface wave mode at the site of transmission to launch a guided surface wave, the phase of the surface current $|J_2|$ far-out should differ from the phase of the surface current $|J_1|$ close-in by the propagation phase corresponding to $e^{-j\beta(\rho_2-\rho_1)}$ plus a constant of approximately 45 degrees or 225 degrees. This is because there are two roots for $\sqrt{\gamma}$, one near $\pi/4$ and one near $5\pi/4$. The properly adjusted synthetic radial surface current is

$$J_\rho(\rho, \phi, 0) = \frac{I_o\gamma}{4} H_1^{(2)}(-j\gamma\rho).$$ (92)

Note that this is consistent with equation (17). By Maxwell's equations, such a $\mathbf{J}(\rho)$ surface current automatically creates fields that conform to

$$H_\phi = \frac{-\gamma I_o}{4} e^{-u_2 z} H_1^{(2)}(-j\gamma\rho),$$ (93)

$$E_\rho = \frac{-\gamma I_o}{4} \left(\frac{u_2}{j\omega\varepsilon_o}\right) e^{-u_2 z} H_1^{(2)}(-j\gamma\rho), \text{ and}$$ (94)

$$E_z = \frac{-\gamma I_o}{4} \left(\frac{-\gamma}{\omega\varepsilon_o}\right) e^{-u_2 z} H_0^{(2)}(-j\gamma\rho).$$ (95)

Thus, the difference in phase between the surface current $|J_2|$ far-out and the surface current $|J_1|$ close-in for the guided surface wave mode that is to be matched is due to the characteristics of the Hankel functions in equations (93)-(95), which are consistent with equations (1)-(3). It is of significance to recognize that the fields expressed by equations (1)-(6) and (17) and equations (92)-(95) have the nature of a *transmission line mode* bound to a lossy interface, *not radiation fields* that are associated with groundwave propagation.

[0157] In order to obtain the appropriate voltage magnitudes and phases for a given design of a guided surface waveguide probe 200e at a given location, an iterative approach may be used. Specifically, analysis may be performed of a given excitation and configuration of a guided surface waveguide probe 200e taking into account the feed currents to the terminals T_1 and T_2, the charges on the charge terminals T_1 and T_2, and their images in the lossy conducting medium 203 in order to determine the radial surface current density generated. This process may be performed iteratively until an optimal configuration and excitation for a given guided surface waveguide probe 200e is determined based on desired parameters. To aid in determining whether a given guided surface waveguide probe 200e is operating at an optimal level, a guided field strength curve 103 (FIG. 1) may be generated using equations (1)-(12) based on values for the conductivity of Region 1 (σ_1) and the permittivity of Region 1 (ε_1) at the location of the guided surface waveguide probe 200e. Such a guided field strength curve 103 can provide a benchmark for operation such that measured field strengths can be compared with the magnitudes indicated by the guided field strength curve 103 to determine if optimal transmission has been achieved.

[0158] In order to arrive at an optimized condition, various parameters associated with the guided surface waveguide probe 200e may be adjusted. One parameter that may be varied to adjust the guided surface waveguide probe 200e is the height of one or both of the charge terminals T_1 and/or T_2 relative to the surface of the lossy conducting medium 203. In addition, the distance or spacing between the charge terminals T_1 and T_2 may also be adjusted. In doing so, one may minimize or otherwise alter the mutual capacitance C_M or any bound capacitances between the charge terminals T_1 and T_2 and the lossy conducting medium 203 as can be appreciated. The size of the respective charge terminals T_1 and/or

T_2 can also be adjusted. By changing the size of the charge terminals T_1 and/or T_2, one will alter the respective self-capacitances C_1 and/or C_2, and the mutual capacitance C_M as can be appreciated.

[0159] Still further, another parameter that can be adjusted is the feed network 209 associated with the guided surface waveguide probe 200e. This may be accomplished by adjusting the size of the inductive and/or capacitive reactances that make up the feed network 209. For example, where such inductive reactances comprise coils, the number of turns on such coils may be adjusted. Ultimately, the adjustments to the feed network 209 can be made to alter the electrical length of the feed network 209, thereby affecting the voltage magnitudes and phases on the charge terminals T_1 and T_2.

[0160] Note that the iterations of transmission performed by making the various adjustments may be implemented by using computer models or by adjusting physical structures as can be appreciated. By making the above adjustments, one can create corresponding "close-in" surface current J_1 and "far-out" surface current J_2 that approximate the same currents $\mathbf{J}(\rho)$ of the guided surface wave mode specified in Equations (90) and (91) set forth above. In doing so, the resulting electromagnetic fields would be substantially or approximately mode-matched to a guided surface wave mode on the surface of the lossy conducting medium 203.

[0161] While not shown in the example of FIG. 16, operation of the guided surface waveguide probe 200e may be controlled to adjust for variations in operational conditions associated with the guided surface waveguide probe 200. For example, a probe control system 230 shown in FIG. 12 can be used to control the feed network 209 and/or positioning and/or size of the charge terminals T_1 and/or T_2 to control the operation of the guided surface waveguide probe 200e. Operational conditions can include, but are not limited to, variations in the characteristics of the lossy conducting medium 203 (*e.g.*, conductivity σ and relative permittivity ε_r), variations in field strength and/or variations in loading of the guided surface waveguide probe 200e.

[0162] Referring now to FIG. 17, shown is an example of the guided surface waveguide probe 200e of FIG. 16, denoted herein as guided surface waveguide probe 200f. The guided surface waveguide probe 200f includes the charge terminals T_1 and T_2 that are positioned along a vertical axis z that is substantially normal to the plane presented by the lossy conducting medium 203 (e.g., the Earth). The second medium 206 is above the lossy conducting medium 203. The charge terminal T_1 has a self-capacitance C_1, and the charge terminal T_2 has a self-capacitance C_2. During operation, charges Q_1 and Q_2 are imposed on the charge terminals T_1 and T_2, respectively, depending on the voltages applied to the charge terminals T_1 and T_2 at any given instant. A mutual capacitance C_M may exist

between the charge terminals T_1 and T_2 depending on the distance there between. In addition, bound capacitances may exist between the respective charge terminals T_1 and T_2 and the lossy conducting medium 203 depending on the heights of the respective charge terminals T_1 and T_2 with respect to the lossy conducting medium 203.

[0163]   The guided surface waveguide probe 200f includes a feed network 209 that comprises an inductive impedance comprising a coil L_{1a} having a pair of leads that are coupled to respective ones of the charge terminals T_1 and T_2. In one embodiment, the coil L_{1a} is specified to have an electrical length that is one-half ($\frac{1}{2}$) of the wavelength at the operating frequency of the guided surface waveguide probe 200f.

[0164]   While the electrical length of the coil L_{1a} is specified as approximately one-half (1/2) the wavelength at the operating frequency, it is understood that the coil L_{1a} may be specified with an electrical length at other values. According to one embodiment, the fact that the coil L_{1a} has an electrical length of approximately one-half the wavelength at the operating frequency provides for an advantage in that a maximum voltage differential is created on the charge terminals T_1 and T_2. Nonetheless, the length or diameter of the coil L_{1a} may be increased or decreased when adjusting the guided surface waveguide probe 200f to obtain optimal excitation of a guided surface wave mode. Adjustment of the coil length may be provided by taps located at one or both ends of the coil. In other embodiments, it may be the case that the inductive impedance is specified to have an electrical length that is significantly less than or greater than $\frac{1}{2}$ the wavelength at the operating frequency of the guided surface waveguide probe 200f.

[0165]   The excitation source 212 can be coupled to the feed network 209 by way of magnetic coupling. Specifically, the excitation source 212 is coupled to a coil L_P that is inductively coupled to the coil L_{1a}. This may be done by link coupling, a tapped coil, a variable reactance, or other coupling approach as can be appreciated. To this end, the coil L_P acts as a primary, and the coil L_{1a} acts as a secondary as can be appreciated.

[0166]   In order to adjust the guided surface waveguide probe 200f for the transmission of a desired guided surface wave, the heights of the respective charge terminals T_1 and T_2 may be altered with respect to the lossy conducting medium 203 and with respect to each other. Also, the sizes of the charge terminals T_1 and T_2 may be altered. In addition, the size of the coil L_{1a} may be altered by adding or eliminating turns or by changing some other dimension of the coil L_{1a}. The coil L_{1a} can also include one or more taps for adjusting the electrical length as shown in FIG. 17. The position of a tap connected to either charge terminal T_1 or T_2 can also be adjusted.

[0167]   Referring next to FIGS. 18A, 18B, 18C and 19, shown are examples of generalized receive circuits for using the surface-guided waves in wireless power delivery

systems. FIGS. 18A and 18B-18C include a linear probe 303 and a tuned resonator 306, respectively. FIG. 19 is a magnetic coil 309 according to various embodiments of the present disclosure. According to various embodiments, each one of the linear probe 303, the tuned resonator 306, and the magnetic coil 309 may be employed to receive power transmitted in the form of a guided surface wave on the surface of a lossy conducting medium 203 according to various embodiments. As mentioned above, in one embodiment the lossy conducting medium 203 comprises a terrestrial medium (or Earth).

[0168]   With specific reference to FIG. 18A, the open-circuit terminal voltage at the output terminals 312 of the linear probe 303 depends upon the effective height of the linear probe 303. To this end, the terminal point voltage may be calculated as

$$V_T = \int_0^{h_e} E_{inc} \cdot dl, \qquad (96)$$

where E_{inc} is the strength of the incident electric field induced on the linear probe 303 in Volts per meter, dl is an element of integration along the direction of the linear probe 303, and h_e is the effective height of the linear probe 303. An electrical load 315 is coupled to the output terminals 312 through an impedance matching network 318.

[0169]   When the linear probe 303 is subjected to a guided surface wave as described above, a voltage is developed across the output terminals 312 that may be applied to the electrical load 315 through a conjugate impedance matching network 318 as the case may be. In order to facilitate the flow of power to the electrical load 315, the electrical load 315 should be substantially impedance matched to the linear probe 303 as will be described below.

[0170]   Referring to FIG. 18B, a ground current excited coil 306a possessing a phase shift equal to the wave tilt of the guided surface wave includes a charge terminal T_R that is elevated (or suspended) above the lossy conducting medium 203. The charge terminal T_R has a self-capacitance C_R. In addition, there may also be a bound capacitance (not shown) between the charge terminal T_R and the lossy conducting medium 203 depending on the height of the charge terminal T_R above the lossy conducting medium 203. The bound capacitance should preferably be minimized as much as is practicable, although this may not be entirely necessary in every instance.

[0171]   The tuned resonator 306a also includes a receiver network comprising a coil L_R having a phase shift Φ. One end of the coil L_R is coupled to the charge terminal T_R, and the other end of the coil L_R is coupled to the lossy conducting medium 203. The receiver network can include a vertical supply line conductor that couples the coil L_R to the charge terminal T_R. To this end, the coil L_R (which may also be referred to as tuned resonator L_R-C_R) comprises a series-adjusted resonator as the charge terminal C_R and the coil L_R are situated in series. The phase delay of the coil L_R can be adjusted by changing the size

and/or height of the charge terminal T$_R$, and/or adjusting the size of the coil L$_R$ so that the phase Φ of the structure is made substantially equal to the angle of the wave tilt Ψ. The phase delay of the vertical supply line can also be adjusted by, e.g., changing length of the conductor.

[0172]   For example, the reactance presented by the self-capacitance C$_R$ is calculated as $1/j\omega C_R$.   Note that the total capacitance of the structure 306a may also include capacitance between the charge terminal T$_R$ and the lossy conducting medium 203, where the total capacitance of the structure 306a may be calculated from both the self-capacitance C$_R$ and any bound capacitance as can be appreciated. According to one embodiment, the charge terminal T$_R$ may be raised to a height so as to substantially reduce or eliminate any bound capacitance.   The existence of a bound capacitance may be determined from capacitance measurements between the charge terminal T$_R$ and the lossy conducting medium 203 as previously discussed.

[0173]   The inductive reactance presented by a discrete-element coil L$_R$ may be calculated as $j\omega L$, where L is the lumped-element inductance of the coil L$_R$. If the coil L$_R$ is a distributed element, its equivalent terminal-point inductive reactance may be determined by conventional approaches. To tune the structure 306a, one would make adjustments so that the phase delay is equal to the wave tilt for the purpose of mode-matching to the surface waveguide at the frequency of operation. Under this condition, the receiving structure may be considered to be "mode-matched" with the surface waveguide. A transformer link around the structure and/or an impedance matching network 324 may be inserted between the probe and the electrical load 327 in order to couple power to the load. Inserting the impedance matching network 324 between the probe terminals 321 and the electrical load 327 can effect a conjugate-match condition for maximum power transfer to the electrical load 327.

[0174]   When placed in the presence of surface currents at the operating frequencies power will be delivered from the surface guided wave to the electrical load 327. To this end, an electrical load 327 may be coupled to the structure 306a by way of magnetic coupling, capacitive coupling, or conductive (direct tap) coupling. The elements of the coupling network may be lumped components or distributed elements as can be appreciated.

[0175]   In the embodiment shown in FIG. 18B, magnetic coupling is employed where a coil L$_S$ is positioned as a secondary relative to the coil L$_R$ that acts as a transformer primary. The coil L$_S$ may be link-coupled to the coil L$_R$ by geometrically winding it around the same core structure and adjusting the coupled magnetic flux as can be appreciated. In addition, while the receiving structure 306a comprises a series-tuned resonator, a parallel-tuned

resonator or even a distributed-element resonator of the appropriate phase delay may also be used.

[0176] While a receiving structure immersed in an electromagnetic field may couple energy from the field, it can be appreciated that polarization-matched structures work best by maximizing the coupling, and conventional rules for probe-coupling to waveguide modes should be observed. For example, a TE_{20} (transverse electric mode) waveguide probe may be optimal for extracting energy from a conventional waveguide excited in the TE_{20} mode. Similarly, in these cases, a mode-matched and phase-matched receiving structure can be optimized for coupling power from a surface-guided wave. The guided surface wave excited by a guided surface waveguide probe 200 on the surface of the lossy conducting medium 203 can be considered a waveguide mode of an open waveguide. Excluding waveguide losses, the source energy can be completely recovered. Useful receiving structures may be E-field coupled, H-field coupled, or surface-current excited.

[0177] The receiving structure can be adjusted to increase or maximize coupling with the guided surface wave based upon the local characteristics of the lossy conducting medium 203 in the vicinity of the receiving structure. To accomplish this, the phase delay (Φ) of the receiving structure can be adjusted to match the angle (Ψ) of the wave tilt of the surface traveling wave at the receiving structure. If configured appropriately, the receiving structure may then be tuned for resonance with respect to the perfectly conducting image ground plane at complex depth $z = -d/2$.

[0178] For example, consider a receiving structure comprising the tuned resonator 306a of FIG. 18B, including a coil L_R and a vertical supply line connected between the coil L_R and a charge terminal T_R. With the charge terminal T_R positioned at a defined height above the lossy conducting medium 203, the total phase shift Φ of the coil L_R and vertical supply line can be matched with the angle (Ψ) of the wave tilt at the location of the tuned resonator 306a. From Equation (22), it can be seen that the wave tilt asymptotically passes to

$$W = |W|e^{j\Psi} = \frac{E_\rho}{E_z} \xrightarrow[\rho \to \infty]{} \frac{1}{\sqrt{\varepsilon_r - j\frac{\sigma_1}{\omega\varepsilon_o}}}, \qquad (97)$$

where ε_r comprises the relative permittivity and σ_1 is the conductivity of the lossy conducting medium 203 at the location of the receiving structure, ε_o is the permittivity of free space, and $\omega = 2\pi f$, where f is the frequency of excitation. Thus, the wave tilt angle (Ψ) can be determined from Equation (97).

[0179] The total phase shift ($\Phi = \theta_c + \theta_y$) of the tuned resonator 306a includes both the phase delay (θ_c) through the coil L_R and the phase delay of the vertical supply line (θ_y). The spatial phase delay along the conductor length l_w of the vertical supply line can be given by $\theta_y = \beta_w l_w$, where β_w is the propagation phase constant for the vertical supply line

conductor. The phase delay due to the coil (or helical delay line) is $\theta_c = \beta_p l_C$, with a physical length of l_C and a propagation factor of

$$\beta_p = \frac{2\pi}{\lambda_p} = \frac{2\pi}{V_f \lambda_0},\qquad(98)$$

where V_f is the velocity factor on the structure, λ_0 is the wavelength at the supplied frequency, and λ_p is the propagation wavelength resulting from the velocity factor V_f. One or both of the phase delays $(\theta_c + \theta_y)$ can be adjusted to match the phase shift Φ to the angle (Ψ) of the wave tilt. For example, a tap position may be adjusted on the coil L$_R$ of FIG. 18B to adjust the coil phase delay (θ_c) to match the total phase shift to the wave tilt angle ($\Phi = \Psi$). For example, a portion of the coil can be bypassed by the tap connection as illustrated in FIG. 18B. The vertical supply line conductor can also be connected to the coil L$_R$ via a tap, whose position on the coil may be adjusted to match the total phase shift to the angle of the wave tilt.

[0180] Once the phase delay (Φ) of the tuned resonator 306a has been adjusted, the impedance of the charge terminal T$_R$ can then be adjusted to tune to resonance with respect to the perfectly conducting image ground plane at complex depth $z = -d/2$. This can be accomplished by adjusting the capacitance of the charge terminal T$_1$ without changing the traveling wave phase delays of the coil L$_R$ and vertical supply line. The adjustments are similar to those described with respect to FIGS. 9A and 9B.

[0181] The impedance seen "looking down" into the lossy conducting medium 203 to the complex image plane is given by:

$$Z_{in} = R_{in} + jX_{in} = Z_o \tanh\bigl(j\beta_o(d/2)\bigr),\qquad(99)$$

where $\beta_o = \omega\sqrt{\mu_o \varepsilon_o}$. For vertically polarized sources over the Earth, the depth of the complex image plane can be given by:

$$d/2 \approx 1/\sqrt{j\omega\mu_1\sigma_1 - \omega^2\mu_1\varepsilon_1},\qquad(100)$$

where μ_1 is the permeability of the lossy conducting medium 203 and $\varepsilon_1 = \varepsilon_r\varepsilon_o$.

[0182] At the base of the tuned resonator 306a, the impedance seen "looking up" into the receiving structure is $Z_\uparrow = Z_{base}$ as illustrated in FIG. 9A. With a terminal impedance of:

$$Z_R = \frac{1}{j\omega C_R},\qquad(101)$$

where C_R is the self-capacitance of the charge terminal T$_R$, the impedance seen "looking up" into the vertical supply line conductor of the tuned resonator 306a is given by:

$$Z_2 = Z_W \frac{Z_R + Z_W \tanh(j\beta_w h_w)}{Z_W + Z_R \tanh(j\beta_w h_w)} = Z_W \frac{Z_R + Z_W \tanh(j\theta_y)}{Z_W + Z_R \tanh(j\theta_y)},\qquad(102)$$

and the impedance seen "looking up" into the coil L$_R$ of the tuned resonator 306a is given by:

$$Z_{base} = R_{base} + jX_{base} = Z_R \frac{Z_2 + Z_R \tanh(j\beta_p H)}{Z_R + Z_2 \tanh(j\beta_p H)} = Z_c \frac{Z_2 + Z_R \tanh(j\theta_c)}{Z_R + Z_2 \tanh(j\theta_c)}.\qquad(103)$$

By matching the reactive component (X_{in}) seen "looking down" into the lossy conducting medium 203 with the reactive component (X_{base}) seen "looking up" into the tuned resonator 306a, the coupling into the guided surface waveguide mode may be maximized.

[0183]   Referring next to FIG. 18C, shown is an example of a tuned resonator 306b that does not include a charge terminal T$_R$ at the top of the receiving structure.   In this embodiment, the tuned resonator 306b does not include a vertical supply line coupled between the coil L$_R$ and the charge terminal T$_R$.   Thus, the total phase shift (Φ) of the tuned resonator 306b includes only the phase delay (θ_c) through the coil L$_R$.   As with the tuned resonator 306a of FIG. 18B, the coil phase delay θ_c can be adjusted to match the angle (Ψ) of the wave tilt determined from Equation (97), which results in $\Phi = \Psi$.   While power extraction is possible with the receiving structure coupled into the surface waveguide mode, it is difficult to adjust the receiving structure to maximize coupling with the guided surface wave without the variable reactive load provided by the charge terminal T$_R$.

[0184]   Referring to FIG. 18D, shown is a flow chart 180 illustrating an example of adjusting a receiving structure to substantially mode-match to a guided surface waveguide mode on the surface of the lossy conducting medium 203.   Beginning with 181, if the receiving structure includes a charge terminal T$_R$ (e.g., of the tuned resonator 306a of FIG. 18B), then the charge terminal T$_R$ is positioned at a defined height above a lossy conducting medium 203 at 184.   As the surface guided wave has been established by a guided surface waveguide probe 200, the physical height (h_p) of the charge terminal T$_R$ may be below that of the effective height.   The physical height may be selected to reduce or minimize the bound charge on the charge terminal T$_R$ (e.g., four times the spherical diameter of the charge terminal).   If the receiving structure does not include a charge terminal T$_R$ (e.g., of the tuned resonator 306b of FIG. 18C), then the flow proceeds to 187.

[0185]   At 187, the electrical phase delay Φ of the receiving structure is matched to the complex wave tilt angle Ψ defined by the local characteristics of the lossy conducting medium 203.   The phase delay (θ_c) of the helical coil and/or the phase delay (θ_y) of the vertical supply line can be adjusted to make Φ equal to the angle (Ψ) of the wave tilt (W). The angle (Ψ) of the wave tilt can be determined from Equation (86).   The electrical phase Φ can then be matched to the angle of the wave tilt.   For example, the electrical phase delay $\Phi = \theta_c + \theta_y$ can be adjusted by varying the geometrical parameters of the coil L$_R$ and/or the length (or height) of the vertical supply line conductor.

[0186]   Next at 190, the load impedance of the charge terminal T$_R$ can be tuned to resonate the equivalent image plane model of the tuned resonator 306a.   The depth ($d/2$) of the conducting image ground plane 139 (FIG. 9A) below the receiving structure can be determined using Equation (100) and the values of the lossy conducting medium 203 (e.g.,

the Earth) at the receiving structure, which can be locally measured. Using that complex depth, the phase shift (θ_d) between the image ground plane 139 and the physical boundary 136 (FIG. 9A) of the lossy conducting medium 203 can be determined using $\theta_d = \beta_o\,d/2$. The impedance (Z_{in}) as seen "looking down" into the lossy conducting medium 203 can then be determined using Equation (99). This resonance relationship can be considered to maximize coupling with the guided surface waves.

[0187] Based upon the adjusted parameters of the coil L$_R$ and the length of the vertical supply line conductor, the velocity factor, phase delay, and impedance of the coil L$_R$ and vertical supply line can be determined. In addition, the self-capacitance (C_R) of the charge terminal T$_R$ can be determined using, e.g., Equation (24). The propagation factor (β_p) of the coil L$_R$ can be determined using Equation (98), and the propagation phase constant (β_w) for the vertical supply line can be determined using Equation (49). Using the self-capacitance and the determined values of the coil L$_R$ and vertical supply line, the impedance (Z_{base}) of the tuned resonator 306a as seen "looking up" into the coil L$_R$ can be determined using Equations (101), (102), and (103).

[0188] The equivalent image plane model of FIG. 9A also applies to the tuned resonator 306a of FIG. 18B. The tuned resonator 306a can be tuned to resonance with respect to the complex image plane by adjusting the load impedance Z_R of the charge terminal T$_R$ such that the reactance component X_{base} of Z_{base} cancels out the reactance component of X_{in} of Z_{in}, or $X_{base} + X_{in} = 0$. Thus, the impedance at the physical boundary 136 (FIG. 9A) "looking up" into the coil of the tuned resonator 306a is the conjugate of the impedance at the physical boundary 136 "looking down" into the lossy conducting medium 203. The load impedance Z_R can be adjusted by varying the capacitance (C_R) of the charge terminal T$_R$ without changing the electrical phase delay $\Phi = \theta_c + \theta_y$ seen by the charge terminal T$_R$. An iterative approach may be taken to tune the load impedance Z_R for resonance of the equivalent image plane model with respect to the conducting image ground plane 139. In this way, the coupling of the electric field to a guided surface waveguide mode along the surface of the lossy conducting medium 203 (e.g., Earth) can be improved and/or maximized.

[0189] Referring to FIG. 19, the magnetic coil 309 comprises a receive circuit that is coupled through an impedance matching network 333 to an electrical load 336. In order to facilitate reception and/or extraction of electrical power from a guided surface wave, the magnetic coil 309 may be positioned so that the magnetic flux of the guided surface wave, H_φ, passes through the magnetic coil 309, thereby inducing a current in the magnetic coil 309 and producing a terminal point voltage at its output terminals 330. The magnetic flux of the guided surface wave coupled to a single turn coil is expressed by

$$\mathcal{F} = \iint_{A_{CS}} \mu_r \mu_o \vec{H} \cdot \hat{n} dA \qquad\qquad (104)$$

where $\mathcal{F}$ is the coupled magnetic flux, μ_r is the effective relative permeability of the core of the magnetic coil 309, μ_o is the permeability of free space, $\vec{H}$ is the incident magnetic field strength vector, $\hat{n}$ is a unit vector normal to the cross-sectional area of the turns, and A_{CS} is the area enclosed by each loop. For an N-turn magnetic coil 309 oriented for maximum coupling to an incident magnetic field that is uniform over the cross-sectional area of the magnetic coil 309, the open-circuit induced voltage appearing at the output terminals 330 of the magnetic coil 309 is

$$V = -N\frac{d\mathcal{F}}{dt} \approx -j\omega\mu_r\mu_0 NHA_{CS}, \qquad\qquad (105)$$

where the variables are defined above. The magnetic coil 309 may be tuned to the guided surface wave frequency either as a distributed resonator or with an external capacitor across its output terminals 330, as the case may be, and then impedance-matched to an external electrical load 336 through a conjugate impedance matching network 333.

[0190]   Assuming that the resulting circuit presented by the magnetic coil 309 and the electrical load 336 are properly adjusted and conjugate impedance matched, via impedance matching network 333, then the current induced in the magnetic coil 309 may be employed to optimally power the electrical load 336. The receive circuit presented by the magnetic coil 309 provides an advantage in that it does not have to be physically connected to the ground.

[0191]   With reference to FIGS. 18A, 18B, 18C and 19, the receive circuits presented by the linear probe 303, the mode-matched structure 306, and the magnetic coil 309 each facilitate receiving electrical power transmitted from any one of the embodiments of guided surface waveguide probes 200 described above. To this end, the energy received may be used to supply power to an electrical load 315/327/336 via a conjugate matching network as can be appreciated. This contrasts with the signals that may be received in a receiver that were transmitted in the form of a *radiated* electromagnetic field. Such signals have very low available power, and receivers of such signals do not load the transmitters.

[0192]   It is also characteristic of the present guided surface waves generated using the guided surface waveguide probes 200 described above that the receive circuits presented by the linear probe 303, the mode-matched structure 306, and the magnetic coil 309 will load the excitation source 212 (e.g., FIGS. 3, 12 and 16) that is applied to the guided surface waveguide probe 200, thereby generating the guided surface wave to which such receive circuits are subjected. This reflects the fact that the guided surface wave generated by a given guided surface waveguide probe 200 described above comprises a transmission line mode. By way of contrast, a power source that drives a radiating antenna that generates a

radiated electromagnetic wave is not loaded by the receivers, regardless of the number of receivers employed.

[0193]   Thus, together one or more guided surface waveguide probes 200 and one or more receive circuits in the form of the linear probe 303, the tuned mode-matched structure 306, and/or the magnetic coil 309 can make up a wireless distribution system.   Given that the distance of transmission of a guided surface wave using a guided surface waveguide probe 200 as set forth above depends upon the frequency, it is possible that wireless power distribution can be achieved across wide areas and even globally.

[0194]   The conventional wireless-power transmission/distribution systems extensively investigated today include "energy harvesting" from radiation fields and also sensor coupling to inductive or reactive near-fields.   In contrast, the present wireless-power system does not waste power in the form of radiation which, if not intercepted, is lost forever.   Nor is the presently disclosed wireless-power system limited to extremely short ranges as with conventional mutual-reactance coupled near-field systems.   The wireless-power system disclosed herein probe-couples to the novel surface-guided transmission line mode, which is equivalent to delivering power to a load by a wave-guide or a load directly wired to the distant power generator.   Not counting the power required to maintain transmission field strength plus that dissipated in the surface waveguide, which at extremely low frequencies is insignificant relative to the transmission losses in conventional high-tension power lines at 60 Hz, all of the generator power goes only to the desired electrical load.   When the electrical load demand is terminated, the source power generation is relatively idle.

[0195]   Referring next to FIGS. 20A-E, shown are examples of various schematic symbols that are used with reference to the discussion that follows.   With specific reference to FIG. 20A, shown is a symbol that represents any one of the guided surface waveguide probes 200a, 200b, 200c, 200e, 200d, or 200f; or any variations thereof.   In the following drawings and discussion, a depiction of this symbol will be referred to as a guided surface waveguide probe P.   For the sake of simplicity in the following discussion, any reference to the guided surface waveguide probe P is a reference to any one of the guided surface waveguide probes 200a, 200b, 200c, 200e, 200d, or 200f; or variations thereof.

[0196]   Similarly, with reference to FIG. 20B, shown is a symbol that represents a guided surface wave receive structure that may comprise any one of the linear probe 303 (FIG. 18A), the tuned resonator 306 (FIGS. 18B-18C), or the magnetic coil 309 (FIG. 19).   In the following drawings and discussion, a depiction of this symbol will be referred to as a guided surface wave receive structure R.   For the sake of simplicity in the following discussion, any reference to the guided surface wave receive structure R is a reference to any one of the linear probe 303, the tuned resonator 306, the magnetic coil 309, or variations thereof.

[0197] Further, with reference to FIG. 20C, shown is a symbol that specifically represents the linear probe 303 (FIG. 18A). In the following drawings and discussion, a depiction of this symbol will be referred to as a guided surface wave receive structure R_P. For the sake of simplicity in the following discussion, any reference to the guided surface wave receive structure R_P is a reference to the linear probe 303 or variations thereof.

[0198] Further, with reference to FIG. 20D, shown is a symbol that specifically represents the tuned resonator 306 (FIGS. 18B-18C). In the following drawings and discussion, a depiction of this symbol will be referred to as a guided surface wave receive structure R_R. For the sake of simplicity in the following discussion, any reference to the guided surface wave receive structure R_R is a reference to the tuned resonator 306 or variations thereof.

[0199] Further, with reference to FIG. 20E, shown is a symbol that specifically represents the magnetic coil 309 (FIG. 19). In the following drawings and discussion, a depiction of this symbol will be referred to as a guided surface wave receive structure R_M. For the sake of simplicity in the following discussion, any reference to the guided surface wave receive structure R_M is a reference to the magnetic coil 309 or variations thereof.

[0200] Turning to FIG. 21, shown is an example of a medical device implanted in a human body according to an embodiment. The medical environment 400 may include a computing environment 403, network 406, guided surface waveguide probe P, one or more guided surface waves 409, a human body 412, and a medical device 415. The computing environment may include a data store 418 and a medical application 421. The data store may include patient data 424 with historical data 427. The patient data 424 may include one or more patient records for one or more patients. The historical data 427 for each patient may include one or more measurements received from a medical device 415. The one or more measurements may be of one or more characteristics of the human body 412 for the patient. The one or more measurements may include repeated measurements of a single characteristic over time and/or repeated measurements of multiple characteristics over time. The computing environment 403 may be connected to network 406. The medical device 415 may communicate via a wireless connection to network 406. The medical application 421 may communicate with one or more medical devices 415 via the network 406.

[0201] According to one embodiment, the medical device 415 may include guided surface wave receive structure R, impedance matching network 431, power circuitry 433, and medical circuitry 436. The guided surface wave receive structure R is configured to receive a guided surface wave 409 transmitted by the guided surface waveguide probe P and generates an AC power signal. According to one embodiment, the guided surface wave receive structure R may comprise a guided surface wave receive structure R_M comprising a

coil that obtains energy from a magnetic field embodied in a guided surface wave as described above. In such case, the coil may be wrapped around various core materials that have a high mu so that a greater amount of magnetic flux can be channeled through such coils to provide a greater amount of energy at the output of the guided surface wave receive structure R_M. Such high mu materials may comprise mu-metals such as nickel-iron soft magnetic alloy having a relative permeability values of 80,000 to 100,000, or other appropriate metals. Alternatively, other guided surface wave receive structures R may be used. For example, it may be possible to use the guided surface wave receive structures R_P and R_R in situations where the medical device 415 resides outside a human body or where electrical leads are exposed outside the human body coupled to a medical device 415 implanted inside the human body.

[0202]   The power circuitry 433 is coupled to the impedance matching network 431. The power circuitry 433 may include a power storage circuit configured to store the power signal. The power circuitry 433 may include AC-to-DC conversion circuitry such as a rectifier, such as a full wave rectifier and/or a half wave rectifier to convert an analog signal to a digital signal. The power storage circuit may include one or more batteries and/or one or more capacitors. The medical circuitry 436 may be coupled to the power circuitry 433, such as via an electrical connection.

[0203]   The medical device 415 may be implanted in a human body, such as the human body 412. For example, a surgeon may cut open a patient and implant the medical device 415 within the human body 412 of the patient. The surgeon may connect leads to various parts of the body to monitor and/or stimulate the body, such as connecting one or more thin insulated wires through a vein into the heart to stimulate the heart. The surgeon may connect one or more stimulating elements to one or more parts of the human body 412 of the patient. The stimulating elements may include one or more of a chemical injector, a laser, an electrical wire, and/or an element that releases nanodevices and/or nanoparticles.

[0204]   The surgeon may connect one or more sensing elements into the body of the patient. For example, the surgeon may implant a pressure sensing device within a vein, artery, or capillary to measure blood pressure and/or a frequency of heart beats. Other sensors may include electrical signal detectors and chemical sensors such as oxygen sensors, carbon dioxide sensors, glucose sensors, motion sensors, geospheres, accelerometers, GPS circuitry, a camera, and/or an x-ray device. The one or more sensors may be configured to detect a leak, such as a leak in a breast implant; detect a level of wear in a component of an artificial body part, such as an artificial hip, knee, or shoulder; detect a flow rate through one or more arteries, veins, and/or capillaries; and/or detect movement of repair or fusion hardware, such as a spine screw, rod, pin, plate, or artificial disc.

[0205] Alternatively, the medical device 415 may not be implanted into a human body. Rather, the medical device 415 may be positioned outside the body and may include electrical leads or other connections that enter the body from the medical device 415.

[0206] The guided surface waveguide probe P may output a guided surface wave 409 at a predefined field strength. According to one embodiment, the guided surface waveguide probe P is configured to transmit at a frequency low enough to propagate around the world. Alternatively, the guided surface waveguide probe P may transmit a guided surface wave at frequencies that propagate to lesser distances. In the event that a guided surface wave is transmitted globally, the resulting field strength will be lower due to geometric spreading at a relative equator with respect to the transmitting guided surface waveguide probe P, than the field strength at the location of the transmitter and at the antipode relative to the transmitting guided surface waveguide probe P. Also, if a guided surface waveguide probe P transmits to a lesser distance such as, for example, within the continental United States, the signal strength experienced at a distance from the guided surface waveguide probe P may not be as strong as the field near the guided surface waveguide probe P due to geometric spreading.

[0207] According to one embodiment, the guided surface waveguide probe P is configured to transmit a minimum power signal output in order to provide enough field strength to operate a medical device 415 at an area with the lowest signal strength, such as when the medical device 415 is located at and/or near the relative equator or on the edge of a transmission area. A measurement of field strength at one or more locations may be monitored by the medical application 421. The medical application 421 may increase and/or decrease the power signal strength output at guided surface waveguide probe P via an excitation source 405. The medical application 421 may increase the power signal strength until a measurement of field strength is received that exceeds or meets a preconfigured threshold, such as meeting a threshold field strength necessary to charge the medical device 415.

[0208] The medical application 421 transmits a power signal via excitation source 405. The excitation source 405 generates a voltage that is applied to the guided surface waveguide probe P. The guided surface waveguide probe P launches a guided surface wave 409 in response to the voltage being applied to the guided surface waveguide probe P. The medical device 415 receives energy from the guided surface wave 409 via guided surface wave receive structure R_M and provides an AC power signal to the power circuitry 433 that stores energy in a battery and/or capacitor for use to power the medical circuitry 436. A battery and/or capacitor in power circuitry 433 may be charged by the power circuitry in cycles when a charge gets down below a predefined threshold.

[0209] Turning to FIG. 22, shown is an example embodiment of medical device 415 according to various embodiments. The medical device 415 includes the guide surface wave receive structure R_M, impedance matching network 431, power circuitry 433, medical circuitry 436, terminals 445 and 448, and potentially other components. The power circuitry includes AC to DC conversion circuitry, power storage circuitry 442, and potentially other components. The guided surface wave receive structure R_M is configured to receive a guided surface wave on a predefined frequency, such as guided surface wave 409 (FIG. 21). Alternatively, the guided surface wave receive structure R_M and the impedance matching network 439 may be configured to receive guided surface waves at multiple different frequencies. To this end, the guided surface wave receive structure R_M and corresponding impedance matching network 439 may represent a plurality of guided surface wave receive structures R_M and corresponding impedance matching networks 439 that operate in parallel to receive power from guided surface waves at multiple different frequencies either one at a time or simultaneously. Alternatively, the physical parameters of the guided surface wave receive structure R_M and/or the impedance matching network 439 may be adjusted from time to time to receive power from guided surface waves at various different frequencies.

[0210] The guided surface wave receiver structure R_M is coupled to the power circuitry 433 through the impedance matching network 439. The power storage circuitry 442 includes terminals 445 and 448. The power circuitry generates a potential difference between terminals 445 and 448. For example, the power circuitry 433 receives a resulting output from the impedance matching network 439. According to one embodiment, the power circuitry 433 may convert that output into a DC power signal using power conversion circuitry 440, which may be provided to medical circuitry 436 and/or stored in power storage circuitry 442. In some embodiments, the power circuitry 443 trickle charges the power storage circuitry 442 continuously. In other embodiments, the power storage circuitry 442 is charged when the power level falls below a predefined threshold.

[0211] With reference to FIG. 23, shown is an example embodiment of medical circuitry 436 according to various embodiments. The medical circuitry 436 may be connected to power circuitry via terminals 445 and 448. Power may be supplied in the form of a DC voltage/current to medical circuitry 436 via the terminals 445 and 448. The medical circuitry 436 may include a stimulus circuit 451, a monitoring circuit 454, a computing device 457, and a wireless networking device 460. The stimulus circuit 451 is configured to provide a stimulus to a human body, such as a stimulus in the form of an electrical pulse, among other stimulus. The monitoring circuit 454 measures one or more characteristics of a human body 412 (FIG. 21). The characteristics may be one or more of a pulse, a blood pressure, a heartbeat frequency, a temperature, a respiration rate, an electric signal, a nerve impulse, a

muscle twitch, a resistance value, a protein turnover level, a carbon dioxide level, an oxygen level, or other characteristic. The stimulus circuit 451 may be configured to activate in response to a change in a characteristic of the human body, such as a measurement from the monitoring circuit 454.

[0212] The computing device 457 may be coupled to the stimulus circuit 451, the monitoring circuit 454, and the wireless networking device 460. The computing device 457 may execute a medical device application, among other software or firmware applications stored in a memory associated with the computing device 457. The computing device 457 may include hardware configured to perform the operations described herein, such as an FPGA, among other known hardware. The computing device may receive one or more measurements from the monitoring circuit 454. The computing device 457 may be coupled to one or more elements within power circuitry 433 to monitor and/or manage power generation, storage, and output.

[0213] The computing device 457 may cause the stimulus circuit 451 to provide the stimulus to the human body 412. The stimulus may include one or more of an electrical stimulus to a peroneal nerve, an electrical stimulus to a heart chamber, an electrical stimulus to the surface of a stomach, an electrical stimulus to an auditory nerve, an auditory stimulus to an auditory nerve, a secretion of insulin, a secretion of one or more other substances, and/or some other stimulus. For example, the monitoring circuit 454 may measure a glucose level in a body and provide the glucose level to computing device 457. The computing device 457 may determine that the glucose level falls outside of a predefined range of acceptable values, and in response to it falling outside of the range, the computing device 457 may signal to stimulus circuit 451 to provide a stimulus to the human body 412. In response to receiving the signal, the stimulus circuit 451 may output a secretion of medicine, such as insulin.

[0214] The computing device 457 may process the one or more characteristics of the human body to calculate more complex measurements. For example, the computing device 457 may calculate a bezometabolic rate by first determining that a person is sleeping based on one or more of a heartbeat frequency, a respiration rate, and a blood pressure, and then monitoring oxygen and carbon dioxide levels in the body during a period of sleep. As another example, a VO_2 max value may be calculated by the computing device 457 based on first determining that a person is in a state of aerobic activity and then monitoring oxygen and carbon dioxide levels in the body.

[0215] With reference to FIG. 24, shown is an example embodiment of power circuitry 433 according to various embodiments. The power circuitry 433 includes a power conversion circuit 440 that may comprise, for example, a full wave rectifier 463 and

smoothing capacitor 466, a power storage circuit 442, a positive input 469, a negative input 472, a positive output 445, and a negative output 448. The impedance matching network 439 is electrically coupled to the guided surface wave receive structure R_M. The impedance matching network 439 is configured reduce a reflection of the power signal and to provide for maximum power transfer at the frequency of operation as can be appreciated. The impedance matching network 439 may be the same as any impedance matching network described above. According to one embodiment, the power circuitry 433 (and medical circuitry 436 coupled thereto) is experienced as a load at an excitation source 405 (FIG. 21).

[0216] The power circuitry 433 is configured to convert an AC signal into a DC signal by way of AC-to-DC converter circuitry. For example, the power circuitry 433 receives an AC signal across positive input 469 and negative input 472 from the impedance matching network 439. The full wave rectifier 463 rectifies the AC signal to generate a DC signal. The smoothing capacitor 466 flattens the signal into a steady DC signal. Other rectifying circuits may be used, such as a half wave rectifier, a silicon controlled rectifier (SCR), a selenium and copper oxide rectifier, and/or silicon and germanium diodes, among other rectifiers as may be appreciated. In addition, other components such as a DC choke may be used to further stabilize the DC voltage. The output of the rectifying circuit 463 may be output directly to medical circuitry 436 (FIG. 21) or may be stored in power storage circuit 442. Power storage circuit 442 may output the stored power to the medical circuit 436 as needed.

[0217] The monitoring circuitry 454 (FIG. 23) may monitor a power level of power storage circuit 442. The computing device 457 may receive the power level from monitoring circuitry 454 and process the power level of power storage circuit 442. The computing device 457 may identify that a power level fails to meet a critical threshold of battery power in the power storage circuit 442 and generate a warning. The critical threshold may include a series of increasing critical thresholds. For example a series of critical thresholds may exist at one or more of 40% power level, 20% power level, 10% power level, 5% power level, 3% power level, 1% power level, or other power level.

[0218] According to one embodiment, the medical device 415 is configured to communicate with a reporting device via a wire lead extending outside the body. In this embodiment, the reporting device generates a warning, such as an audible warning. In yet another embodiment, the medical device 415 is not implanted in the body, but rather attached on the outside, such as an insulin pump.

[0219] The warning for each of the levels may increase in urgency as the power storage circuit 442 decreases in power level. The warning may be one or more of an audible noise, a physical pulse, and/or an electronic notification, such as an email or a text message. For example, the computing device 457 may transmit an email notifying that the power storage

circuit has a power level below 40%, but may submit an electric pulse into the body to cause a muscle to twitch when the power level falls below 5%. Causing a muscle to twitch may be a startling event for a person, but a risk associated with a power level for medical device 415 falling below a critical threshold may outweigh startling the person.

[0220] The computing device 457 may also store the power level associated with a time of measurement in a memory device associated with the computing device 457, such as memory devices 524 and 533 (FIG. 27). The computing device 457 may transmit the power level to a remote server for processing and storage, such as computing environment 403 (FIG. 21). The computing device 457 may store a history of the power levels in the memory device until a syncing event occurs. The computing device 457 may verify the power level history has been transferred to the remote server. The computing device 457 may clear the history from the memory device in response to verifying the power level history was transferred successfully. The computing device 457 and/or remote server may process a history of power levels for a medical device 415 to determine an estimated life for the power storage circuitry 442. The ability for power storage circuitry 442 to store power may deteriorate over time and require the medical device 415 be extracted and the power storage circuitry 442 be replaced. For example, a battery and/or capacitor may deteriorate over time.

[0221] Referring next to FIG. 25, shown is a flowchart of a medical stimulus process 475 that provides one example of the operation of a portion of the medical device 415 according to various embodiments. It is understood that the flowchart of FIG. 25 provides merely an example of the many different types of functional and/or physical arrangements that may be employed to implement the operation of the portion of the medical device 415 as described herein. As an alternative, the flowchart of FIG. 25 may be viewed as depicting an example of steps of a method implemented in the medical device 415 (FIG. 21) according to one or more embodiments.

[0222] At box 478, the medical stimulus process 475 includes receiving energy from a guided surface wave transmitted by a guided surface waveguide probe P. For example, the medical device 415 receives energy from a guided surface wave 409 (FIG. 21) by way of guided surface wave receive structure R_M (FIG. 21). At box 481, the medical stimulus process 475 includes generating a power signal based on the received guided surface wave. For example, the guided surface wave receive structure R_M outputs a power signal to the power circuitry 433 (FIG. 21) through the impedance matching circuitry 439. At box 484, the medical stimulus process 475 includes generating a power signal from the AC signal obtained from the guided surface wave receive structure R_M. For example, the power circuitry 433 may generate a DC power signal from the AC power signal generated by the

guided surface wave receive structure R_M. The DC power signal may be used to power the medical device 415 in real time or by storing the generated power signal in a power storage device, such as the power storage circuitry 442 (FIG 22). The power storage circuitry 442 may provide power stored from the power signal to the medical device 415.

[0223] At box 487, the medical stimulus process 475 includes determining a measurement from a human body. For example, monitoring circuit 454 (FIG. 23) of medical device 415 may obtain one or more measurements from a human body 412 (FIG. 21) via one or more sensing elements. The monitoring circuit 454 may include the one or more sensing elements and/or the one or more sensing elements may be separate elements. The monitoring circuit 454 may transmit the one or more measurements to the computing device 457 (FIG. 23). The measurements may be transmitted via a messaging protocol implemented in both the monitoring circuit 454 and computing device 457. The measurements may be transmitted by one or more outputs of monitoring circuit 454 being connected to one or more General Purpose Input/Output ("GPIO") lines of computing device 457. The output may be an analog signal and require an Analog-to-Digital converter circuit between the GPIO line of the computing device 457 and monitoring circuit 454. Each of the one or more outputs of the monitoring circuit 454 may correspond to a different measurement from a different sensing element. A single output of the monitoring circuit 454 may send more than one measurement from more than one sensing elements.

[0224] At box 490, the medical stimulus process 475 includes calculating a variance in the measurement. For example, the computing device 457 may process one or more measurements from the monitoring circuit 454 and one or more historical measurements stored in a memory device associated with the computing device 457 to determine a variance in one or more measurements. The variance may be a statistical measure. For example, the computing device 457 may compute an average value for one of the measurements over a history and calculate a standard deviation of the current measurement from the average value. The computing device 457 may perform a regression analysis on the history of measurements in memory, determine a predicted value of the current measurement based on the regression analysis, and determine a variance between the predicted value and the current measurement. For example, the regression analysis may identify a history of a blood pressure spike of 20% after eating at 5:00PM, but determine a large variance if a measurement at 5:00PM shows an increase of 50%, whereas an increase of only 20% would have no variance.

[0225] At box 493 the medical stimulus process 475 includes determining whether the variance meets a predefined threshold. For example, computing device 457 may compare a variance, such as the variance calculated in box 490, to determine whether the variance

meets a predefined threshold. The predefined threshold may be stored in a memory device associated with the computing device 457. The predefined threshold may be modified, updated, or changed based in part on one or more characteristics of the human body the medical device 415 is implanted into. For example, the computing device 457 may store measurements of the effect of a dosage of insulin on the level of glucose in the body adjust a threshold for injecting insulin based in part on the effect. The effect of the dosage may change over time based in part on an increased resistance of the body to insulin, and thus the threshold may be changed over time by the computing device 457. A remote server, such as computing environment 403 (FIG. 21), may transmit a message via a network, such as network 406 (FIG. 21), to the medical device 415 instructing the computing device 457 to adjust the threshold stored in memory. If the threshold is met (e.g. Yes), the medical stimulus process 475 proceeds to box 496. If the threshold is not met (e.g. No), the medical stimulus process 475 proceeds to box 499.

[0226]   At box 496, the medical stimulus process 475 includes providing a stimulus to the human body. For example, the computing device 457 may transmit an indication to a stimulus circuit 451 (FIG. 23) to cause the stimulus circuit 451 to provide or output a stimulus. For example, the computing device 457 may raise and/or lower a GPIO line connected to the stimulus circuit 451 to indicate that a stimulus should be provided. The computing device 457 may need to transmit a message to stimulus circuit 451 with parameters describing characteristics of the stimulus to be output. The stimulus circuit 451 may respond with a message confirming the instructions and the stimulus circuit 451 may require an acknowledgement from the computing device 457 before applying the stimulus. The communication between the stimulus circuit 451 and the computing device 457 may be encrypted. The stimulus circuit 451 provides the stimulus in response to receiving the indication from the computing device 457.

[0227]   Referring next to FIG. 26, shown is a flowchart of an update process 500 that provides one example of the operation of a portion of the medical device 415 according to various embodiments. It is understood that the flowchart of FIG. 26 provides merely an example of the many different types of functional arrangements that may be employed to implement the operation of the portion of the medical device 415 as described herein. As an alternative, the flowchart of FIG. 26 may be viewed as depicting an example of steps of a method implemented in the medical device 415 (FIG. 21) according to one or more embodiments.

[0228]   At box 503, the update process 500 includes receiving a request to perform an update from a server. For example, the medical application 421 (FIG. 21) of computing environment 403 (FIG. 21) may transmit a message via network 406 (FIG. 21) to medical

device 415. The request may be a request for the medical device 415 to transmit a history of measurements to the medical application 421 from a memory device associated with the computing device 457 (FIG. 23). The request may be to update or modify one or more thresholds for providing a stimulus including data describing the new or modified thresholds. The request may be a request to update software or firmware associated with the computing device 457. For example, the medical application 421 may request that the computing device 457 update firmware and set thresholds, for example, for a specific patient prior to installing the device and/or in an existing patient when updates become necessary or desirable.

[0229] At box 506, the update process 500 includes authenticating the server. For example, the computing device 457 may authenticate the medical application 421 prior to responding to any requests. The authentication may be based in part on one or more of a security credential, a digital signature, and/or a biometric feedback. The medical device 415 may be programmed prior to being implanted with a trusted security key known only to a doctor of the patient. The patient may be asked to specify security credentials to the doctor prior to the implant and those security credentials may be preloaded into the medical device 415.

[0230] The patient may authenticate the server based in part on flexing a muscle in a predefined manner, such as repeatedly flexing a chest muscle 3 times sequentially and a bicep two times. The computing device 457 may transmit a series of required biometric feedback steps required to authenticate the request to the medical application 421. The medical application 421 may render a user interface instructing the patient to perform the steps in order to validate the server. The biometric feedback may include pressing a button on the medical device 415 through the skin of the patient.

[0231] The wireless networking device 460 (FIG. 23) may be configured to communicate only within a preconfigured range, such as by using Near Field Communication (NFC). The wireless networking device 460 may limit a range that a wireless transmitter of network 406 must be within in order to communicate with the computing device 457. For example, the wireless networking device 460 may be an NFC transceiver that only transmits within a 1 foot radius of the medical device 415.

[0232] At box 509, the update process 500 includes verifying the update. For example, the computing device 457 may verify a hash of an update received from medical application 421. The computing device 457 may calculate a signature for a software update downloaded from the medical application 421, such as an MD5, checksum, and/or CRC. The signature may be compared to a signature embedded within the software update. The computing device 457 may transmit the signature to the medical application 421, and the

medical application 421 may acknowledge the signature and/or instruct the computing device 457 to apply the software update, download the software update again, discard the software update, and/or cancel the software update. The computing device 457 may transmit a confirmation message and receive an acknowledgement prior to applying an update to one or more thresholds. The computing device 457 may verify the request by transmitting a history of measurements to the medical application 421 when requested.

[0233] At box 512, the update process 500 includes applying the update. For example, the computing device 457 may store an update to a memory device. The computing device 457 may store a software update to a memory device associated with the computing device 457. The computing device 457 may execute the stored software update in response to successfully saving the update. The computing device 457 may store an update to one or more thresholds to memory locations preconfigured to store the one or more thresholds. For example, the computing device 457 may store a new variance threshold in a specific address in a Non-Volatile Ram (NV Ram) assigned to the variance threshold. The specific address may be an address used when determining if a threshold is exceeded, such as in box 493 (FIG. 25).

[0234] With reference to FIG. 27, shown is a schematic block diagram of the computing environment 403 (FIG. 21) and/or computing device 457 (FIG, 27) according to an embodiment of the present disclosure. The computing environment 403 and/or computing device 457 include one or more computing devices 518. Each computing device 518 includes at least one processor circuit, for example, having a processor 521 and a memory 524/533, both of which are coupled to a local interface 530. To this end, each computing device 518 may comprise, for example, at least one server computer or like device. The local interface 530 may comprise, for example, a data bus with an accompanying address/control bus or other bus structure as can be appreciated. The computing device 518 may include one or more I/O 527, such as a serial port, a network port, a GPIO, a USB port, among other known I/O.

[0235] Stored in the memory 524/533 are both data and several components that are executable by the processor 521. In particular, stored in the memory 524/533 and executable by the processor 521 are one or more application including an application executed in computing device 457 and the medical application 421, and potentially other applications. Also stored in the memory 524/533 may be a data store 418 (FIG. 21) and other data. In addition, an operating system may be stored in the memory 524/533 and executable by the processor 521.

[0236] It is understood that there may be other applications that are stored in the memory 524/533 and are executable by the processor 521 as can be appreciated. Where

any component discussed herein is implemented in the form of software, any one of a number of programming languages may be employed such as, for example, C, C++, C#, Objective C, Java®, JavaScript®, Perl, PHP, Visual Basic®, Python®, Ruby, Flash®, or other programming languages.

[0237]   A number of software components are stored in the memory 524/533 and are executable by the processor 521. In this respect, the term "executable" means a program file that is in a form that can ultimately be run by the processor 521. Examples of executable programs may be, for example, a compiled program that can be translated into machine code in a format that can be loaded into a random access portion of the memory 524/533 and run by the processor 521, source code that may be expressed in proper format such as object code that is capable of being loaded into a random access portion of the memory 524/533 and executed by the processor 521, or source code that may be interpreted by another executable program to generate instructions in a random access portion of the memory 524/533 to be executed by the processor 521, *etc.* An executable program may be stored in any portion or component of the memory 524/533 including, for example, random access memory (RAM), read-only memory (ROM), hard drive, solid-state drive, USB flash drive, memory card, optical disc such as compact disc (CD) or digital versatile disc (DVD), floppy disk, magnetic tape, or other memory components.

[0238]   The memory 524/533 is defined herein as including both volatile and nonvolatile memory and data storage components. Volatile components are those that do not retain data values upon loss of power. Nonvolatile components are those that retain data upon a loss of power. Thus, the memory 524/533 may comprise, for example, random access memory (RAM), read-only memory (ROM), hard disk drives, solid-state drives, USB flash drives, memory cards accessed via a memory card reader, floppy disks accessed via an associated floppy disk drive, optical discs accessed via an optical disc drive, magnetic tapes accessed via an appropriate tape drive, and/or other memory components, or a combination of any two or more of these memory components. In addition, the RAM may comprise, for example, static random access memory (SRAM), dynamic random access memory (DRAM), or magnetic random access memory (MRAM) and other such devices. The ROM may comprise, for example, a programmable read-only memory (PROM), an erasable programmable read-only memory (EPROM), an electrically erasable programmable read-only memory (EEPROM), or other like memory device.

[0239]   Also, the processor 521 may represent multiple processors 521 and/or multiple processor cores and the memory 524/533 may represent multiple memories 524/533 that operate in parallel processing circuits, respectively. In such a case, the local interface 530 may be an appropriate network that facilitates communication between any two of the

multiple processors 521, between any processor 521 and any of the memories 524/533, or between any two of the memories 524/533, *etc.* The local interface 530 may comprise additional systems designed to coordinate this communication, including, for example, performing load balancing. The processor 521 may be of electrical or of some other available construction.

[0240] Although an application executed in computing device 457 and the medical application 421, and other various systems described herein may be embodied in software or code executed by general purpose hardware as discussed above, as an alternative the same may also be embodied in dedicated hardware or a combination of software/general purpose hardware and dedicated hardware. If embodied in dedicated hardware, each can be implemented as a circuit or state machine that employs any one of or a combination of a number of technologies. These technologies may include, but are not limited to, discrete logic circuits having logic gates for implementing various logic functions upon an application of one or more data signals, application specific integrated circuits (ASICs) having appropriate logic gates, field-programmable gate arrays (FPGAs), or other components, *etc.* Such technologies are generally well known by those skilled in the art and, consequently, are not described in detail herein.

[0241] The flowcharts of FIGS. 25 and 26 show the functionality and operation of an implementation of portions of the application executed in computing device 457 and/or functionality of the hardware in computing device 457. If embodied in software, each block may represent a module, segment, or portion of code that comprises program instructions to implement the specified logical function(s). The program instructions may be embodied in the form of source code that comprises human-readable statements written in a programming language or machine code that comprises numerical instructions recognizable by a suitable execution system such as a processor 521 in a computer system or other system. The machine code may be converted from the source code, *etc.* If embodied in hardware, each block may represent a circuit or a number of interconnected circuits to implement the specified logical function(s).

[0242] Although the flowcharts of FIGS. 25 and 26 show a specific order of execution, it is understood that the order of execution may differ from that which is depicted. For example, the order of execution of two or more blocks may be scrambled relative to the order shown. Also, two or more blocks shown in succession in FIGS. 25 and 26 may be executed concurrently or with partial concurrence. Further, in some embodiments, one or more of the blocks shown in FIGS. 25 and 26 may be skipped or omitted. In addition, any number of counters, state variables, warning semaphores, or messages might be added to the logical flow described herein, for purposes of enhanced utility, accounting, performance

measurement, or providing troubleshooting aids, *etc.* It is understood that all such variations are within the scope of the present disclosure.

[0243] Also, any logic or application described herein, including an application executed in computing device 457 and the medical application 421, that comprises software or code can be embodied in any non-transitory computer-readable medium for use by or in connection with an instruction execution system such as, for example, a processor 521 in a computer system or other system. In this sense, the logic may comprise, for example, statements including instructions and declarations that can be fetched from the computer-readable medium and executed by the instruction execution system. In the context of the present disclosure, a "computer-readable medium" can be any medium that can contain, store, or maintain the logic or application described herein for use by or in connection with the instruction execution system.

[0244] The computer-readable medium can comprise any one of many physical media such as, for example, magnetic, optical, or semiconductor media. More specific examples of a suitable computer-readable medium would include, but are not limited to, magnetic tapes, magnetic floppy diskettes, magnetic hard drives, memory cards, solid-state drives, USB flash drives, or optical discs. Also, the computer-readable medium may be a random access memory (RAM) including, for example, static random access memory (SRAM) and dynamic random access memory (DRAM), or magnetic random access memory (MRAM). In addition, the computer-readable medium may be a read-only memory (ROM), a programmable read-only memory (PROM), an erasable programmable read-only memory (EPROM), an electrically erasable programmable read-only memory (EEPROM), or other type of memory device.

[0245] Further, any logic or application described herein, including an application executed in computing device 457 and the medical application 421, may be implemented and structured in a variety of ways. For example, one or more applications described may be implemented as modules or components of a single application. Further, one or more applications described herein may be executed in shared or separate computing devices or a combination thereof. For example, a plurality of the applications described herein may execute in the same computing device 518 or in multiple computing devices 518 in the same computing environment 403 and/or computing device 457. Additionally, it is understood that terms such as "application," "service," "system," "engine," "module," and so on may be interchangeable and are not intended to be limiting.

[0246] Disjunctive language such as the phrase "at least one of X, Y, or Z," unless specifically stated otherwise, is otherwise understood with the context as used in general to present that an item, term, etc., may be either X, Y, or Z, or any combination thereof (*e.g.,* X,

Y, and/or Z). Thus, such disjunctive language is not generally intended to, and should not, imply that certain embodiments require at least one of X, at least one of Y, or at least one of Z to each be present.

[0247]   In addition to the foregoing, the various embodiments of the present disclosure include, but are not limited to, the embodiments set forth in the following clauses:

[0248]   Clause 1. An apparatus, comprising: a guided surface wave receive structure configured to receive a guided surface wave traveling along a terrestrial medium generated by a guided surface waveguide probe; a power circuit electrically coupled to the guided surface wave receive structure, the power circuit generating a power signal from an alternating current signal generated by the guided surface wave receive structure; and a medical circuit electrically coupled to the power circuit, the medical circuit comprising a monitoring circuit configured to measure a characteristic of a human body.

[0249]   Clause 2. The apparatus of clause 1, wherein the medical circuit comprising a stimulus circuit configured to provide a stimulus to the human body.

[0250]   Clause 3. The apparatus of any of clauses 1-2, wherein apparatus is implanted in the human body.

[0251]   Clause 4. The apparatus of any of clauses 1-3, wherein the power circuit comprises a power storage circuit configured to store the power signal.

[0252]   Clause 5. The apparatus of any of clauses 1-4, wherein the monitoring circuit is configured to measure at least one of: a pulse, a blood pressure, a temperature, a respiration rate, an electric signal, a nerve impulse, a muscle twitch, a resistance value, a protein turnover level, or an oxygen level.

[0253]   Clause 6. The apparatus of clause 2, wherein the medical circuit further comprises a computing device coupled to the stimulus circuit and the monitoring circuit, the computing device configured to at least: receive at least one measurement from the monitoring circuit; and cause the stimulus circuit to provide the stimulus to the human body.

[0254]   Clause 7. The apparatus of clauses 2 or 6, wherein the stimulus circuit is configured to stimulate the human body in response to a change in value of at least one measurement by the monitoring circuit.

[0255]   Clause 8. The apparatus of any of clauses 1-7, wherein the guided surface wave receive structure is coupled to the power circuit through an impedance matching network, the impedance matching network configured to minimize a reflection of the alternating current signal back to the guided surface wave receive structure.

[0256]   Clause 9. The apparatus of clauses 2, 6, or 7, wherein the stimulus comprises at least one of: an electrical stimulus to a peroneal nerve, an electrical stimulus to a heart

chamber, an electrical stimulus to the surface of a stomach, an electrical stimulus to an auditory nerve, or a secretion of insulin.

[0257] Clause 10. The apparatus of clauses 2, 6, 7, or 9, wherein the medical circuit comprises a computing device connected to the power circuit and the computing device is configured to obtain a measurement from a sensing device and initiate the stimulus to the human body based at least in part on the measurement.

[0258] Clause 11. The apparatus of claim 2, 6, 7, 9, or 10, wherein the guided surface wave receive structure further comprises a coil wrapped around a high-mu material.

[0259] Clause 12. A system comprising: a guided surface waveguide probe configured to transmit a guided surface wave traveling along a terrestrial medium; and a medical device comprising a guided surface wave receive structure, the guided surface wave receive structure being configured to generate an alternating current (AC) signal from the guided surface wave for the medical device, the medical device being experienced as a load at an excitation source coupled to the guided surface waveguide probe.

[0260] Clause 13. The system of clause 12, wherein the medical device is configured to stimulate the human body in response to a change in value of at least one measurement by the medical device.

[0261] Clause 14. The system of clause 12 or 13, wherein the medical device further comprises a rectifying circuit configured to convert the AC signal into a direct current (DC) signal.

[0262] Clause 15. The system of clause 14, wherein the rectifying circuit comprises a full-wave bridge rectifier.

[0263] Clause 16. The system of clause 14 or 15, wherein the medical device further comprises a power storage circuit configured to store energy from the DC signal in a storage device and provide stored power to the medical device from the storage device, the storage device comprising at least one of a battery or a capacity.

[0264] Clause 17. The system of any of clauses 12-14, wherein the guided surface wave receive structure comprises a magnetic coil.

[0265] Clause 18. A method comprising: generating an alternating current (AC) signal, via at least one guided wave receive structure, from at least one guided surface wave; supplying, via power circuitry, electrical energy generated embodied in the AC signal to medical circuitry comprising a monitoring circuit and a stimulus circuit; determining, via the monitoring circuit, at least one measurement from a human body; and providing, via the stimulus circuit, the stimulus circuit to provide a stimulus to the human body.

[0266] Clause 19. The method of clauses 18, wherein the medical circuitry further comprises at least one computing device and the method further comprises: receiving, via

70

the at least one computing device, the at least one measurement from the monitoring circuit; and causing, via the at least one computing device, the stimulus circuit to provide the stimulus.

[0267] Clause 20. The method of clauses 19, further comprising: receiving, via the at least one computing device, at least one preconfigured impulse; and transmitting, via the at least one computing device, information describing at least one measurement from the monitoring circuit over a network connection.

[0268] Clause 21. The method of any of clauses 19 and 20, further comprising: receiving, via the at least one computing device, a request to modify at least one threshold for providing the stimulus; modifying, via the at least one computing device, the at least one threshold based at least in part on the request to generate at least one modified threshold; and causing, via the at least one computing device, the stimulus circuit to provide the stimulus based in part on the at least one modified threshold.

[0269] Clause 22. The method of any of clauses 19-21, further comprising: receiving, via the at least one computing device, a software package via a network connection, the software package including a hash of the software package; verifying, via the at least one computing device, the software packaged based at least in part on the hash; receiving, via the at least one computing device, a request to program the software package into a memory associated with the computing device; storing, via the at least one computing device, the software package in the memory; validating, via the at least one computing device, the software package was successfully stored; and executing, via the at least one computing device, the software package.

[0270] Clause 23. The method of any of clauses 19-22, further comprising: receiving, via the at least one computing device, a request from a server via a network connection; and authenticating, via the at least one computing device, the request based at least in part on at least one security credential.

[0271] It should be emphasized that the above-described embodiments of the present disclosure are merely possible examples of implementations set forth for a clear understanding of the principles of the disclosure. Many variations and modifications may be made to the above-described embodiment(s) without departing substantially from the spirit and principles of the disclosure. All such modifications and variations are intended to be included herein within the scope of this disclosure and protected by the following claims. In addition, all optional and preferred features and modifications of the described embodiments and dependent claims are usable in all aspects of the disclosure taught herein. Furthermore, the individual features of the dependent claims, as well as all optional

and preferred features and modifications of the described embodiments are combinable and interchangeable with one another.

CLAIMS

Therefore, the following is claimed:

1.   An apparatus, comprising:

a guided surface wave receive structure configured to receive a guided surface wave traveling along a terrestrial medium generated by a guided surface waveguide probe;

a power circuit electrically coupled to the guided surface wave receive structure, the power circuit generating a power signal from an alternating current signal generated by the guided surface wave receive structure; and

a medical circuit electrically coupled to the power circuit, the medical circuit comprising a monitoring circuit configured to measure a characteristic of a human body.

2.   The apparatus of claim 1, wherein the medical circuit comprising a stimulus circuit configured to provide a stimulus to the human body.

3.   The apparatus of any of claims 1-2, wherein apparatus is implanted in the human body.

4.   The apparatus of any of claims 1-3, wherein the power circuit comprises a power storage circuit configured to store the power signal.

5.   The apparatus of any of claims 1-4, wherein the monitoring circuit is configured to measure at least one of: a pulse, a blood pressure, a temperature, a respiration rate, an electric signal, a nerve impulse, a muscle twitch, a resistance value, a protein turnover level, or an oxygen level.

6.   The apparatus of claim 2, wherein the medical circuit further comprises a computing device coupled to the stimulus circuit and the monitoring circuit, the computing device configured to at least:

receive at least one measurement from the monitoring circuit; and

cause the stimulus circuit to provide the stimulus to the human body.

7.   The apparatus of any of claims 1-6, wherein the guided surface wave receive structure is coupled to the power circuit through an impedance matching network, the impedance matching network configured to minimize a reflection of the alternating current signal back to the guided surface wave receive structure.

8.   The apparatus of claims 2 or 6, wherein the stimulus comprises at least one of: an electrical stimulus to a peroneal nerve, an electrical stimulus to a heart chamber, an electrical stimulus to the surface of a stomach, an electrical stimulus to an auditory nerve, or a secretion of insulin.

9.   The apparatus of claim 2, 6, or 8, wherein the medical circuit comprises a computing device connected to the power circuit and the computing device is configured to obtain a measurement from a sensing device and initiate the stimulus to the human body based at least in part on the measurement.

10.   A method comprising:

generating an alternating current (AC) signal, via at least one guided wave receive structure, from at least one guided surface wave;

supplying, via power circuitry, electrical energy generated embodied in the AC signal to medical circuitry comprising a monitoring circuit and a stimulus circuit;

determining, via the monitoring circuit, at least one measurement from a human body; and

providing, via the stimulus circuit, the stimulus circuit to provide a stimulus to the human body.

11.   The method of claim 10, wherein the medical circuitry further comprises at least one computing device and the method further comprises:

receiving, via the at least one computing device, the at least one measurement from the monitoring circuit; and

causing, via the at least one computing device, the stimulus circuit to provide the stimulus.

12.   The method of claim 11, further comprising:

receiving, via the at least one computing device, at least one preconfigured impulse; and

transmitting, via the at least one computing device, information describing at least one measurement from the monitoring circuit over a network connection.

13.   The method of any of claims 11 and 12, further comprising:

receiving, via the at least one computing device, a request to modify at least one threshold for providing the stimulus;

modifying, via the at least one computing device, the at least one threshold based at least in part on the request to generate at least one modified threshold; and

causing, via the at least one computing device, the stimulus circuit to provide the stimulus based in part on the at least one modified threshold.

14.   The method of any of claims 11-13, further comprising:

receiving, via the at least one computing device, a software package via a network connection, the software package including a hash of the software package;

verifying, via the at least one computing device, the software packaged based at least in part on the hash;

receiving, via the at least one computing device, a request to program the software package into a memory associated with the computing device;

storing, via the at least one computing device, the software package in the memory;

validating, via the at least one computing device, the software package was successfully stored; and

executing, via the at least one computing device, the software package.

15.   The method of any of claims 11-14, further comprising:

receiving, via the at least one computing device, a request from a server via a network connection; and

authenticating, via the at least one computing device, the request based at least in part on at least one security credential.
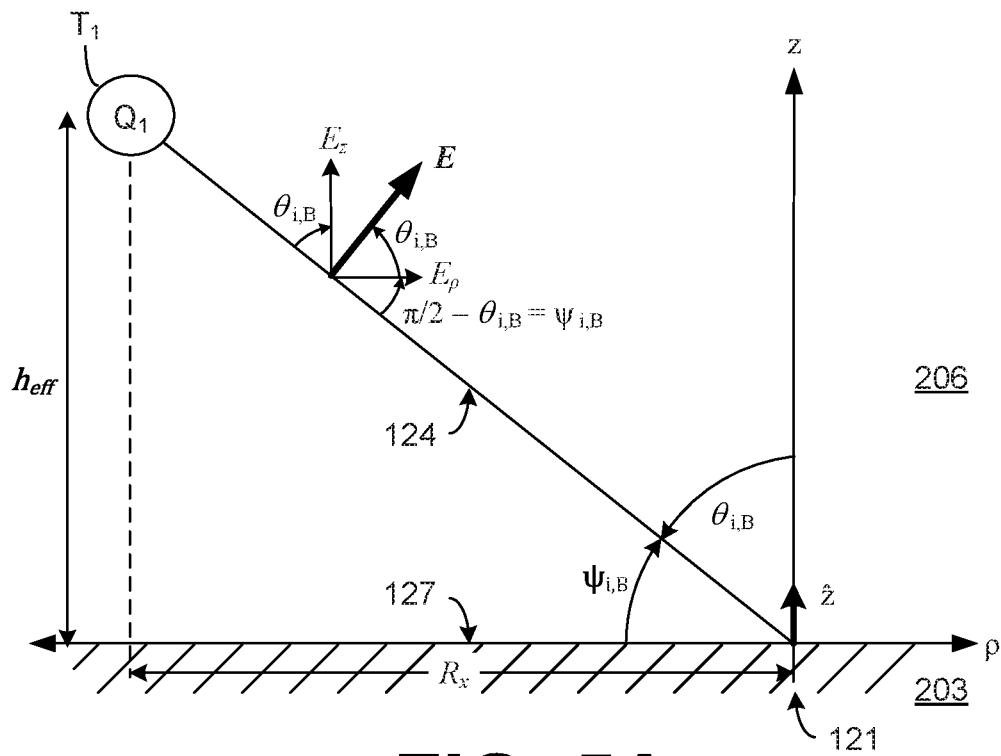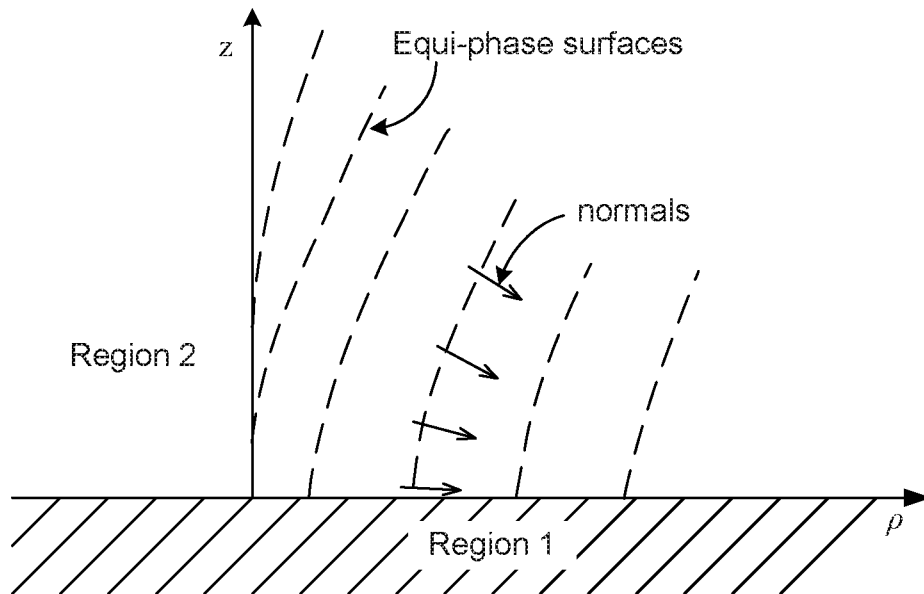
FIG. 1

FIG. 2

FIG. 3

Distance to Crossover Point

FIG. 4

FIG. 5A

FIG. 5B

FIG. 6

FIG. 7

FIG. 8C

FIG. 8B

FIG. 8A

FIG. 9A

FIG. 9B

FIG. 10

FIG. 11

$$D_1 = H_1 + d/2 + d/2 = H_1 + d$$

$$D_2 = H_2 + d/2 + d/2 = H_2 + d$$

FIG. 12

FIG. 13

FIG. 14

FIG. 15A

FIG. 15B

$$D_1 = H_1 + d/2 + d/2 = H_1 + d$$

$$D_2 = H_2 + d/2 + d/2 = H_2 + d$$

FIG. 16

FIG. 17

FIG. 18A

FIG. 18B

306b

321

L_R

L_S

Impedance
Matching
Network
324

Electric
Load
327

203

FIG. 18C

START

181

Charge
terminal?

Y

Position charge terminal

184

N

Match electrical phase of
receiving structure with
complex wave tilt angle

187

180

FIG. 18D

Resonate equivalent
image plane model

190

END
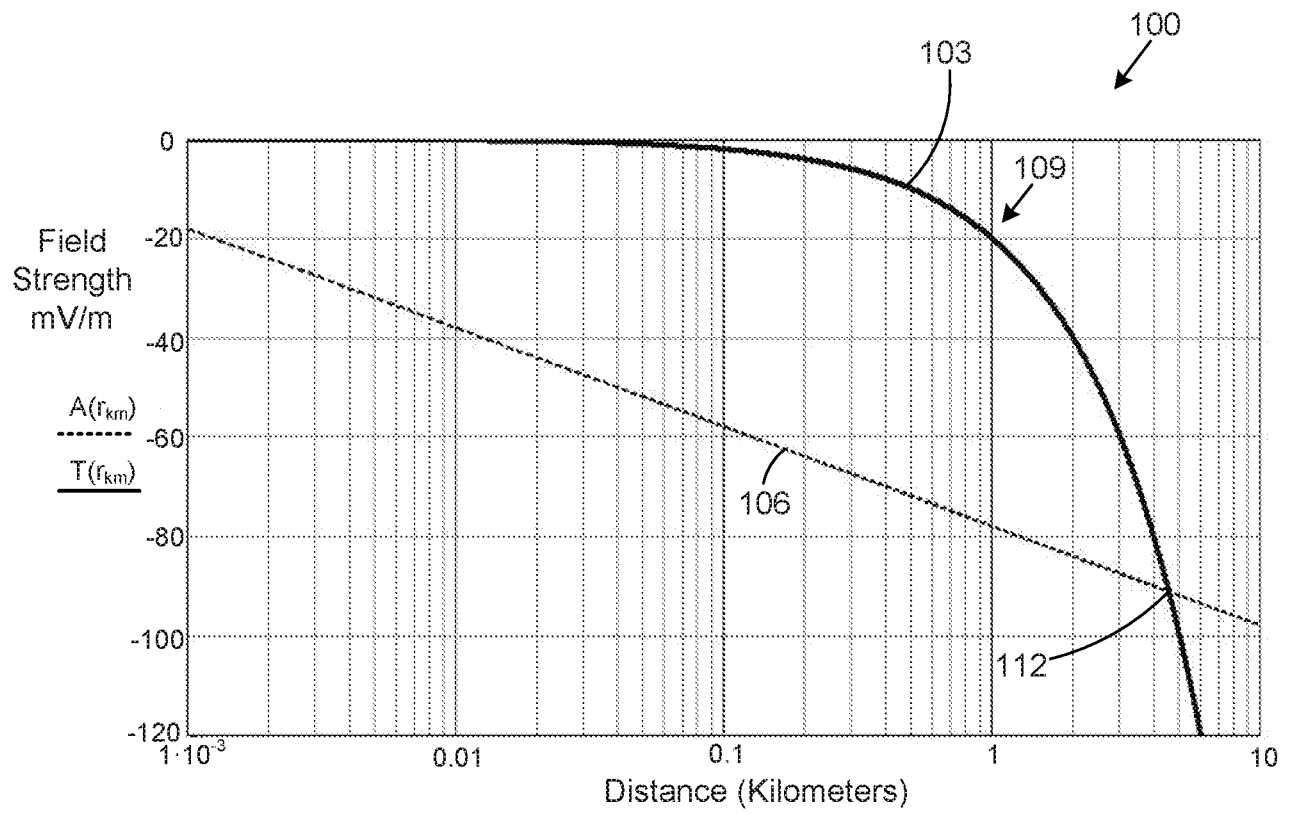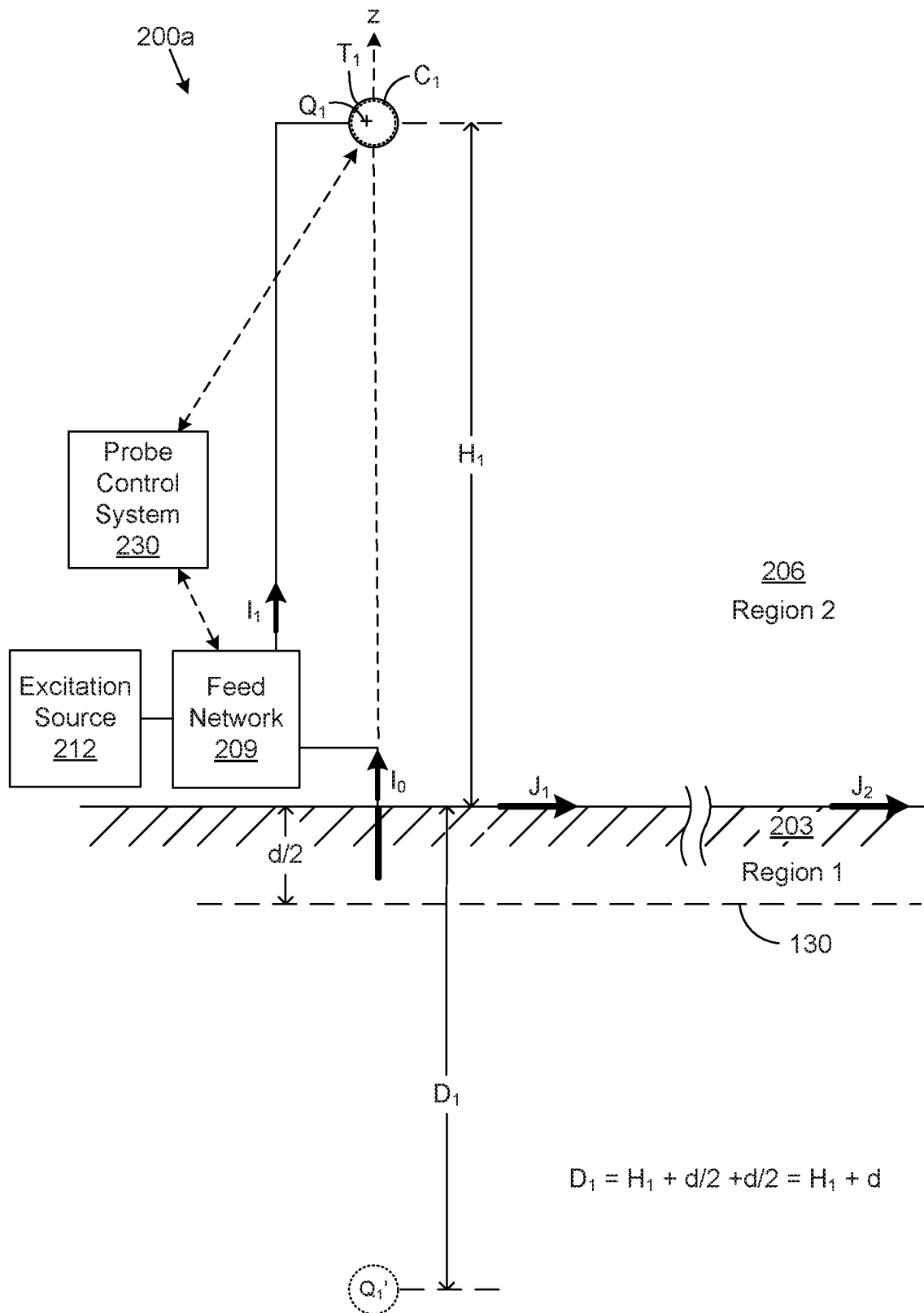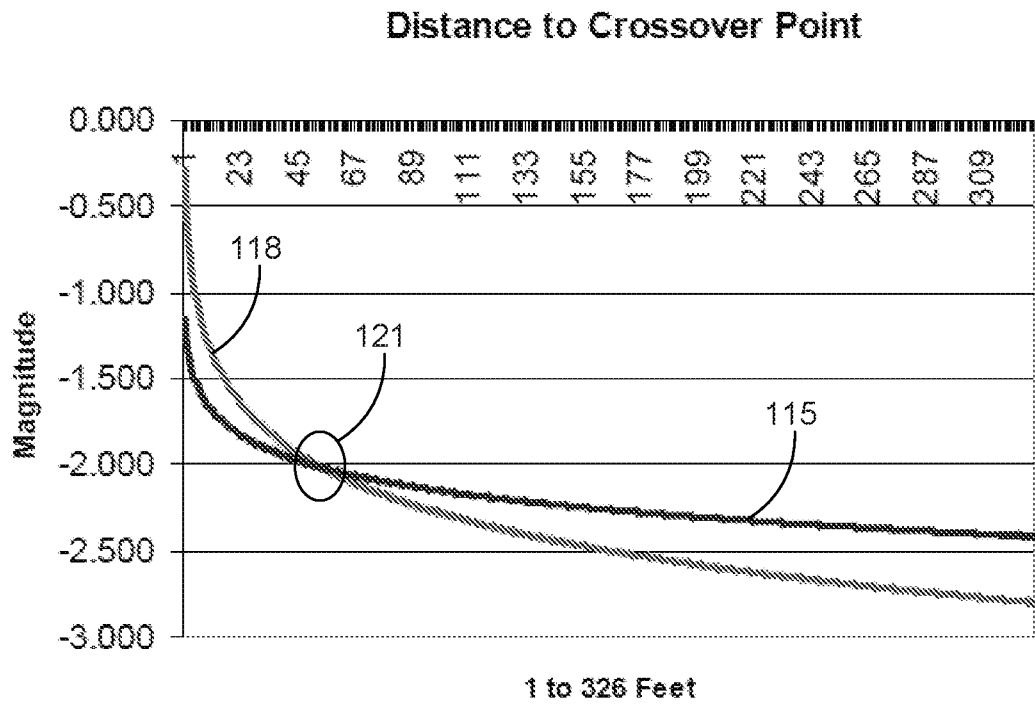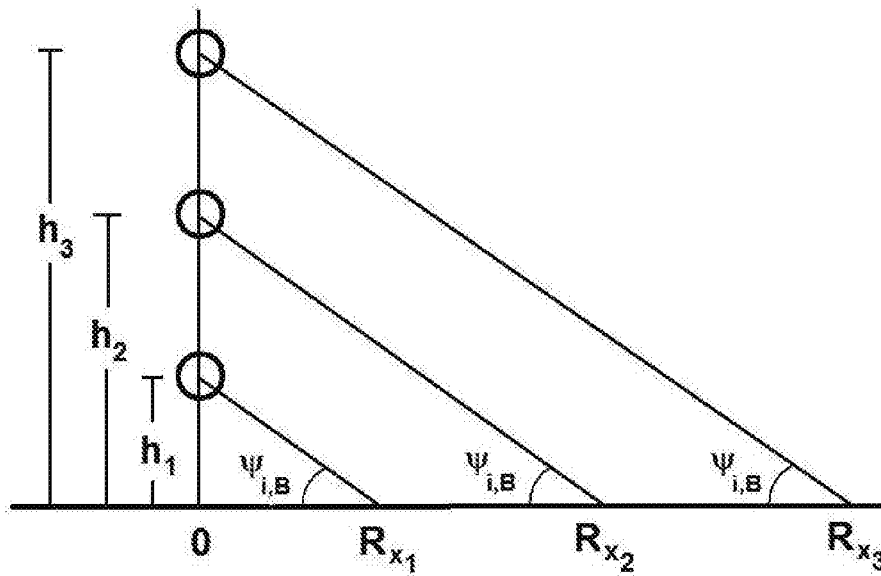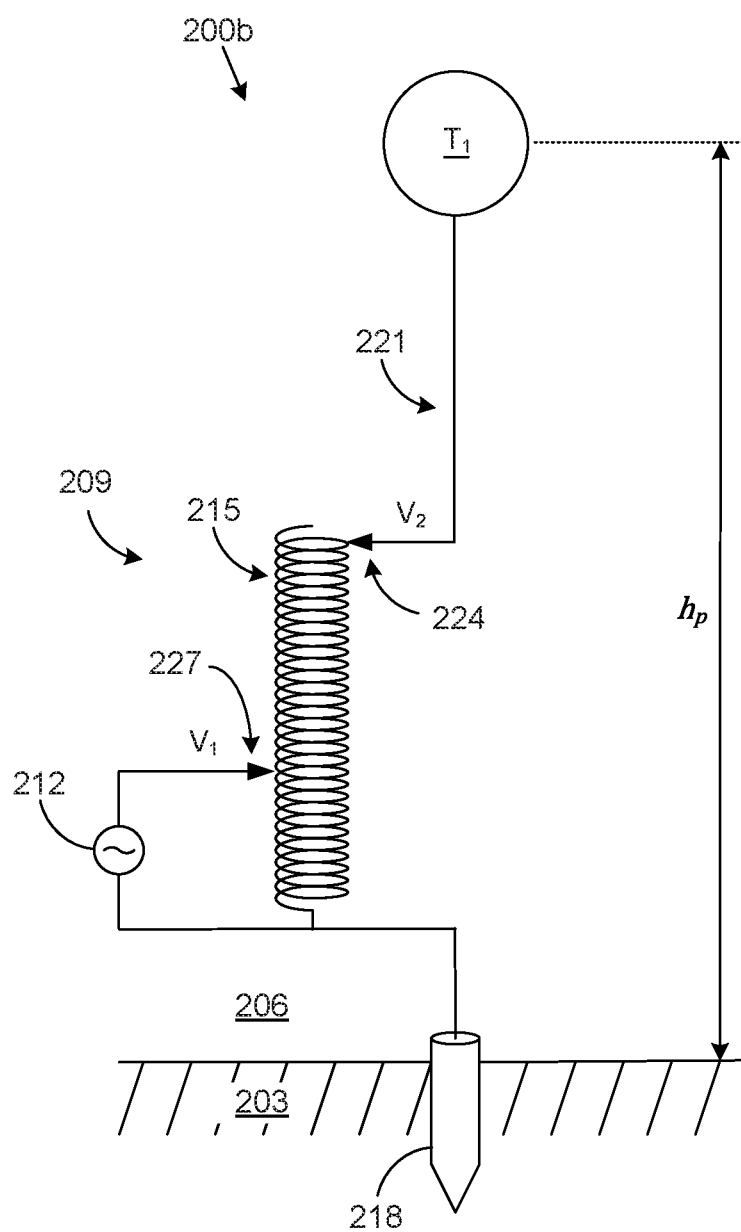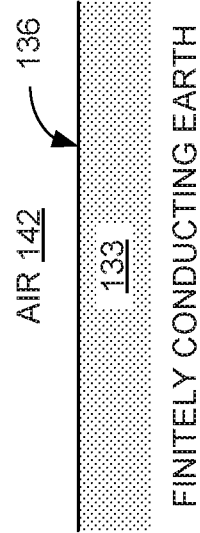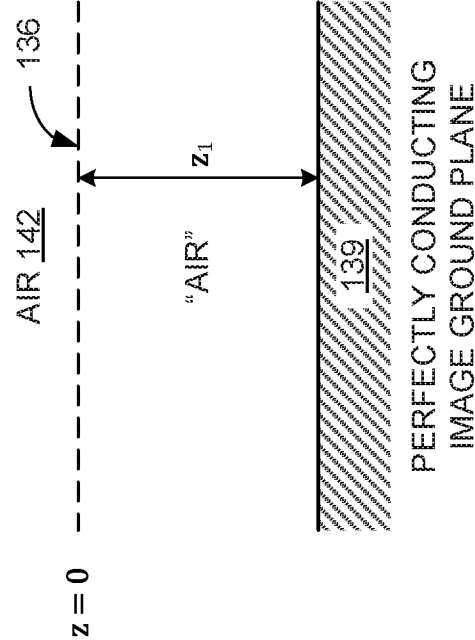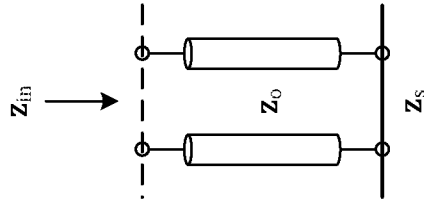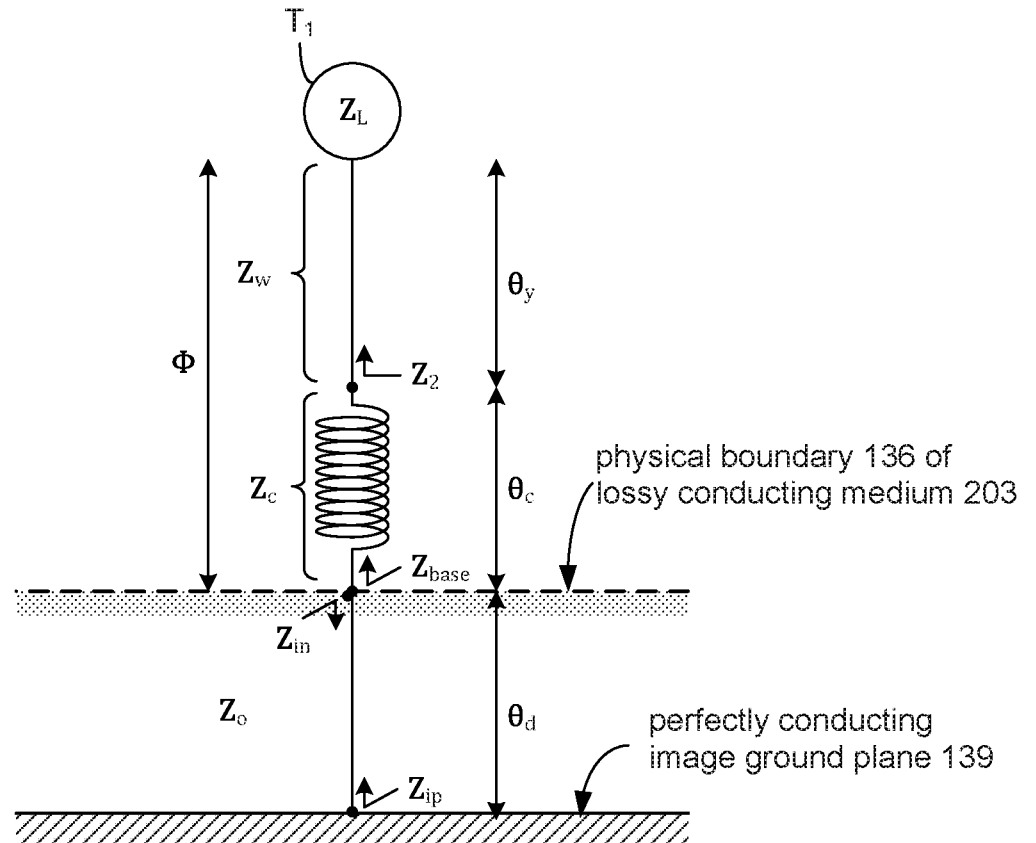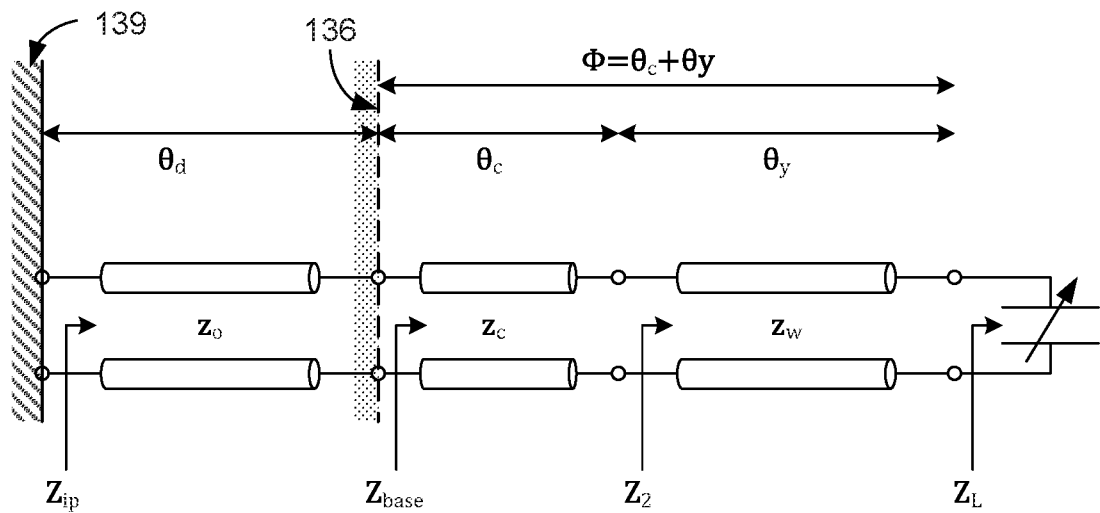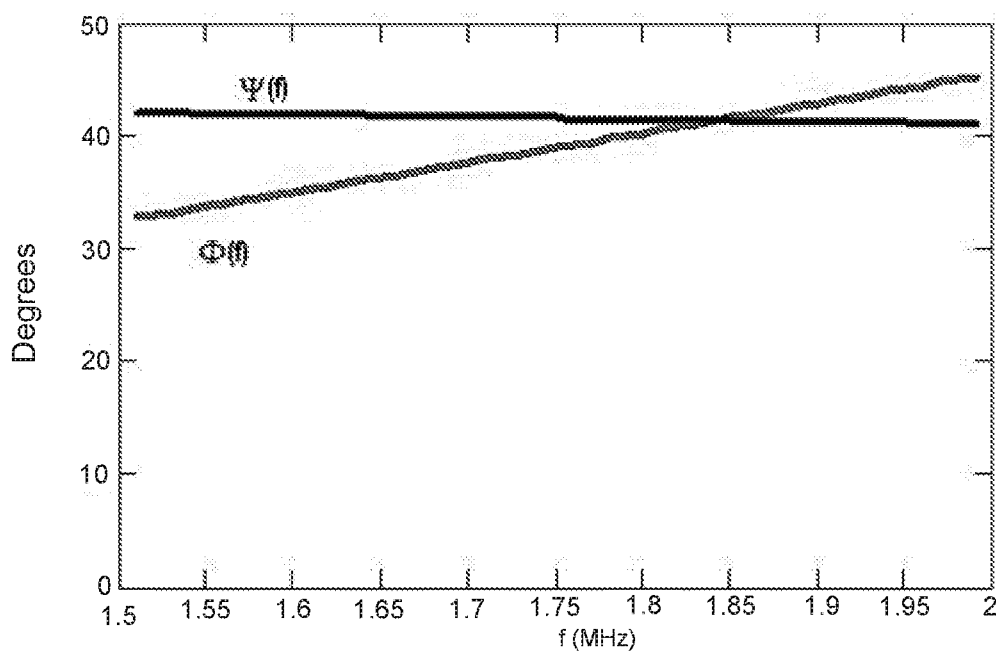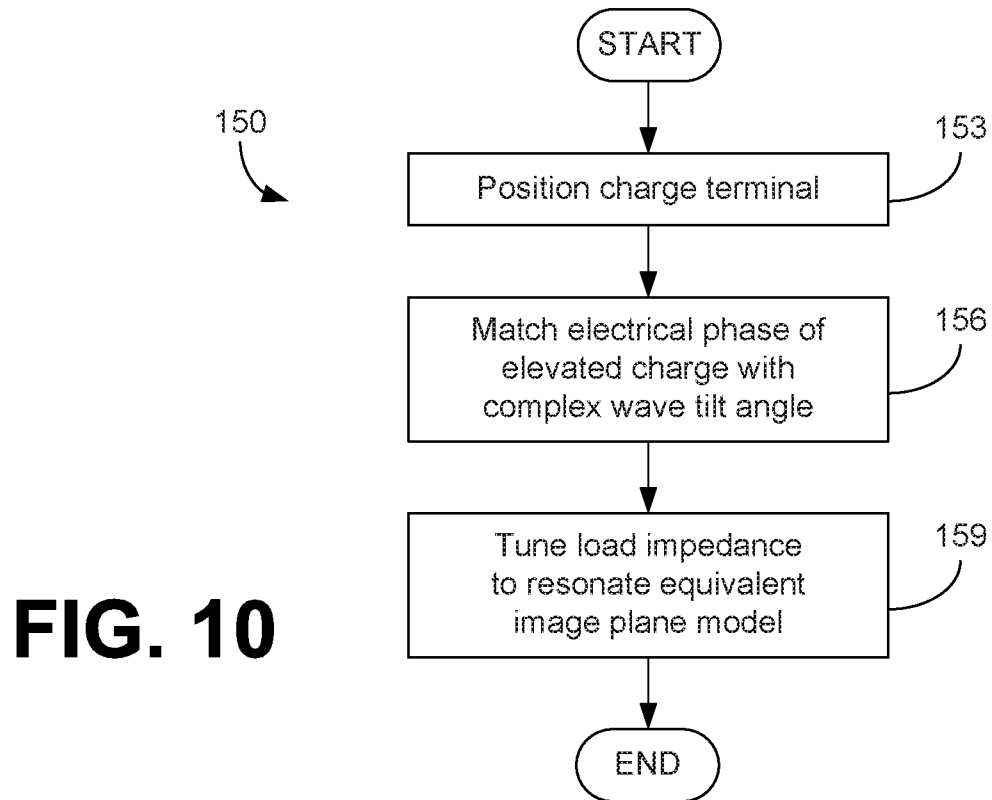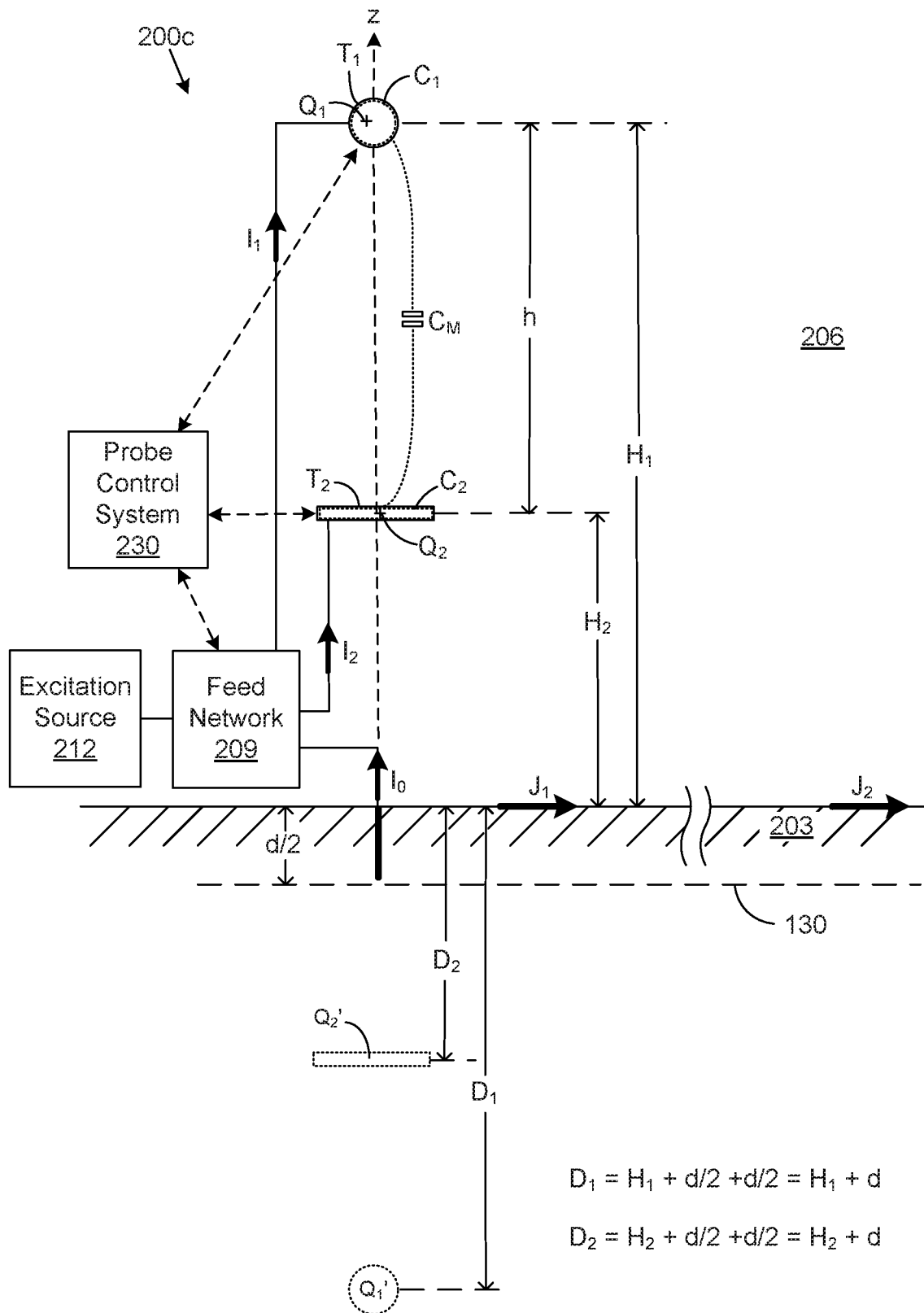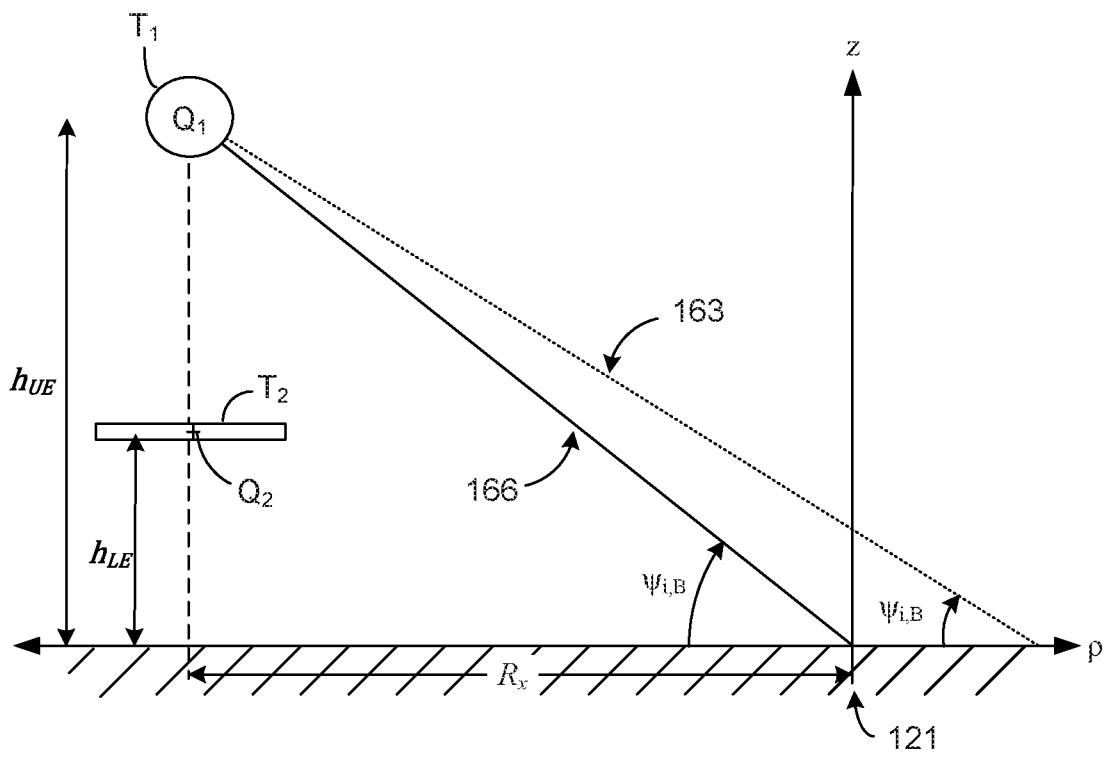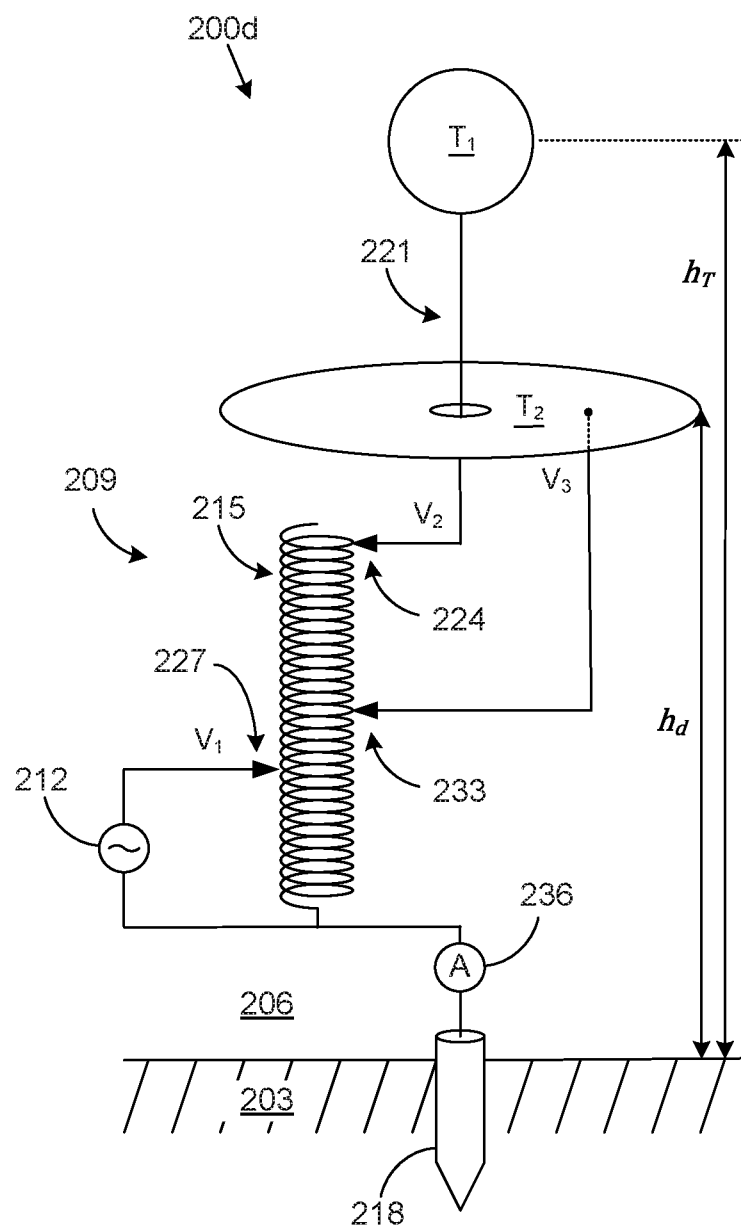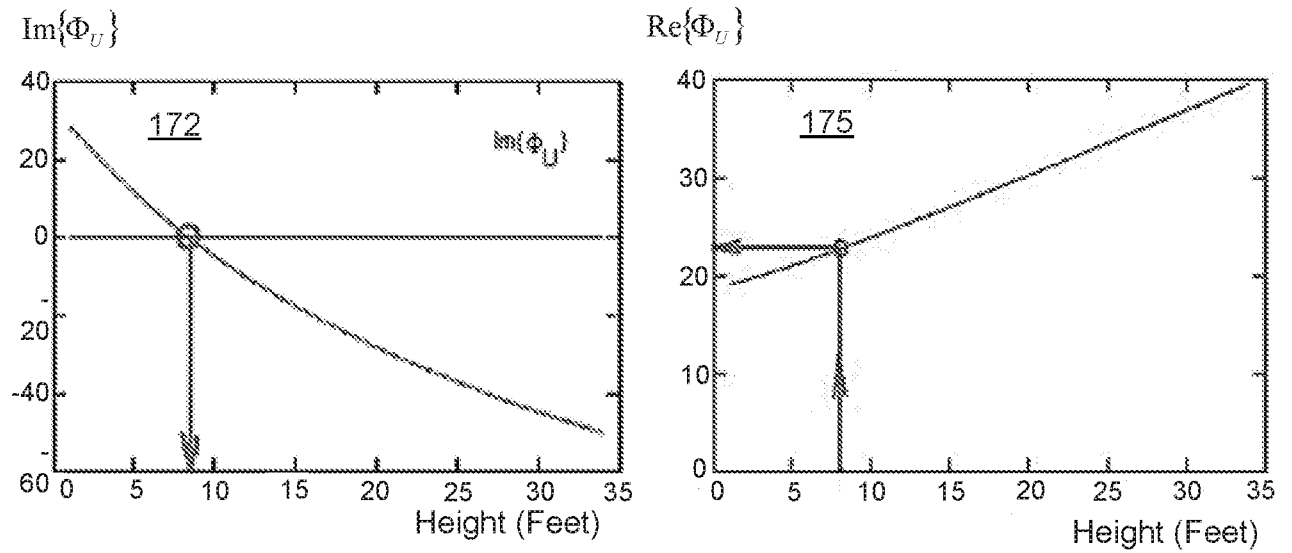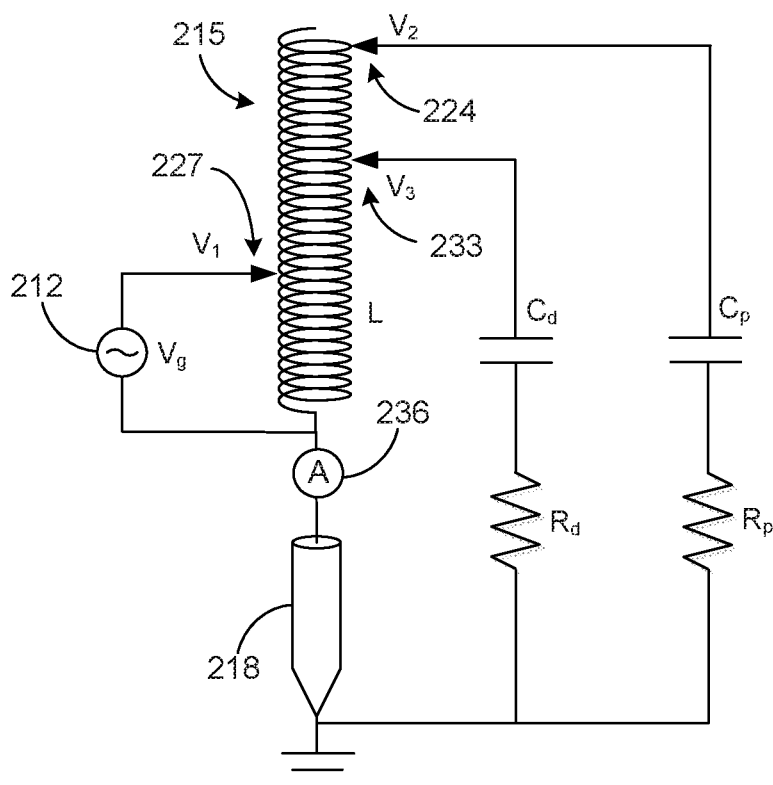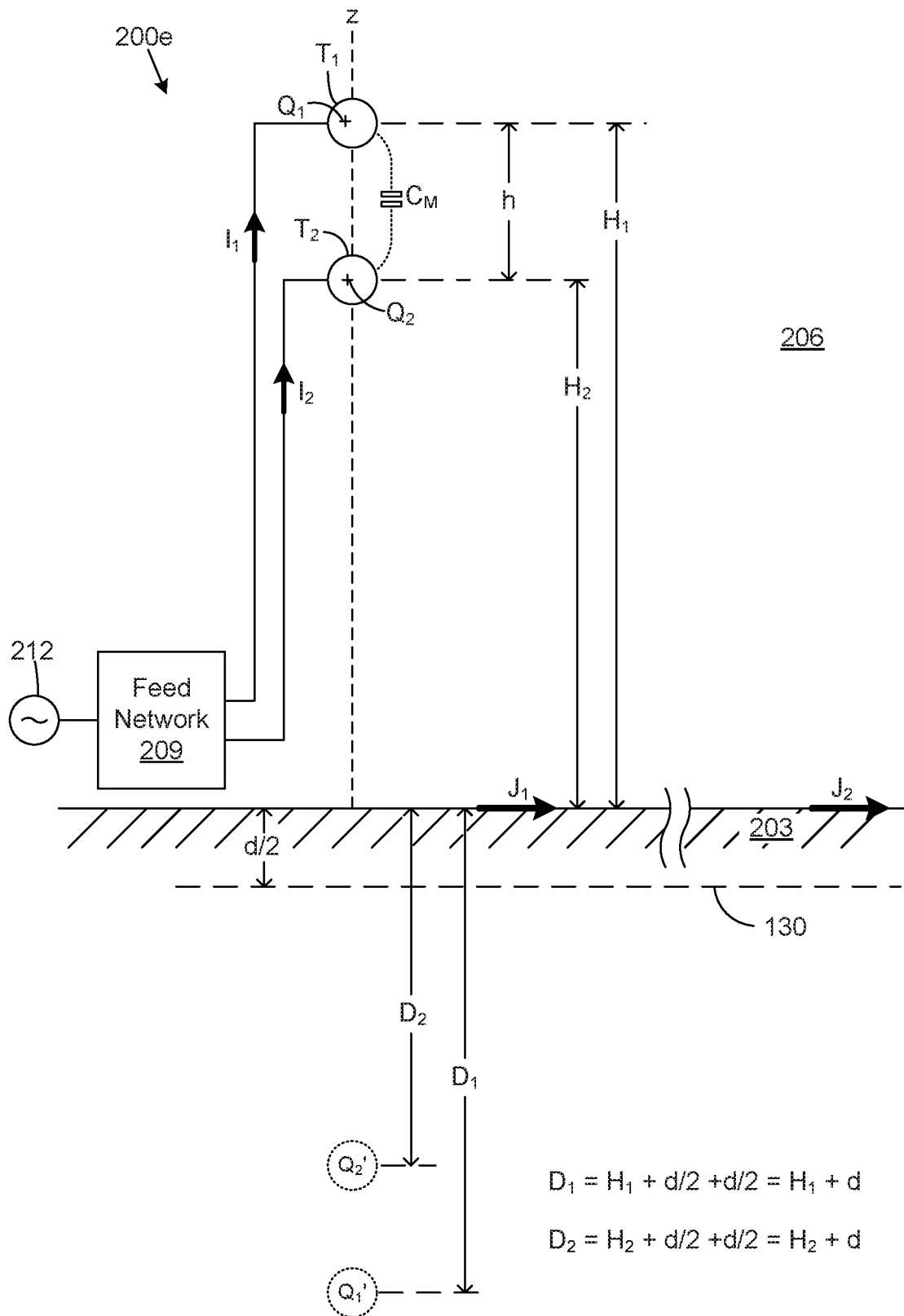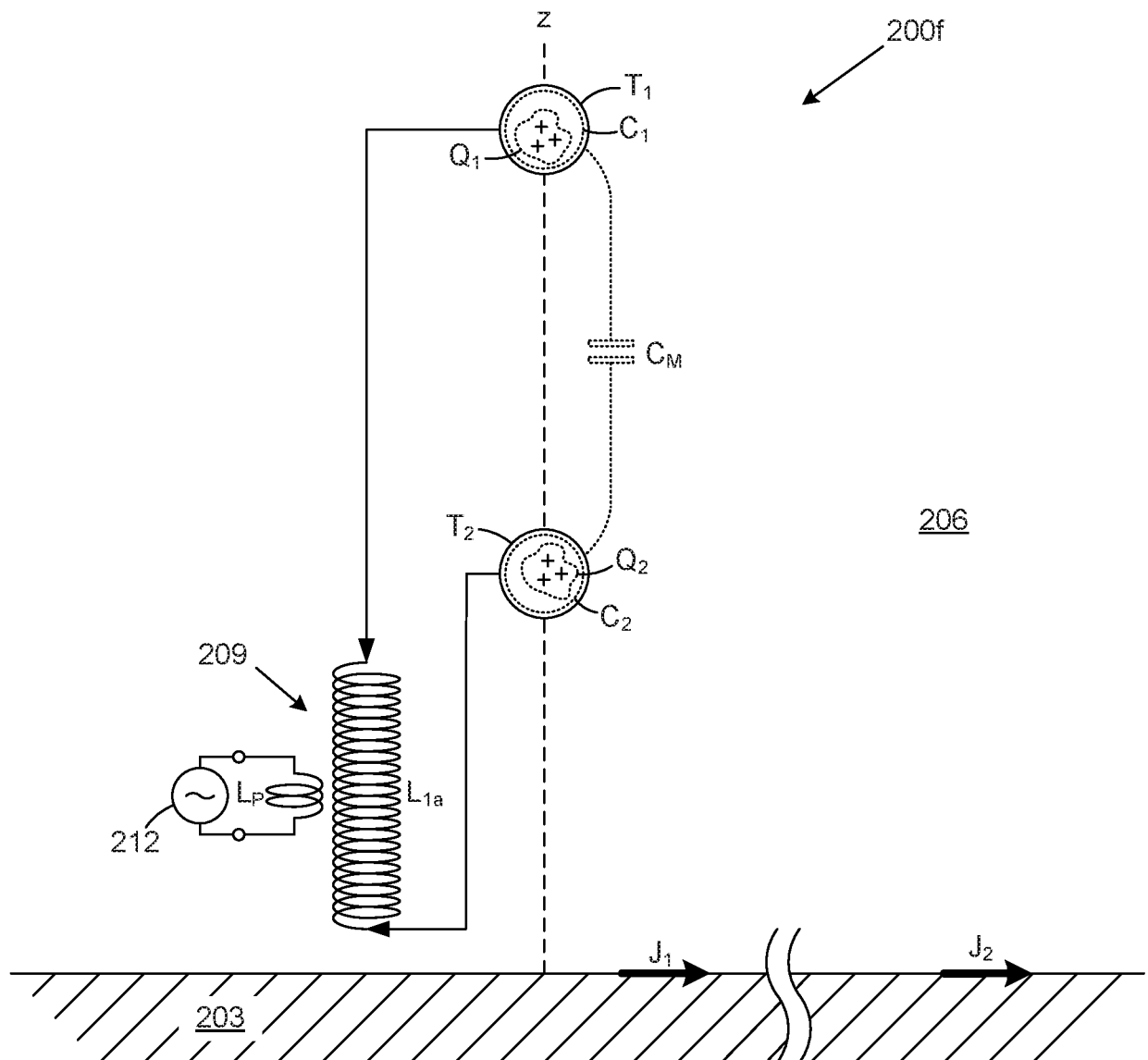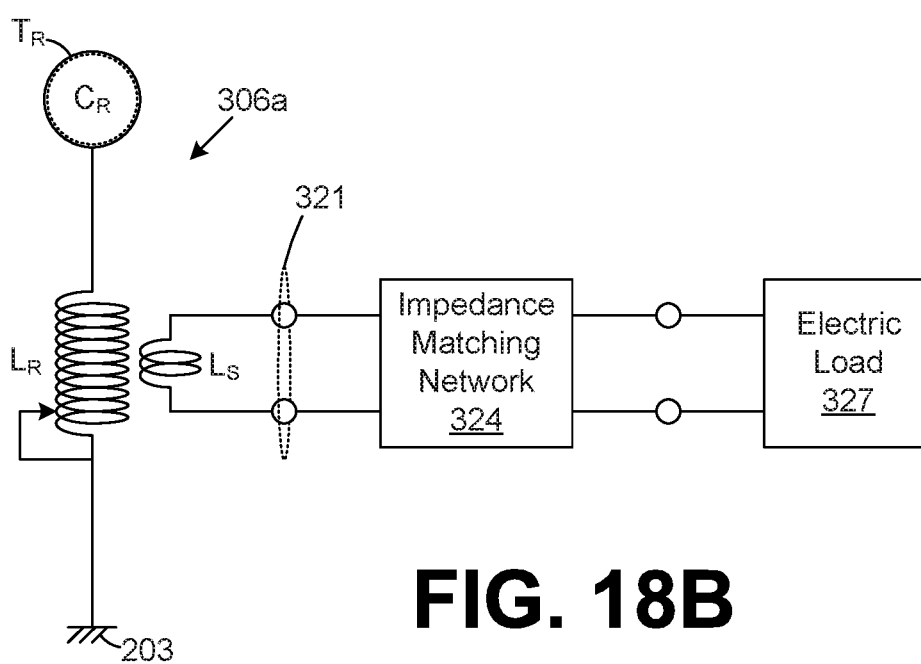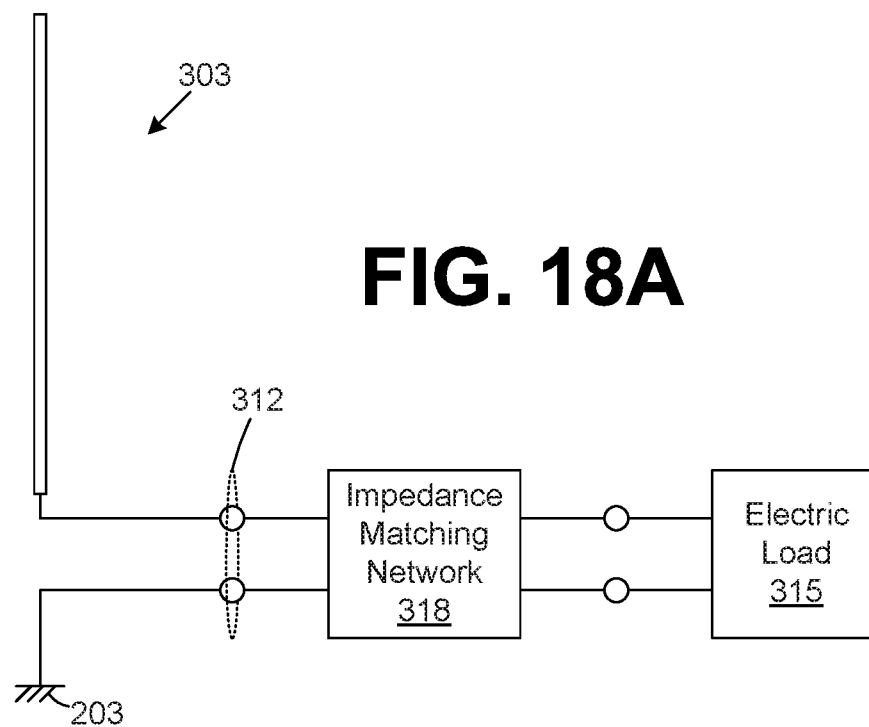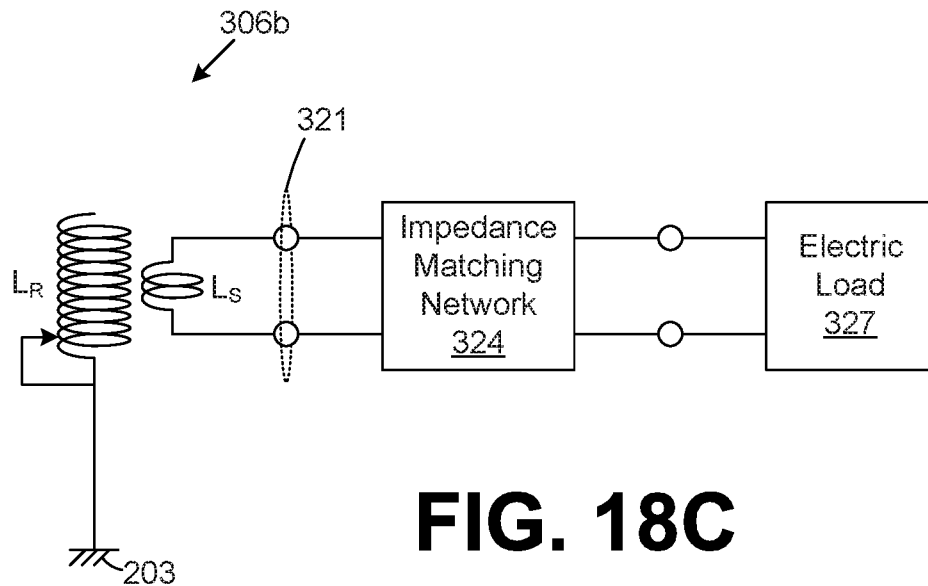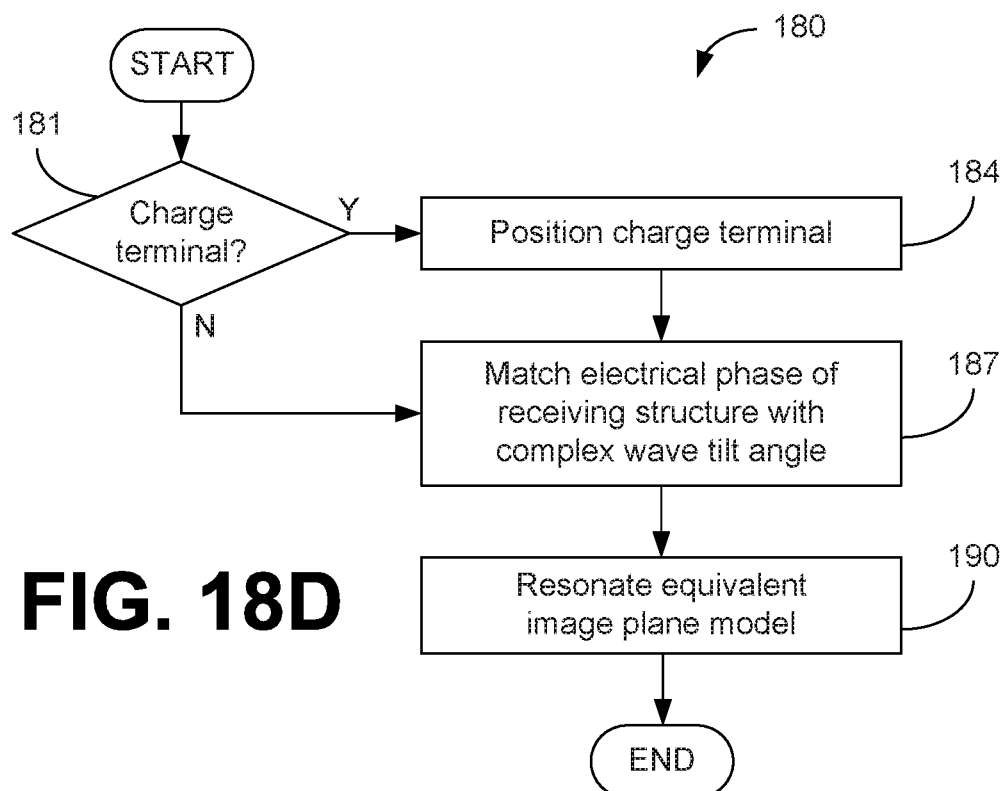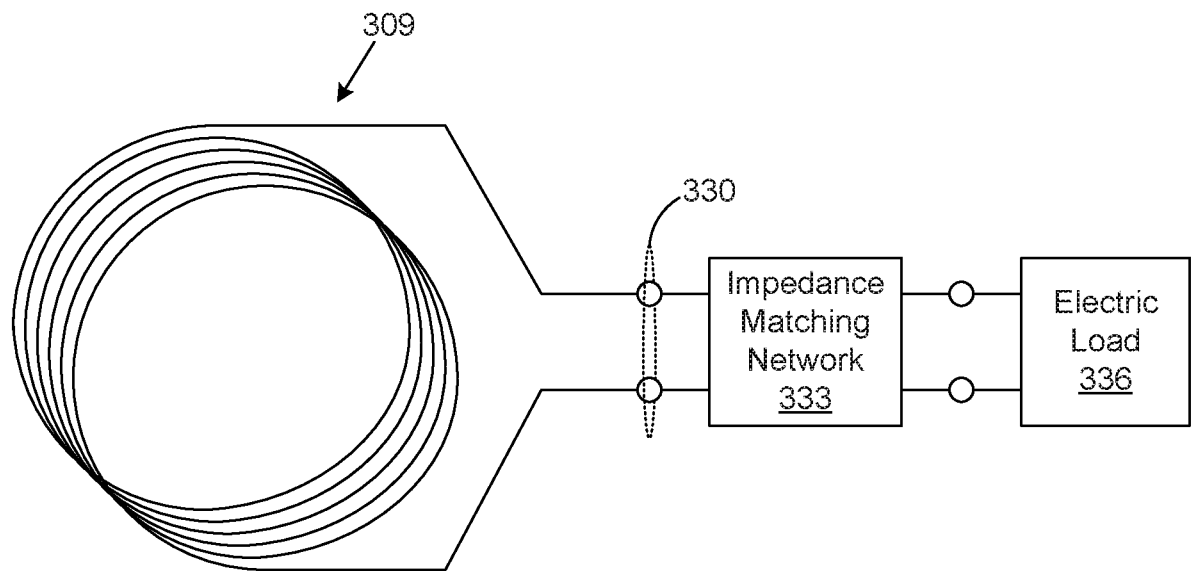
FIG. 19
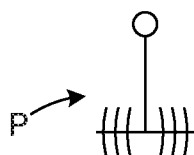
FIG. 20A

FIG. 20B

FIG. 20C

FIG. 20D
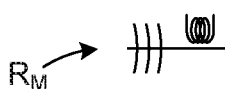
FIG. 20E
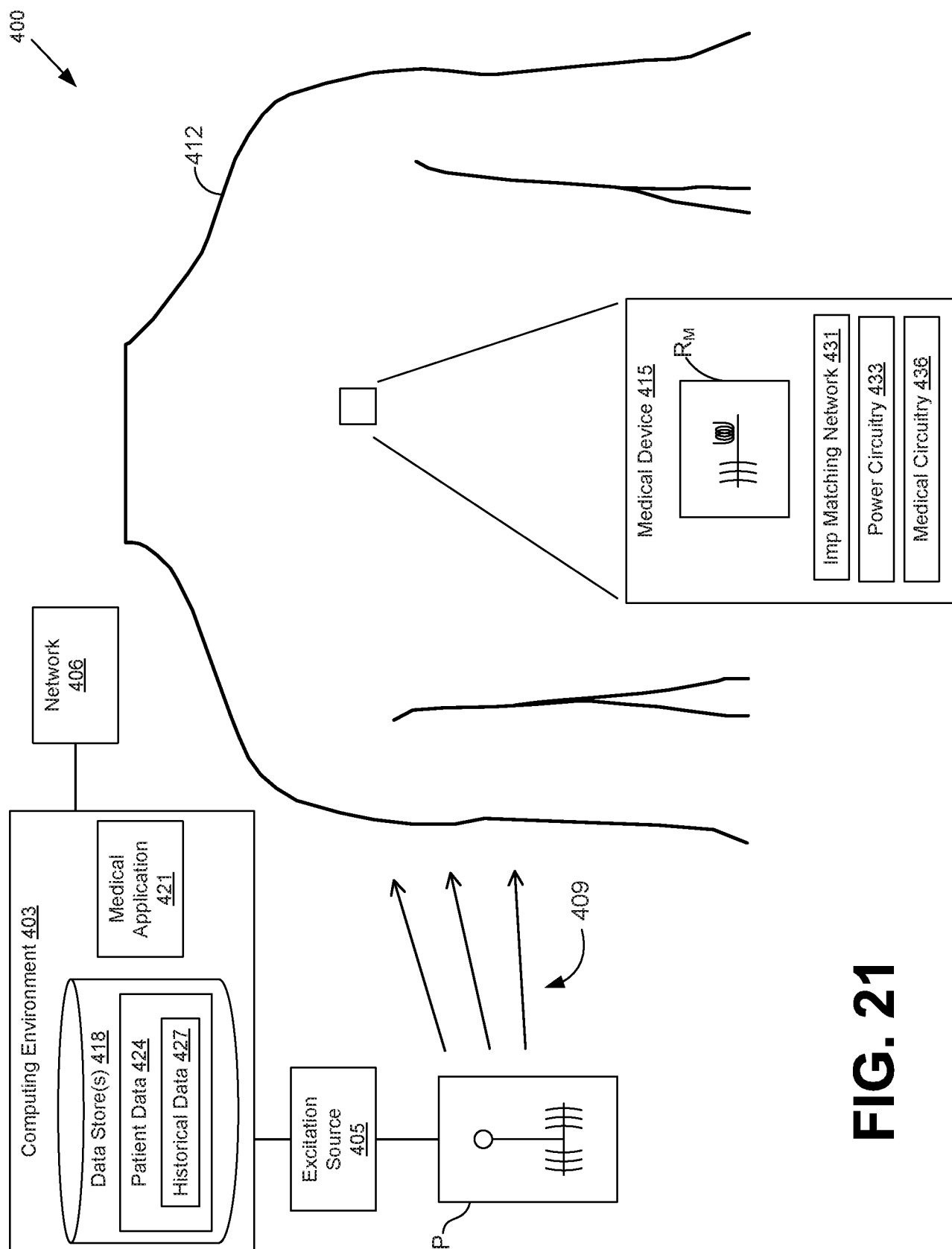
FIG. 21
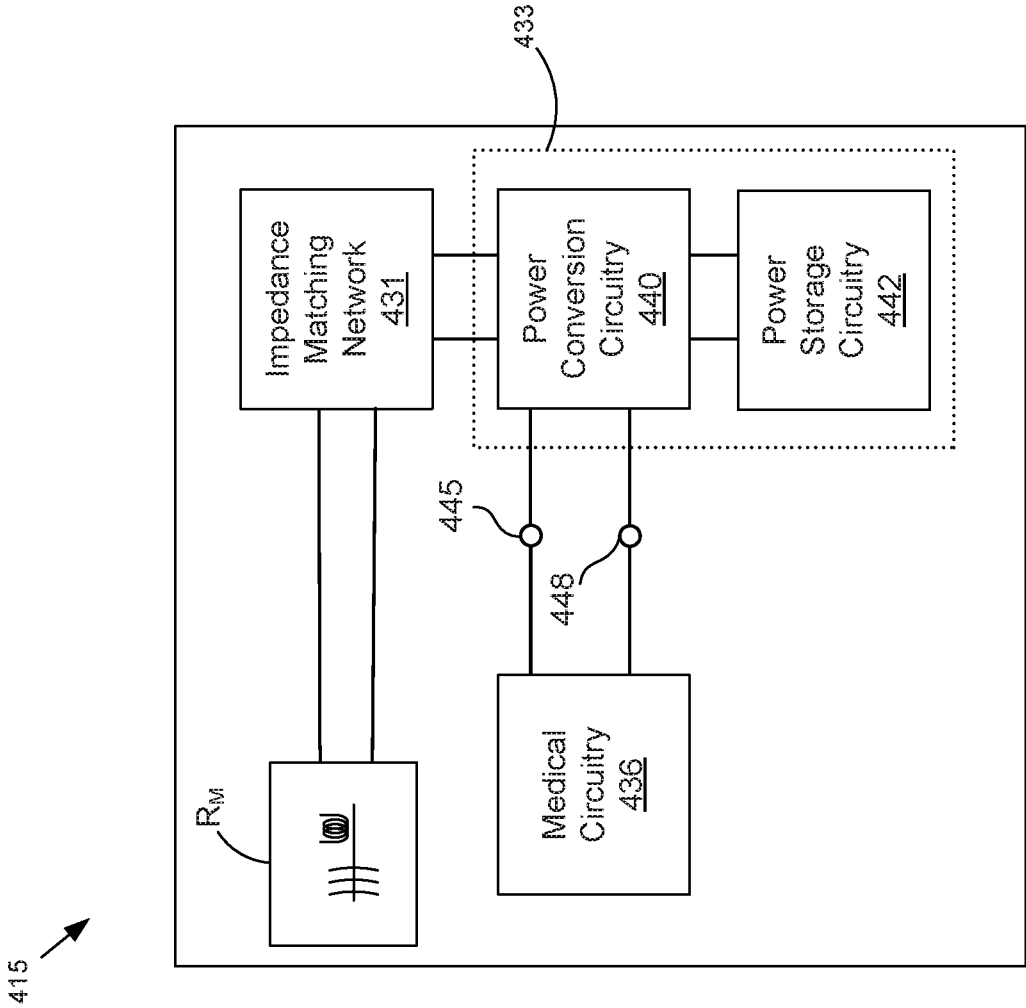
FIG. 22
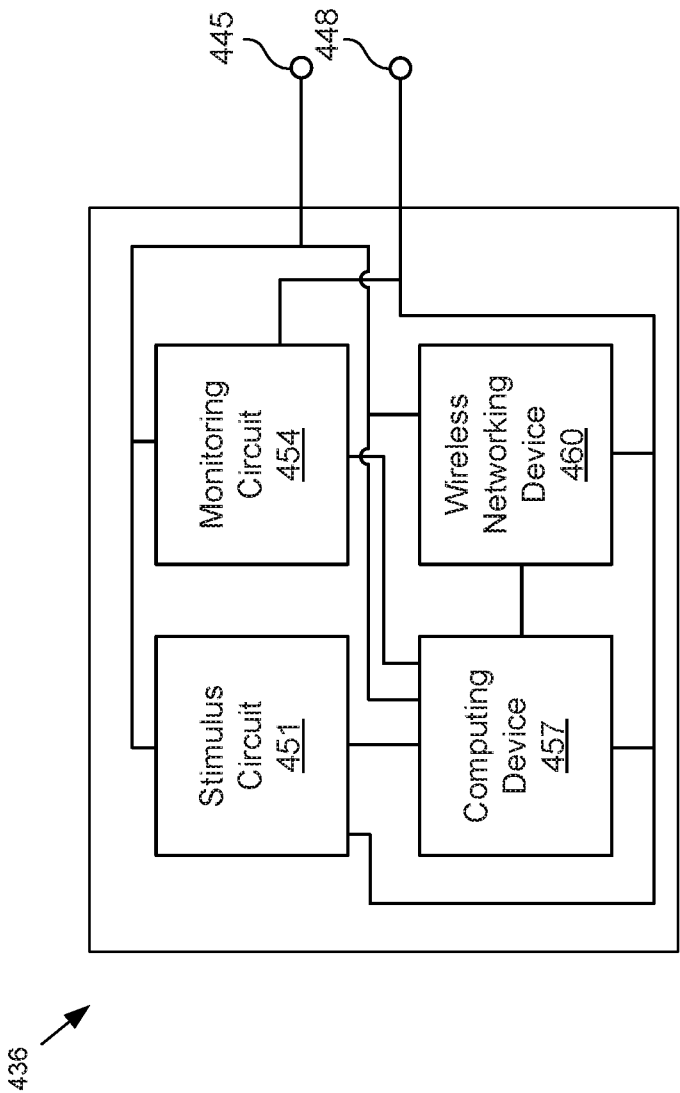
FIG. 23

FIG. 24

```
                    ┌─────────────┐
                    │    Start    │
                    └──────┬──────┘
                           │                          475
                           ▼                          ↙
           ┌───────────────────────────────┐
           │   Receive a guided surface wave│
           │             478                │
           └───────────────┬───────────────┘
                           │
                           ▼
           ┌───────────────────────────────┐
           │  Generate an AC signal based on│
           │      guided surface wave       │
           │             481                │
           └───────────────┬───────────────┘
                           │
                           ▼
           ┌───────────────────────────────┐
           │ Generate DC power signal from the│
           │   guided surface wave signal   │
           │             484                │
           └───────────────┬───────────────┘
                           │
                           ▼
           ┌───────────────────────────────┐
           │  Determine a measurement from a│
           │          human body            │
           │             487                │
           └───────────────┬───────────────┘
                           │
                           ▼
           ┌───────────────────────────────┐
           │   Calculate a variance in the  │
           │         measurement            │
           │             490                │
           └───────────────┬───────────────┘
                           │
                           ▼
                       ◇─────────◇
                      ╱    Does    ╲                ┌──────────────┐
                     ╱   Variance   ╲    Yes        │   Provide    │
                    ◇ meet a predefined◇────────────▶│ stimulus to  │
                     ╲   threshold?  ╱                │ human body   │
                      ╲    493      ╱                 │     496      │
                       ◇─────────◇                    └──────┬───────┘
                           │                                 │
                           No                                │
                           ▼                                 │
                    ┌─────────────┐                          │
                    │     End     │◀─────────────────────────┘
                    │     499     │
                    └─────────────┘
```
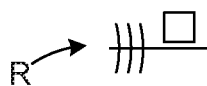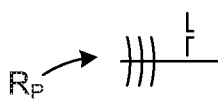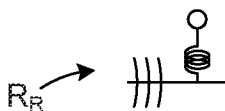
FIG. 25

```
        ┌─────────────┐
        │    Start     │
        └──────┬──────┘
               │
               ▼
┌──────────────────────────────────┐        500
│ Receive a request to perform an  │      ↙
│         update                   │
│         from a server            │
│            503                   │
└──────────────┬───────────────────┘
               │
               ▼
┌──────────────────────────────────┐
│      Authenticate the server      │
│              506                  │
└──────────────┬───────────────────┘
               │
               ▼
┌──────────────────────────────────┐
│         Verify the update         │
│              509                  │
└──────────────┬───────────────────┘
               │
               ▼
┌──────────────────────────────────┐
│        Applying the update        │
│              512                  │
└──────────────┬───────────────────┘
               │
               ▼
        ┌─────────────┐
        │     End      │
        │     515      │
        └─────────────┘
```

FIG. 26

518

| Processor 521 | RAM 524 | I/O 527 |

530

Memory Device 533

FIG. 27

INTERNATIONAL SEARCH REPORT

A. CLASSIFICATION OF SUBJECT MATTER

INV. A61N1/372
ADD. A61N1/362   A61N1/39   A61N1/365

According to International Patent Classification (IPC) or to both national classification and IPC

B. FIELDS SEARCHED

Minimum documentation searched (classification system followed by classification symbols)

A61M A61N

Documentation searched other than minimum documentation to the extent that such documents are included in the fields searched

Electronic data base consulted during the international search (name of data base and, where practicable, search terms used)

EPO-Internal, WPI Data

C. DOCUMENTS CONSIDERED TO BE RELEVANT

Category*	Citation of document, with indication, where appropriate, of the relevant passages	Relevant to claim No.
X	WO 2009/120490 A1 (MEDTRONIC INC [US]; CORNDORF ERIC D [US]; MEEKS LUCAS JM [NL]) 1 October 2009 (2009-10-01) pages 4,5; figures 2,5 -----	1-9
A	US 2014/252886 A1 (CORUM JAMES F [US] ET AL) 11 September 2014 (2014-09-11) cited in the application abstract; figure 1 -----	1-9

☐ Further documents are listed in the continuation of Box C.   ☒ See patent family annex.

* Special categories of cited documents :

"A" document defining the general state of the art which is not considered to be of particular relevance

"E" earlier application or patent but published on or after the international filing date

"L" document which may throw doubts on priority claim(s) or which is cited to establish the publication date of another citation or other special reason (as specified)

"O" document referring to an oral disclosure, use, exhibition or other means

"P" document published prior to the international filing date but later than the priority date claimed

"T" later document published after the international filing date or priority date and not in conflict with the application but cited to understand the principle or theory underlying the invention

"X" document of particular relevance; the claimed invention cannot be considered novel or cannot be considered to involve an inventive step when the document is taken alone

"Y" document of particular relevance; the claimed invention cannot be considered to involve an inventive step when the document is combined with one or more other such documents, such combination being obvious to a person skilled in the art

"&" document member of the same patent family

Date of the actual completion of the international search	Date of mailing of the international search report
22 November 2016	02/12/2016

Name and mailing address of the ISA/	Authorized officer
European Patent Office, P.B. 5818 Patentlaan 2 NL - 2280 HV Rijswijk Tel. (+31-70) 340-2040, Fax: (+31-70) 340-3016	Edward, Vinod

1

Form PCT/ISA/210 (second sheet) (April 2005)

INTERNATIONAL SEARCH REPORT	International application No.
	PCT/US2016/047375

Box No. II   **Observations where certain claims were found unsearchable (Continuation of item 2 of first sheet)**

This international search report has not been established in respect of certain claims under Article 17(2)(a) for the following reasons:

1. [X] Claims Nos.:   10-15
   because they relate to subject matter not required to be searched by this Authority, namely:

   Due to the step of providing a stimulus to the human body, claim 15 relates to a method of treatment of the human body by therapy, contrary to the requirements of Art. 39.1(iv) PCT. Therefore, claims 10-15 were not searched and cannot be examined.

2. [ ] Claims Nos.:
   because they relate to parts of the international application that do not comply with the prescribed requirements to such an extent that no meaningful international search can be carried out, specifically:

3. [ ] Claims Nos.:
   because they are dependent claims and are not drafted in accordance with the second and third sentences of Rule 6.4(a).

Box No. III   **Observations where unity of invention is lacking (Continuation of item 3 of first sheet)**

This International Searching Authority found multiple inventions in this international application, as follows:

1. [ ] As all required additional search fees were timely paid by the applicant, this international search report covers all searchable claims.

2. [ ] As all searchable claims could be searched without effort justifying an additional fees, this Authority did not invite payment of additional fees.

3. [ ] As only some of the required additional search fees were timely paid by the applicant, this international search report covers only those claims for which fees were paid, specifically claims Nos.:

4. [ ] No required additional search fees were timely paid by the applicant. Consequently, this international search report is restricted to the invention first mentioned in the claims; it is covered by claims Nos.:

Remark on Protest   [ ] The additional search fees were accompanied by the applicant's protest and, where applicable, the payment of a protest fee.

[ ] The additional search fees were accompanied by the applicant's protest but the applicable protest fee was not paid within the time limit specified in the invitation.

[ ] No protest accompanied the payment of additional search fees.

Form PCT/ISA/210 (continuation of first sheet (2)) (April 2005)

INTERNATIONAL SEARCH REPORT

Information on patent family members

Patent document cited in search report		Publication date	Patent family member(s)		Publication date
WO 2009120490	A1	01-10-2009	US	2009248115 A1	01-10-2009
			US	2012188096 A1	26-07-2012
			WO	2009120490 A1	01-10-2009
US 2014252886	A1	11-09-2014	NONE		

摘要

公开的是一种可植入的医疗设备和使用该医疗设备的方法。医疗设备可以包括被引导的表面波接收结构，其被配置为接收由被引导的表面波导探头发送的被引导的表面波。当接收到被引导的表面波时，医疗设备中的被引导的表面波接收结构产生交流信号。医疗设备包括被耦合到被引导的表面波接收结构的电力电路。电力电路包括用于存储电力信号的电力存储电路。医疗设备包括医疗电路，该医疗电路包括刺激电路、监测电路以及可能的其他组件。刺激电路为人体提供刺激。监测电路测量人体的特性。

$$D_1 = H_1 + d/2 + d/2 = H_1 + d$$